

CHARACTERIZING AND REDUCING HEAD ACCELERATION EVENTS IN CONTACT SPORTS

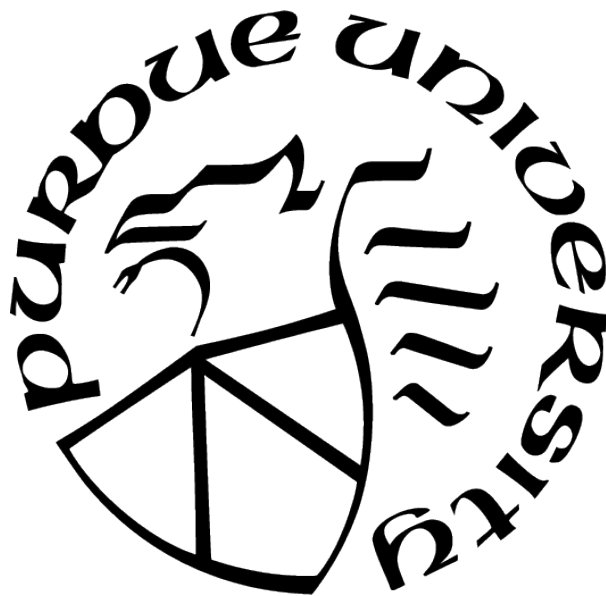
by
Taylor Lee

A Dissertation

Submitted to the Faculty of Purdue University

In Partial Fulfillment of the Requirements for the degree of

Doctor of Philosophy



School of Mechanical Engineering

West Lafayette, Indiana

May 2021

**THE PURDUE UNIVERSITY GRADUATE SCHOOL
STATEMENT OF COMMITTEE APPROVAL**

Dr. Eric Nauman, Chair

School of Mechanical Engineering, Weldon School of Biomedical Engineering, Department
of Basic Medical Sciences

Dr. Thomas Talavage

Department of Electrical and Computer Engineering, Weldon School of Biomedical
Engineering

Dr. Jeffrey Rhoads

School of Mechanical Engineering

Dr. Scott Lawrance

Department of Health and Kinesiology

Approved by:

Dr. Nicole Key

I would like to dedicate this dissertation to my incredible family (Barbara, Jason, Mary, Carolyn, and Patrick Lee) for their unwavering love and support during this adventure and friends (Abi Banan, Chauncey Fry, Becky Creech, Megan Hubbard, Annie Dooley, and Maddie Riordan) without whom my time at Purdue would not have been the same. I would also like to dedicate this work to my HIRRT lab (Roy Lycke, Jacob McGough, Murat Horasan, Michael Dziekan, Kevin McIver, Brie Lawson, Nathan Knodel, Nicolas Leiva-Molano, Breana Cappuccilli, Sean Bucherl, Kelly Torolski, Leonardo de Freitas Silva, Ninad Trifale, Josh Auger, and Jacob Music), PNG (Nicole Vike, Ikbeom Jang, Sumra Bari, Yukai Zou, Ho-Ching Yang, Caroline Cudal, and Mitchell Arndt), and AUT SPRINZ (Josh McGeown, Renata Gottgroy, and Dr. Hannah Wyatt) colleagues, without whom this work would not have been possible. Special dedications to my former soccer coach, Howie Hawver, and undergraduate advisor, Dr. Lisa Pruitt, for inspiring me to pursue a graduate degree in this field.

ACKNOWLEDGMENTS

I would like to thank my committee members Dr. Tom Talavage, Dr. Jeffrey Rhoads, and Dr. Scott Lawrance for their invaluable expertise and mentorship through my PhD. I would like to thank my thesis advisor, Dr. Eric Nauman, for his guidance and knowledge that helped me grow, professionally and personally. I would also like to thank, Dr. Paul Auerbach for his irreplaceable collaboration on these projects. I would like to thank Professor Patria Hume for her pivotal mentorship during my time in New Zealand. Lastly, I would like to thank Dr. Roy Lycke for his instrumental mentorship and input on the design, processing, and reporting of these works.

I would like to acknowledge the following for their financial support: Purdue University, Purdue Research Foundation, Stanford Department of Emergency Medicine (Dr. Paul Auerbach), Auckland University of Technology, Collaboration in Translational Research grant from the Indiana Clinical and Translational Sciences Institute (PI: Newman), Allied Milk Producers, X2 Biosystems (for supplying sensors), NVIDIA Corporation (donation of Titan Xp GPU), grants from the BrainScope Company (on behalf of a grant from GE-NFL Head Health Initiative), Indiana Clinical and Translational Sciences Institute Spinal Cord and Brain Injury Research Fund (SCBI #207-5 and #207-32), Core Facilities Grant from the Indiana Clinical and Translational Sciences Institute, the National Science Foundation Graduate Research Fellowships Program (Grant No. DGE-1333468), and the Fulbright New Zealand US Graduate Student Program.

TABLE OF CONTENTS

LIST OF TABLES	10
LIST OF FIGURES	12
LIST OF SYMBOLS	16
ABBREVIATIONS	17
ABSTRACT	19
1 INTRODUCTION	22
1.1 Motivation	22
1.2 Objectives	24
2 LEVEL OF PLAY IN FOOTBALL AND GIRLS' SOCCER	26
2.1 Introduction	26
2.2 Methods	28
2.2.1 Participants	28
2.2.2 Data Collection	28
2.2.3 Data Analysis	29
2.2.4 Statistical Analysis	30
2.3 Results	31
2.3.1 Group-Based Analysis	31
2.3.2 Player-Based Analysis	31
2.4 Discussion and Implications	33
2.4.1 Football vs. Girls' Soccer	33
2.4.2 Girls' Soccer Levels of Play	35
2.4.3 Football Levels of Play	35
2.4.4 Limitations	37
2.5 Conclusion	38

3	PLAY TYPE AND STANCE: PILOT STUDY	48
3.1	Introduction	48
3.2	Methods	50
3.2.1	Subjects	50
3.2.2	Impact Data Collection and Analysis	50
3.2.3	Video Data Collection and Analysis	51
3.2.4	Statistics	52
3.3	Results	53
3.4	Discussion	55
3.5	Conclusion	57
4	PLAY TYPE AND STANCE: CONFIRMATION STUDY	58
4.1	Introduction	58
4.2	Methods	58
4.2.1	Subjects	58
4.2.2	Assignment of Stance	60
4.2.3	Modified Game Rules	60
4.2.4	HAE Data Collection and Analysis	60
4.2.5	Video Data Collection and Analysis	61
4.2.6	Offensive Linemen Stance	62
4.2.7	Statistics	62
4.3	Results	63
4.4	Discussion	68
4.4.1	Effect of Position on HAEs	69
4.4.2	Factors Affecting the HAE Rate	69
4.4.3	Limitations	71
4.5	Conclusion	72
5	WHITE MATTER	73
5.1	Introduction	73
5.2	Methods	76

5.2.1	Subjects	76
5.2.2	Magnetic Resonance Image Acquisition and Data Processing	76
	Data Acquisition	76
	Data Pre-Processing	77
	DTI Metric Session Value Comparison	77
	DTI Metric Difference Comparison	78
5.2.3	Football Athlete Relative Region of Interest Change Factor Visualization	78
	Statistics	79
5.3	Results	80
5.3.1	Comparison of Football vs. Control Athlete at Pre-Season	80
5.3.2	Comparison of Football vs. Control Athlete Over a Season	81
5.3.3	Comparison of Football vs. Control Athlete at Post-Season	82
5.3.4	ROI Likelihood Factor Analysis	83
5.4	Discussion	85
5.4.1	Monte Carlo Simulation to Investigate Trends	87
5.4.2	Limitations	88
5.5	Conclusion	89
6	RUGBY HAE STUDY	90
6.1	Introduction	90
6.2	Methods	90
6.2.1	Participants	90
6.2.2	HAE Data Collection	91
6.2.3	HAE Data Analysis	91
6.2.4	Video Analysis	91
6.2.5	Statistics	92
6.3	Results	93
6.4	Discussion	94
6.4.1	Difference by Position	94
6.4.2	Difference by Possession	95

6.4.3	Difference by Cause of HAE	96
6.4.4	Comparison to Previous Rugby Studies	96
6.4.5	Sport Comparison: Rugby vs. Football	97
6.4.6	Limitations	98
6.5	Conclusion	98
7	INSTRUMENTED HELMET	99
7.1	Introduction	99
7.2	Methods	100
7.2.1	Circuitry Components and Design	100
	Strain Gauges	100
	Multiplexer	101
	Wheatstone Bridge and Differential Amplifier	102
	Development Board	102
	Time Sync Data Processing	103
7.2.2	Bench Top Bending Test	105
	Bending Test Sample	105
	Bending Test Set Up	106
	Bending Test Data Processing	107
7.2.3	Strain Gauge Testing on Hybrid III Headform	110
	Manufacturing Process	110
	Data Acquisition	110
	Data Post-Processing	113
7.3	Results	113
7.3.1	Four Point Bending Test	113
7.3.2	Strain Gauge Testing on Hybrid III Headform	114
	Single Rosette	114
	Full Array	114
7.4	Discussion	122
7.5	Conclusion	124

8	SUMMARY	125
8.1	Level of Play	125
8.2	Stance Analysis	125
8.3	White Matter	125
8.4	Rugby	126
8.5	Instrumented Helmet	126
	REFERENCES	127
A	APPENDIX A: METHODS	148
A.1	Outlier Analysis	148
A.2	Repair Data Calculation	148
B	APPENDIX B: METRIC GENERATION	150
B.1	Histograms	150
B.2	Number of HAEs	150
B.3	Cumulative PTA and PAA	150
B.4	Contact Sessions	151
B.5	Linear Regressions	151
	VITA	152
	PUBLICATIONS	155

LIST OF TABLES

2.1	Number of players in each group with full seasons of data (FSD) and partial seasons of data (PSD). Also listed are the ranges of the maximum number of monitored sessions for FSD players at each level of play.	29
2.2	Sport and level of play player medians of median HAEs per contact session, total HAEs, cumulative PTA, and cumulative PAA per season with the statistical difference noted in the column to the right of the metric of interest.	42
2.3	Average number of contact sessions in a season and the percentage of sessions in a season that had contact for each sport and level with the statistical difference noted in the column to the right of the metric of interest.	43
2.4	Comparison of the teams in this study to similar data that has been collected by others. All values below are calculated or estimated means.	47
3.1	HAEs by position as a function of practices (session 1, 2, 3) and game.	53
4.1	Number of study participants for both games for each position and team. This includes players that played on two teams in one day.	59
4.2	Number of HAEs sustained by each position separated by team and game (G1, G2, All Games).	64
4.3	Head acceleration event (HAE) rates for different play/stance combinations when matched and mismatched offensive line skill (OLS; low or high) teams play each other. Note that when matched OLS teams play each other, lower OLS teams had lower HAE rates than when two high OLS teams played each other. When mismatched OLS teams played each other, the HAE rate for lower OLS team increased, but decreased for the higher OLS team for certain combinations relative to playing a team matched OLS.	67
4.4	Variables and coefficients from logistic regression analysis. Main effects were included in the model if interaction effect with the variable was significant (p-value < 0.05 noted by *).	68
5.1	Combinations of DTI metrics and their biological meaning [121], [128], [129], [131], [133], [134], [137]–[139], [141], [144]–[147], [150]–[154], [156], [157], [160], [172], [173].	74
5.2	Comparison between pre-season and post-season likelihood factors for each ROI (L/R: Left-Right hemisphere) and FA/MD category, along with which session was significantly greater than the other. P-values are derived from the distribution generated from permutations (n = 1,000,000) of the Wilcoxon signed-rank. . . .	83
6.1	The estimated number of HAEs per game sustained by each position and all players. Values in the cell are the mean, median (lower quartile, upper quartile). There were no significant differences between the number of HAEs sustained by forwards and backs at any of the different threshold levels.	93

7.1	Strain gauge nominal values and ranges (if applicable). The subscript i represents the value for all of the strain gauges in the rosette (A, B, or C). Specific values for individual strain gauges are provided if necessary.	102
7.2	Wheatstone bridge and differential op amp values.	103
7.3	Test specimen and bending test set up values used to calculate the Euler's stress and strain and the strain from the designed circuit [197], [198].	107
7.4	Location classification accuracy.	120
7.5	Multiple linear regression coefficients for model correlating rosette effective $\epsilon_{EQnorm,i}$ to hit peak force.	121
7.6	Multiple linear regression coefficients for model correlating rosette effective $\epsilon_{EQnorm,i}$ to hit impulse.	122

LIST OF FIGURES

1.1	Example of an SN-curve.	24
1.2	A modified SN-curve for how repetitive impacts sustained in contact sports may cause neurological changes in these athletes.	24
2.1	The xPatch sensor and an example of (a) placement on a player's head, (b) waveform of the translational acceleration, and (c) waveform of the angular velocity.	40
2.2	Normalized distribution of HAE PTA magnitudes by level of play. There was no statistical difference between FB levels of play ($p=.190$), and GS V differed from both GS JV ($p=.001$) and GS JV-V ($p=.006$) distributions. High school FB and GS distributions were significantly different from each other ($p=.001$). Less than 1% of HAEs occurred above 120 g for each level.	41
2.3	Cumulative PTA (g) for the season versus the total number of HAEs per player per season for (a) FB and (b) GS, and cumulative PAA ($\text{rad} \cdot \text{sec}^{-2}$) for the season versus the total number of HAEs per player per season for (c) FB and (d) GS. For cumulative PTA, there was no statistical difference across of the levels of play in terms of the slope (FB: $p=.367$, ANOVA; GS: $p=.615$; KW), or between high school FB and GS ($p=.702$; KW). For cumulative PAA, there was no statistical difference between any of the slopes among the different levels of play (FB: $p=.933$, KW; GS: $p=.146$, ANOVA). There was a significant difference between PAA regressions between high school FB and GS ($p<.001$, ANOVA). To demonstrate the difference in scale, the dashed lines in (a) are the same as in (b), and the dashed lines in (c) are the same as in (d).	44
2.4	Total number of HAEs per season per FB player versus the median number of HAEs per contact session (CS). The plots have the players grouped by level of play as follows: (a) all players (b) V (c) JV-V (d) JV (e) FR (f) MS. The dashed lines on these plots are the same as those used in Fig. 2.5 to demonstrate the differences in scale. There is a significant difference in the slopes between V and MS ($p=.001$; KW), JV-V and MS ($p<.001$; KW), and JV and MS ($p<.001$; KW). The filled data point in (a) and (f) indicates a player who accumulated 40% or more of the HAEs for the season in a single session and was not included in the regression analysis.	45
2.5	Total number of HAEs per season per GS player versus the median number of HAEs per contact session (CS). The plots have the players grouped by level as follows: (a) all players (b) V (c) JV-V (d) JV. The dashed lines on the plots are the same as the lines shown in Fig. 2.4 to demonstrate the differences in scale. There was a statistical difference between JV and JV-V ($p=.014$; ANOVA) and JV and V ($p=.048$; ANOVA).	46

3.1	The players on the offensive line began each play in a (a) 2-point, (b) 3-point, or (c) 4-point stance. A 2-point stance was considered the “up” stance and a 3-point or 4-point stance was considered a “down” stance.	52
3.2	HAE distribution by position (DB, DL, LB, OL, TE, RB, WR, QB/K/P) for all three practice sessions.	54
3.3	HAE distribution by position (DB, DL, LB, OL, TE, RB, WR, QB/K/P for the exhibition game.	54
3.4	Comparison of the average number of play-related HAEs (exceeding 20 g) observed across all monitored players on the field during plays intended to be passing vs. running.	55
3.5	Comparison of the rate that OL and TEs sustain impacts separated by play type (pass vs. run) and stance (up vs. down).	55
4.1	Histogram of the PLA for all hits sustained in the games. Offensive linemen had a significantly different distribution (indicated by *) than: DB, LB, RB, WR, Skill.	65
4.2	Hits sustained on each play by play type. Run plays had statistically more hits per play than pass (p-value < 0.001) and punt plays (p-value = 0.001).	66
4.3	HAE rate of the players on the offensive line. The HAE rates for run down and run up were both statistically greater than pass down (p-value < 0.001 and p-value = 0.001, respectively) and pass up (p-value = 0.001 and p-value = 0.004, respectively).	67
4.4	HAE rate for players on the offensive line separated by skill level. For (a) higher skill level, both pass up and pass down stances had significantly lower HAE rates compared to run up (p-value = 0.001 and p-value = 0.002, respectively) and run down (p-value < 0.001 and p-value = 0.001, respectively). For (b) lower skill, pass down had a significantly lower HAE rate than pass up (p-value < 0.001) and run up (p-value < 0.001). Lower skill players also had a significantly higher HAE rate when up compared to down (p-value = 0.005).	68
5.1	Ellipsoid representations of changes in eigenvalues such that a) FA+/MD+, b) FA-/MD+, c) FA+/MD-, and d) FA-/MD-. The direction of the arrows indicates the change in the eigenvalue with respect to the original eigenvalues [174]. . . .	75
5.2	Football players have a significantly higher percentage of voxels in each of the categories compared to controls indicating football athletes are different from controls in pre-season.	80
5.3	Percentage of control and football athletes’ voxels that are considered significantly different in either difference in FA or difference in MD at post-season sorted into the four different groups compared to the difference in controls (retest-test). . .	81

5.4	Football players have a significantly higher percentage of voxels in each of the categories compared to controls indicating football athletes are different from controls in post-season.	82
5.5	Relative ROI change factor maps in the coronal, sagittal and transverse planes for a) FA+/MD+, b) FA-/MD+, c) FA+/MD, and d) FA-/MD- for pre-season and post-season values compared to control test values. Shade of the color indicates the median factor by which football athletes have more voxels in the ROI/obtained white matter intersection that fell into the respective group than control groups. Note that the darkest shades (width = 3) represent a range twice that of the other shades (width = 1.5).	84
5.6	Results from a Monte Carlo Simulation of eigenvalues to quantify the effect of noise on FA and MD sorted values. The simulation reveals a similar trend seen in both controls and football athletes with opposing changes in FA and MD occurring more frequently than concurrent changes.	88
6.1	When HAE PTA is analyzed by a) position (MW, $p = 0.992$), b) possession (MW, $p = 0.232$), or c) mechanism (tackle or ruck; MW, $p = 0.391$), there are no differences between the different groups.	94
6.2	Differences in the PTA of a HAE when considering possession and cause of the HAE (KW, $p = 0.031$). There was a significant difference between a defensive and offensive ruck (MW, $p = 0.008$).	95
7.1	Schematic of the circuit and its components. The voltage above the strain gauge was fed to a multiplexer to iterate through multiple inputs. That voltage was then fed into one input of the op amp and the other op amp input was the second half of the Wheatstone bridge. The configuration of the op amp magnified the difference between the voltage difference at the inputs before sending the data to the development board. Abbreviation and values can be found in Tables 7.1 and 7.2.	100
7.2	Image of the HBK rosette. The three strain gauges are stacked where the A and C strain gauges are orthogonal to each other and the B strain gauge is angled half way so that it is offset 45° from both axes (necessary values found in Table 7.1).	101
7.3	Schematic for how a differential op amp works.	103
7.4	Both boards completely wired up for data collection.	104
7.5	The theoretical signal used to time sync the strain gauge and hammer data. . .	104
7.6	An example of how to use the pulse wave to sync the parent board and child board signals. Starting with the (a) raw pulse waves, the pulses were then (b) pre-processed to remove samples collected by the child board before the parent board is turned and then, (c) the delay between the two signals is found and removed to align the pulses.	105

7.7	The rosette strain gauge adhered to the bending test sample.	106
7.8	The four point bending test (a) set up and (b) free body diagram. The rosettes were adhered to the aluminum sample and placed at approximately the middle of the sample.	108
7.9	Strain gauge rosette location on the Riddell Speedflex.	111
7.10	H3H testing set up consisted of: the instrumented helmet on the H3H (left), modal hammer (on top of yellow foam), both wired boards (in front of yellow foam), DAQ (right of the boards), laptop to control the boards, and workstation running LabVIEW (right) to collect hammer and accelerometer data.	112
7.11	The (a) principal strains and (b) percent error from a four point bending test to evaluate the strain gauge circuit, data alignment method, and calculations. . . .	115
7.12	The unfiltered signal from a single rosette fixed to the Speedflex hinge.	116
7.13	A single rosette tested on the H3H set-up indicated the values of components in the circuit were correctly assigned.	116
7.14	Boxplot for (a) rosette 4 and (b) rosette 10. Rosette 4 was located on the left side of the helmet at the front and rosette 10 was located on the left side of the helmet at the back.	117
7.15	The (a) mean effective equivalent strain and (b) mean normalized effective equivalent strain for each rosette by hit location. This demonstrated the advantage to normalizing each rosette by it's own value. Standard deviation bars were included for the (c) mean effective equivalent strain and (d) mean normalized effective equivalent strain for each rosette by hit location to determine which rosettes should represent each hit location.	119
7.16	Multiple linear regression for (a) front, (b) right, (c) back, and (d) left classified hits and the peak force of the hit.	121
7.17	Multiple linear regression for (a) front, (b) right, (c) back, and (d) left classified hits and the impulse of the hit.	122

LIST OF SYMBOLS

λ	eigenvalue
g	acceleration due to gravity (9.81 m/s ²)
Ω	ohm
$k\Omega$	kilohm
k	gauge factor
q	transverse sensitivity
α_i	temperature coefficient for material i
$\Delta \bullet$	change in \bullet
ϵ	strain
γ	shear strain
ν	Poisson's Ratio
σ	stress
τ	shear stress

ABBREVIATIONS

CTE	Chronic Traumatic Encephalopathy
TBI	Traumatic Brain Injury
HAE	Head Acceleration Event
MRI	Magnetic Resonance Image\Imaging
PLA	Peak Linear Acceleration
PTA	Peak Translational Acceleration
PAA	Peak Angular Acceleration
PRA	Peak Rotational Acceleration
rad	Radian
DB	Defensive Back
DL	Defensive Lineman\Linemen
LB	Linebacker
OL	Offensive Lineman\Linemen
TE	Tight End
RB	Running Back
WR	Wide Receiver
QB	Quarterback
K	Kicker
P	Punter
DTI	Diffusion Tensor Imaging
MRS	Magnetic Resonance Spectroscopy
FA	Fractional Anisotropy
MD	Mean Diffusivity
R	Resistance
V	Voltage
EQ	Equivalent
m	Meter(s)
mm	Millimeter(s)

s	Second(s)
lbf	Pound Force

ABSTRACT

Since the discovery of chronic traumatic encephalopathy (CTE) in retired professional football players, the long-term neurological safety of these athletes has been called into question. Studies revealed that those who play football are at higher risk for developing neurological deficits such as Parkinson's and Alzheimer's diseases. It has also been observed that participation in contact sports can result in neurological changes detectable with magnetic resonance imaging (MRI) that do not present with any easily observable clinical symptoms. Changes in brain chemistry, structure, and blood flow have been observed over the course of a season of contact sports. These changes are thought to be caused by the repetitive head acceleration events (HAEs) sustained by contact sport athletes, with the magnitude and number of HAEs correlating with some changes. This dissertation aims to characterize and reduce the HAEs sustained by contact sport athletes with a specific focus on football players.

Studies of middle school and high school football players revealed that there are likely offsetting effects that result in similar HAEs between the two groups. As one plays at higher levels of play with typically bigger, stronger, faster athletes that should result in higher magnitude HAEs, there is likely an improvement in tackling technique used at higher levels that make it so there are similar HAEs among different levels of play. Examining middle school football and high school football and girls' soccer athletes indicate that players that play on two teams (i.e. a player that plays both Varsity and Junior Varsity) may be at an increased risk for neurological changes due to over-exposure. It was revealed when studying post-collegiate football the up stance offensive linemen may help reduce the frequency of HAEs compared to the down stance. However, the skill of the offensive lineman needs to be accounted for to determine if it is beneficial for players to start in this stance.

Repetitive HAEs (rHAEs), whether due to body or direct head impacts arising from participation in contact sports, are correlated with alterations in white matter health. Fractional anisotropy (FA) and mean diffusivity (MD), two metrics used to assess white matter structural integrity, typically change in opposite directions (one increases while the other decreases) after brain injury. This study investigated the manner in which participation in

American football affects the percentage of white matter exhibiting the four possible change combinations: increased FA, increased MD; decreased FA, increased MD; increased FA, decreased MD; decreased FA, decreased MD. Diffusion tensor imaging data of 61 high school football and 15 non-contact athletes were analyzed. After a season of participation, football athletes exhibited a significantly greater percentage of deviant voxels in each of the four categories than were observed from test-retest of non-contact athletes. Even prior to a season of participation, football athletes exhibited significantly more voxels in each of the categories, relative to controls. Of particular concern is that voxels exhibiting jointly decreased FA and MD—a change typically associated with cell death—were observed at a significantly higher rate within football athletes than non-contact athletes. This finding suggests that rHAEs may increase the incidence of cell death, and argues for the greater adoption of methods aimed at reducing mechanical loading on the brain from rHAEs, both through reduction of the number of HAEs, and development of better protective equipment.

Rugby is a sport that is very similar to football in terms of physicality and overall objective, but there are marked differences in protective equipment and style of play. These differences in protective equipment result in different tackling rules and styles between the two sports that may influence the effect repetitive HAEs can have on neurological health. Therefore, the HAEs experienced over the course of the season by New Zealand collegiate (ages 16+) rugby athletes were characterized. The number of HAEs were compared by position (forward vs. backs) and the peak translation acceleration (PTA) of the HAE was analyzed by position, possession (offense vs. defense), and cause of HAE (tackle vs. ruck). Forwards (although not significantly) tended to sustain more HAEs than backs, but there were no differences in the magnitude of the HAEs by any of the types of comparisons. However, when considering possession and type of HAE simultaneously, it was found that HAEs in a defensive ruck are more severe than those sustained in an offensive ruck. This could be a potential place to work on player technique to reduce the PTA during these situations.

There are numerous studies that have utilized accelerometers to quantify head motion during a contact event, but a current gap in the field is quantification of the impact force. In order to capture high force events, an instrumented helmet using strain was built to capture

this data. Strain gauges were adhered to the inside of a Riddell Speedflex helmet shell and then mounted onto a Hybrid III Headform for testing. The helmet was hit at four different locations (front, right, back, and left) and at different impulse ranges (2-5 Ns, 5-8 Ns, 8-11 Ns, and 11+ Ns). The strain gauges were able to classify the location of the hit with about 95% accuracy and were correlated the impact peak force and impulse. This suggests that it is possible to build an instrumented helmet to be worn by a football player during collision events to capture real impact force and location data.

1. INTRODUCTION

1.1 Motivation

A traumatic brain injury, or TBI, occurs when an external force causes a change in brain pathology or function [1]. Sports are a common place for TBI to occur, with 1.6-3.8 million sports-related TBIs each year in the United States [2]–[4]. This estimate is most likely an underestimation of the actual number of sports-related TBIs due to the underreporting of concussions, a type of mild TBI, and concussion symptoms [5], [6]. It was projected that in 2010, TBI would result in total lifetime costs of \$76.5 billion [7]. This means that TBI is not just a short-term injury that is resolved over several weeks or months, but may have lasting effects and in certain cases, the symptoms do not present themselves until years after the initial injury.

Chronic traumatic encephalopathy (CTE) is one such type of neurodegenerative disease caused by TBI. Symptoms of CTE include reduced cognitive function, emotional volatility, and suicidal tendencies [8]. It was originally discovered in pugilists in the 1920’s and was thought to be the result of the blows to the head sustained by these athletes [9], [10]. In the 2000’s, the first case of CTE in a retired professional American football player was reported [11] and CTE has since been confirmed in over 100 retired professional players, as well as collegiate and high school football players [12]–[14]. Since it’s discovery in football players, research has indicated the development of CTE does not correlate with a history of diagnosed concussion, but does correlate with a history of repetitive head trauma, suggesting that the continuous exposure to head impacts is the critical mechanism contributing to CTE [15]–[18].

With the discovery of CTE in football players and its correlation to a history of repetitive head trauma, the long-term safety of these players has come into question. Of specific concern is the fact that younger players at the high school level are also sustaining repetitive head trauma, which may contribute to the development of CTE later in life. Researchers began to study these players to determine if there is any indication of neurological changes at this point in their athletic career. Studies of high school football players have revealed there exists a group of players that sustain asymptomatic neurological changes, meaning these players do not display any symptoms, but through magnetic resonance imaging (MRI),

demonstrate significant differences from their preseason baseline scans or from the control group consisting of age-matched non-contact athletes that, in some cases, are comparable to players who have been diagnosed with a concussion [19]–[24]. Since these players do not display any outward symptoms, they are not removed from sessions and continue to sustain repetitive head traumas which can further exacerbate their neurological changes. Specifically, it is believed that the critical aspect of these repetitive head traumas that cause neurological changes is the acceleration of the head during the contact event.

There are several reasons that the acceleration is thought to be the cause of the neurological changes. By Newton’s second law, $\Sigma \mathbf{F}_{CoM} = m_{head} \mathbf{a}_{CoM}$, if the acceleration of the center of mass (CoM) is known, then the forces at the CoM can be estimated and translated to stress and strain on the brain tissue. Also, the velocity of the system can be determined from the acceleration and can approximate the kinetic energy (KE) transferred to the head by $KE = \frac{1}{2}mv^2$. Stress, strain, and energy transfer may be the mechanisms that actually cause changes at the cell and tissue level [25], [26].

The long-term neurological changes seen in contact sport athletes appears similar to fatigue failure of engineering materials. Fatigue failure is when a material is cyclically loaded over a period of time and eventually fails, not due to a single catastrophic event, but because of its continuous use. To predict when this failure will occur in engineering materials, there are SN-curves which relate the applied stress to the number of cycles to failure (Fig. 1.1). However, for real world applications, it is highly unlikely that a material will be loaded at a single stress level. Miner’s rule (Equation 1.1) is a way to determine the life of a material subjected to varying loads [27]. Miner’s rule takes the number of cycles sustained at a given stress level (n_{S_i}) and divides it by the number of cycles to failure for that stress level (N_{S_i}), then adds all of those fractions together for all of the different stress loads experienced. If the sum is greater than one, then the material will fail.

$$\sum_{i=1}^k \frac{n_{S_i}}{N_{S_i}} = c \quad (1.1)$$

Fatigue analysis is applicable to engineering materials, but is not yet widely applied to biological materials. However, based on the delayed symptoms seen with repetitive head

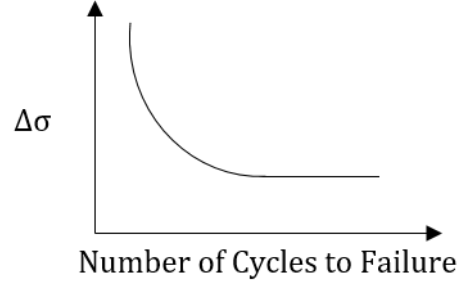


Figure 1.1. Example of an SN-curve.

trauma, there might be a similar “SN-curve” for this situation where instead of stress being the load, it may be acceleration of the head and instead of number of cycles to failure, it may be number of cycles to changes or symptoms (Fig. 1.2). It is likely that there will be a distribution of hits will be sustained during the season, so a similar approach to Miner’s rule may also have to be implemented to fully understand the complexity of changes in brain health due to non-uniform, repetitive head trauma.

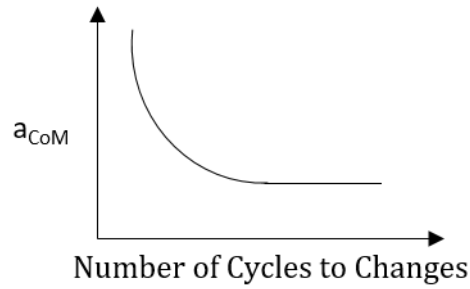


Figure 1.2. A modified SN-curve for how repetitive impacts sustained in contact sports may cause neurological changes in these athletes.

1.2 Objectives

Many studies have been performed to monitor the neurological changes due to participation in American football and other contact sports, but there is still no true understanding of what part of the repetitive head impacts causes these changes to occur. Therefore, investigating the accelerations of the head and impact characteristics during contact events and

better understanding what component of the event leads to neurological changes is a major objective of this study.

Although it is not fully understood what part of the impacts cause neurological changes, the number of impacts is theorized to play at least a partial role in the severity of the changes, with an increase in the number of sustained hits leading to more drastic changes. With this information, another major objective of this study is to determine if there are certain technique changes that may decrease the number of impacts sustained by players, therefore reducing their overall risk for neurological changes.

This work first examines how head acceleration events (HAEs) differ by sport (football vs. girls' soccer) and levels of play from middle school to varsity high school to provide a better understanding of how these factors influence HAEs. Next, simple changes in starting stance of players on the offensive line are studied to determine if this intervention reduces the number of HAEs sustained by these players. An extension of a previous analysis on white matter changes in football athletes investigates simultaneous changes in fractional anisotropy and mean diffusivity to better understand physiological changes in the white matter. The HAEs sustained in rugby are then examined to see how this contact sport compares to football. And finally, the last part of this work details a design about an instrumented football helmet to capture impact location and force data, with the idea of deploying it during a practice session to gather in vivo impact data. Together, these studies aim to find ways to improve player safety for contact sport athletes.

2. LEVEL OF PLAY IN FOOTBALL AND GIRLS' SOCCER

This is a non-final version of an article published in final form in the Journal of Engineering in Medicine: T. Lee, R. Lycke, J. Auger, J. Music, M. Dziekan, S. Newman, T. Talavage, L. Levenenz, and E. Nauman, “Head acceleration event metrics in youth contact sports more dependent on sport than level of play,” *Proceedings of the Institution of Mechanical Engineers, Part H: Journal of Engineering in Medicine* (vol. 235, no. 2) pp. 208–221 Copyright ©2021 (SAGE Publications). DOI: 10.1177/0954411920970812. https://journals.sagepub.com/doi/10.1177/0954411920970812?url_ver=Z39.88-2003&rfr_id=ori:rid:crossref.org&rfr_dat=cr_pub%20%20pubmed [28]

2.1 Introduction

In the United States, approximately 1.6-3.8 million traumatic brain injuries (TBIs) occur each year due to sports-related activities [2]–[4]. In reality, this number is considerably higher due to documented underreporting of symptoms [5], [6]. Traditionally among high school contact sports, football exhibits the highest rate of concussions, a type of TBI, followed by women’s soccer [29]–[32]. Every year, tackle football and women’s soccer have about 1 million and 400,000 high school participants, respectively, making them some of the most popular high school sports for student athletes, and subsequently putting a greater population at risk for sustaining a sports-related TBI [33].

There has been growing concern regarding the long-term effects playing football can have on a player’s cognitive health [34]–[36]. The problem was first identified and documented in football players by Omalu et al. when a series of ex-NFL players’ autopsies revealed they had a neurodegenerative disease known as chronic traumatic encephalopathy (CTE) [11]–[13], previously observed only in retired pugilists [9], [10]. Chronic traumatic encephalopathy has since been confirmed postmortem in more than 120 retired professional, 55 collegiate, and 10 high school football players [14], [37]–[41]. The development of CTE has no correlation with history of diagnosed concussions, but does correlate with a history of repetitive brain trauma, suggesting that continuous exposure to impacts that do not cause a diagnosed concussion may be the critical aspect contributing to CTE [15]–[18].

These findings are consistent with the results of studies by Talavage and colleagues, who determined that over the course of a season, repetitive head trauma can cause high school contact sport athletes to significantly deviate from baseline neuroimaging measures or significantly differ from high school non-contact athletes [2], [19]–[21], [26], [42]–[49]. These short-term changes may result in long-term consequences. In a retrospective study that included 43 football players from the Mayo Clinic brain bank, Bieniek and colleagues found there is approximately a 30% chance of developing CTE for males that played up to high school football, and a 50% chance if they played up to college [41]. Although CTE has mainly been studied in professional athletes, these data indicate all those who participate in football in their youth may be at risk for developing CTE.

Similarly, it has been observed that participation in soccer and repeated heading of a soccer ball can also produce neurological alterations [50]–[56]. While female soccer players traditionally have the highest rate of concussion after football, few studies have been conducted on this group of athletes to adequately characterize how heading and other head acceleration events (HAEs) in soccer contribute to the neurological deficits [22], [29]–[32], [57]–[59].

To more accurately determine those at risk for short- and long-term neurological changes, it must first be determined how HAE exposure depends on sport, age, or skill level. Consequently, this study was designed to examine the hypothesis that HAEs are dependent on sport and level of play of the athlete. To this end, this study examined differences in HAE characteristics at different competition levels – middle school (MS), high school freshman (FR), high school junior varsity (JV), high school junior varsity-varsity (JV-V), and high school varsity (V) – for football and girls’ soccer. High school athletes are assigned to one of these levels based on their skill level, which better reflects a player’s size, speed, and/or technical skill relative to simply age or grade. HAE characteristics such as the distribution of HAEs by peak translational acceleration (PTA), number of HAEs per session (practice/game), number of HAEs per season, relation of the number of HAEs per season to cumulative peak acceleration measurements, and number and percent of sessions that resulted in sustaining at least one HAE were analyzed to examine the differences in frequency of HAEs between the groups and to determine if the number of HAEs can be used to effec-

tively and accurately determine the cumulative head acceleration exposure for each group. This relationship between number and cumulative acceleration measures could indicate that the number of HAEs is a simple measurement that could be controlled by teams and coaches to reduce the cumulative acceleration exposure for an athlete during a season of play. These metrics were selected since there is a relationship between these HAE metrics and functional neurological changes that have been measured using magnetic resonance imaging (MRI) [2], [19], [20], [22], [24], [48], [49], [59]–[63].

2.2 Methods

2.2.1 Participants

All research methods involving human participants were approved by Purdue’s Institutional Review Board prior to beginning the study. For participants at least 18 years of age, written informed participant consent was obtained. For participants under the age of 18, parental consent and participant assent were obtained.

This study consists of 123 football (FB) athletes, 107 from three high schools (ages 14-18, 106 male and 1 female) and 16 from one middle school (MS; ages 12-14, all male), observed for one season. Data from high school girls’ soccer (GS) players were collected from two schools over two consecutive seasons (season 1 n=31; season 2 n=34), resulting in a total of 65 player observations (ages 14-18). A partial season is defined as a player who missed three or more consecutive weeks of play (FB n=12: 1 female, 11 male; GS n=4).

Within each sport, the high school athletes were divided into levels of play based on the amount of playing time received at the different levels of play (Table 2.1). Several players spent substantial time playing on both V and JV, and typically played more than those who only played at one level. Since these players cannot be solely specified as only a JV or V player, they were labeled as JV-V players and it was considered its own level of play.

2.2.2 Data Collection

Head acceleration events (HAEs) were monitored using the xPatch (X2 Biosystems; Seattle, WA; Figure 2.1). Each practice and each game was considered a separate “session”. Sen-

Table 2.1. Number of players in each group with full seasons of data (FSD) and partial seasons of data (PSD). Also listed are the ranges of the maximum number of monitored sessions for FSD players at each level of play.

Sport	Level of Play	FSD	PSD	Range of maximum number of sessions for each level
Football	MS	16	0	32-33
Football	FR	11	0	40-42
Football	JV	28	5	49-62
Football	JV-V	8	2	49-62
Football	V	48	5	44-54
Girls' Soccer	JV	11	2	45-50
Girls' Soccer	JV-V	15	1	64-74
Girls' Soccer	V	35	1	56-72

sors were placed on FB players if the session required full pads and were used in all sessions for GS. An xPatch sensor was affixed behind a player's right ear with an adhesive patch after cleaning the area with rubbing alcohol [58], [64]. Each head impact was recorded as a separate "event" on the sensor when the PTA projected on any axis was greater than 10 g. Data were downloaded using the Head Impact Monitoring System software (X2 Biosystems; Seattle, WA) after sessions.

2.2.3 Data Analysis

For the purposes of this study, the clack recognition algorithm (X2 Biosystems; Seattle, WA) was not used so as to include events caused by different mechanisms [58], [64]. This study analyzed all substantial head accelerations, whether they are the result of direct head impacts or whiplash events (caused by impacts to the body), noting that the latter are no less deleterious to brain health [65]–[73]. Data from the sensors were processed using a custom MATLAB (MathWorks; Natick, MA) program to isolate events that occurred within the valid time window of each session and registered a PTA greater than or equal to 20 g. While the sensors collected low acceleration events (10-20 g), these were excluded from the analysis since they are typically caused by non-impact (sharp changes of direction, kicking the ball, etc.) mechanisms [58]. Data were also analyzed to remove sessions when sensors

exhibited ringing or other forms of errors (see Appendix A for details). Following HAE validation, data for players with full seasons were adjusted for times where a participant was playing without a sensor (e.g. the sensor had fallen off) and for sessions removed by outlier analysis. Data interpolated to account for missing collection time are referred to as repair data and were added to the validated raw data to obtain a more complete account of the overall exposure (number of HAEs, cumulative PTA, cumulative peak angular acceleration [PAA]; see Appendix A for details).

Data were analyzed for full-season athletes on a per player basis, and the following impact metrics were established: median number of HAEs per contact session (a session where at least one HAE occurred), total number of HAEs per season, cumulative PTA per season, cumulative PAA per season, number of contact sessions, and percent of contact sessions (see Appendix B for details). Head acceleration events without repair data for full and partial season players were used to generate the HAE PTA magnitude histogram (Figure 2.2). Regressions for each level of play were used to determine the relationship between the following metrics: cumulative PTA per season and total number of HAEs, cumulative PAA per season and total number of HAEs, and total number of HAEs and median number of HAEs per contact session (see Appendix B for details).

2.2.4 Statistical Analysis

Statistical analyses were performed using SAS 9.4 (SAS Institute; Cary, NC) to determine if the metrics were significant ($p < 0.05$) as a function of the level of play. The χ^2 test was used to compare histograms. If the overall χ^2 test indicated statistical significance between the levels, then pairwise χ^2 tests with a Bonferroni correction were used to determine which levels were different. Analysis of variance (ANOVA) was used if the normality (Shapiro-Wilk) and constant variance (Brown and Forsythe) assumptions were met, and the Kruskal-Wallis (KW) test was used if they were not. If ANOVA indicated a significant difference between levels, Tukey's post hoc test was used to determine which levels were different. If the KW test was used, Dunn's post hoc test was used to compare differences between levels [74]. These methods were used to test the median number of HAEs per contact session, total HAEs per season, cumulative PTA/PAA per season, number of contact sessions, and percent of

contact sessions. Similar tests were conducted to compare the regressions. The slope was computed for each data point and then slopes were grouped by level of play. Comparisons were performed within each sport to analyze differences between levels. High school FB levels were grouped to compare against grouped GS levels for a between-sport/sex comparison.

2.3 Results

2.3.1 Group-Based Analysis

Over the course of a season, the 95 full-season male high school FB players collectively accounted for 29,978 HAEs (15,948 practice; 14,030 game) and the 16 MS players collectively accounted for 4,118 HAEs (2,702 practice; 1,416 game). The number of HAEs in a season for a single FB player ranged from 23 to 1,352. Of the 29,978 HAEs, V, JV-V, JV, and FR players accounted for 17,704 (9,516 practice; 8,188 game), 3,100 (1,570 practice; 1,530 game), 6,437 (3,438 practice; 2,999 game), and 2,737 (1,424 practice; 1,313 game) HAEs, respectively.

The 61 full-season GS players sustained 8,414 HAEs (5,192 practice; 3,222 game) with V players accounting for 4,991 HAEs (2,925 practice; 2,066 game), JV-V taking 2,502 of the HAEs (1,662 practice; 840 game), and JV players accounting for 921 HAEs (605 practice; 316 game). The number of HAEs in a season for a single GS player ranged from 22 to 411.

The HAE PTA magnitude distribution was examined for each sport and level of play. For FB, there was no significant difference between levels of play ($p=.190$). For GS, V was significantly different JV ($p=.001$) and JV-V ($p=.006$). There was a significant difference between the high school FB distribution and the GS distribution ($p=.001$; Figure 2.2).

2.3.2 Player-Based Analysis

All other results were calculated on a per player basis (i.e. reported numbers reflect medians and averages for a single player in the indicated group). The MS level of play had a significantly greater median number of HAEs per contact session than JV for FB ($p=.018$; KW; Table 2.2), but there was no statistical difference between the levels of play for GS ($p=.675$; KW; Table 2.2). However, there was a statistical difference in the median number of

HAEs per contact session based on sport ($p<.001$; KW), with GS recording fewer HAEs per contact session than high school FB, regardless of level of play.

There was no significant difference between the levels of play for total HAEs ($p=.133$; KW), cumulative PTA ($p=.104$; KW), or cumulative PAA ($p=.193$; KW) for FB (Table 2.2). For GS, the JV-V level exhibited significantly more total HAEs ($p=.041$; KW) and greater cumulative PAA ($p=.031$; KW) than the JV level (Table 2.2).

High school FB players registered significantly greater season totals for number of HAEs (median: 262), cumulative PTA (median: 10.0×10^3 g), and cumulative PAA (median: 16.8×10^5 rad/s²) than GS players (respective medians: 107, 4.05×10^3 g, 7.55×10^5 rad/s²; $p<0.001$; KW).

The number of contact sessions in a season were compared for each of the different levels in each sport (Table 2.3). For FB, MS had fewer total contact sessions than JV ($p<.001$; KW), JV-V ($p<.001$; KW), and V ($p=.009$; KW), FR had less than JV ($p=.019$; KW) and JV-V ($p<.001$; KW), and JV-V had more than V ($p=.033$; KW). When the number of contact sessions were normalized by the total number of sessions in a season, there was only a significant difference between MS and JV, with MS having a significantly higher percentage of contact sessions in a season ($p=.032$; KW).

For GS, JV had significantly fewer contact sessions than JV-V and V ($p=.001$ and $p=.003$, respectively; ANOVA), but no levels differed regarding percent of contact sessions ($p=.060$; ANOVA). High school FB had statistically more contact sessions in a season (35.2; $p=.039$, KW) and a higher percentage of contact sessions (77.4%; $p<.001$, KW) than GS (31.5 and 56.4%, respectively).

There was no statistical difference between any of the regressions for the different levels of play (Figure 2.3a, 2.3b) when examining the cumulative PTA for a season versus the total number of HAEs in a season for FB ($p=.367$; ANOVA) or GS ($p=.615$; KW), nor was there a significant difference between high school FB and GS ($p=.702$; KW). When the levels are combined for each sport, the total number of HAEs in a season serves as a good predictor (FB $R^2 = 0.97$; GS $R^2 = 0.96$) of the cumulative PTA.

Similarly for PAA, there was no statistical difference between any of the levels of play in terms of the regression trends for either sport (FB $p=.933$, KW; GS $p=.146$, ANOVA;

Figure 2.3c,2.3d). The slope of the regression line for GS is significantly steeper than the one for high school FB ($p<.001$; ANOVA).

In comparing the median number of HAEs in a session to the total number of HAEs sustained during an entire FB season, some slopes differed between levels (Figure 2.4). Middle school was different from JV ($p<.001$; KW), JV-V ($p<.001$; KW) and V ($p=.001$; KW) levels. Since the JV-V players played in both JV and V events, they had the greatest number of contact sessions (45.4 ± 6.63) and this level of play has the steepest slope relating median number of HAEs in a session to the total number of HAEs in a season (Figure 2.4c).

For GS, JV compared to JV-V and V showed significantly different regressions for the total HAEs in a season versus median HAEs in a session ($p=.014$ and $p=.048$, respectively; ANOVA; Figure 2.5). Similar to FB, the JV-V level of play in GS exhibited the steepest slope (Figure 2.5c) as this level participated in the greatest number of contact events (36.1 ± 11.0).

2.4 Discussion and Implications

The purpose of this study was to determine whether HAE metrics are dependent on level of play and/or sport. Since FB and GS players usually exhibit the highest rates of diagnosed concussions, characterizing all HAEs is an important step in understanding how HAEs contribute to TBI in athletes [29]–[32]. While differences observed between sports could reflect contributions from both sport and sex, the findings regarding level of play within a given sport have important implications for potential interventions.

2.4.1 Football vs. Girls' Soccer

The hypothesis that HAE characteristics are dependent upon sport was not supported for certain metrics. Although football and soccer are vastly different in terms of rules, game play, and equipment, high school FB and GS players exhibit similar PTA characteristics for individual HAEs (Figure 2.3a,2.3b). Since this is the only aspect in which these two groups of athletes are similar, the player average PTA per HAE may indicate that the average translational biomechanical reaction to direct or body impacts that cause HAEs is similar

between high school males and females. The mechanisms by which HAEs arise differ in football and soccer, but a more thorough analysis of the biomechanics of the head and neck during these HAEs may lead to a better understanding of the factors responsible for the player average PTA per HAE to be similar between the two sports.

Differences in the way FB and GS players acquire HAEs result in differences for certain HAE metrics. In football, contact with another player, either through blocking or tackling, is a fundamental component of the game and is almost guaranteed to happen once per play for multiple positions. Even though heading is an important aspect of the game of soccer, it generally occurs less frequently than contact in football. This increased frequency is what leads to higher season totals (total number of HAEs, cumulative PTA/PAA) for FB players and the possibility of greater neurological alterations (Table 2.2). Interestingly, the observation that GS players have a greater player average PAA per HAE than high school FB players (Figure 2.3c,2.3d) suggests that HAEs from heading a ball in soccer, how a majority of HAEs in soccer occur, are fundamentally different in mechanics than HAEs from the tackling experienced in football. The greater average PAA per HAE for GS players may also be due to the lack of or minimal protective head gear worn by these athletes, while FB players wear helmets that reduce some of the rotational acceleration that would otherwise be experienced by the head [75].

It has been observed in literature that total HAEs, cumulative PTA, and cumulative PAA can represent the mechanical load on the brain and is indicated that cumulative exposure is important when determining whether neurological changes occur [2], [15], [19], [20], [22], [24], [26], [58]–[60], [76]. The cumulative PTA and PAA correlate strongly with the total HAEs ($R^2 \geq 0.94$), making total HAEs an accurate measure for predicting cumulative PTA and PAA for a season and only necessitate tracking the number of HAEs with a PTA over the threshold instead of having to record the PTA and PAA for each individual HAE. Therefore, a player's HAEs per contact session can serve as a fluid metric to predict total HAEs (and by extension cumulative PTA and PAA), such that monitoring HAEs on a session basis could allow for adjustment of a player's technique or participation in contact sessions during a season to proactively limit cumulative exposure. This relationship is valid for FB ($0.59 \leq R^2 \leq 0.92$), as

long as the level of play is known, but is not as reliable for GS ($0.58 \leq R^2 \leq 0.73$). This trend appears to reflect the difference in how FB and GS players accumulate HAEs.

2.4.2 Girls' Soccer Levels of Play

Girls' soccer demonstrated significant differences between levels of play among different HAE metrics. Junior varsity players may be at less risk of experiencing neurological changes than JV-V or V players. Players at the JV level, due to their lower skill level relative to JV-V and V players, are less likely to utilize headers to control the ball as noted by observations during data collection and trends reported by McCuen et al. (2015), resulting in substantially, but not always significantly, lower season totals (total number of HAEs, cumulative PTA/PAA), number of contact sessions, and percent of contact sessions [58]. Reducing the number of heading sessions in a season would help to reduce the season totals for the JV-V and V players.

2.4.3 Football Levels of Play

Relative to GS, FB was internally more consistent between levels of play for HAE metrics. Examining FB levels indicates MS players may be at the same or greater risk of developing neurological deficits compared to high school players. Even though MS players have a shorter season than the high school players, they still accumulated comparable season totals. Middle school teams typically have fewer players than high school teams, requiring players to play both offense and defense and likely leading to a greater accumulation of HAEs. This is especially concerning since it has been observed that the age at which a brain injury occurs can be a factor for the type and severity of short-term neurological problems and ones that develop later in life, with younger participants possibly developing more serious complications [16], [18], [77]–[81]. Teaching proper tackling technique to players should reduce the PTA and PAA for individual HAEs, overall HAE accumulation, and provide better protection from long-term consequences.

While increased playing time can explain the similarities between HAE totals for MS and high school FB players, the lack of significant difference between their individual HAE

magnitudes may be due to physical differences, primarily neck strength, between the groups [82]. It has been hypothesized that players under the age of 14 should not play tackle football because they are exposed to greater risk relative to older, more physically developed players who possess greater neck strength to better protect and brace themselves for tackles [83]. While MS players are physically smaller and unlikely to generate the same forces as high school players while tackling, their HAE data were comparable to the high school players, suggesting other biomechanical factors contribute to HAE characteristics. More MS teams should also be studied to determine if the trends extend to schools in different leagues.

The JV-V level is more at risk to be exposed to a higher frequency of HAEs, possibly making them more at risk for asymptomatic neurological changes. These players participated in the greatest number of contact sessions per season (Table 2.3) and although not statistically significant, these players also tended to have higher HAE season totals than other levels. The most concerning metric from the JV-V level was that they had the steepest slope ($y = 56.7x$) for correlating the season HAEs to the session HAEs (Figure 2.4c). These players are essentially playing on two teams and participate in more contact sessions than a player that is only active on a single level. Just like the MS players, the JV-V players are at a greater risk of overexposure due to increased playing time. Previously, neuroimaging (primarily MRI) has been used to quantify and monitor chemical, structural, and hemodynamic neurological changes in contact sport athletes due to repetitive HAEs [2], [19]–[22], [24], [48], [59]–[63], [84]. Such investigations have strongly suggested increased risk of neurological changes for overexposed players. If it is known a player is going to be playing in two games during a certain week, coaches and athletic trainers may consider making a practice session a non-contact session for the player to reduce the total number of HAEs the player will sustain that week.

To confirm that the results of this study are applicable to high school FB players in general, the teams in this study were compared to other teams analyzed in similar studies (Table 2.4) [2], [19], [60], [85]–[88]. This comparison demonstrates the MS team is experiencing HAEs similar to high school teams in general. If teams are registering more HAEs than the teams examined here at comparable level of play, it can be inferred those teams will experience increased asymptomatic changes in neurological function [2], [19]. This also pro-

vides evidence that sensors and data analysis in this study are consistent with other sensor systems.

2.4.4 Limitations

Use of the xPatch to monitor HAEs is a limitation of the study since it has been shown that this sensor typically exhibits PTA errors on the order of 20% for any given HAE, but an average error of approximately 5% which is sufficient for comparing PTA distributions and cumulative exposures [64], [89]. The sensor demonstrated PAA errors on the order of 50% for any given HAE and an average error of approximately 20%, which limits the comparison between FB and GS for average PAA per HAE [64], [89]. The error indicates the inaccuracy of the xPatch in terms of measuring PAA, which may be attributed to HAE location, cause of HAE, and relative velocity of approach, but the sensor is thought to be precise which would still allow for a comparison between the two groups. Also, the objective of this study was not to determine the HAEs that would induce a brain injury, but to measure all HAEs sustained. This study examined the frequency and peak translational and angular accelerations of HAEs sustained by two groups of athletes. Although HAE duration has been examined in relation to concussion, this study aimed to examine all HAEs and not just those associated with symptomatic head trauma [90]–[92]. Accounting for duration of the HAE may improve the fit between HAE metrics and neurological changes observed via MRI, but current research has been able to correlate HAE peak accelerations and frequency with observed changes [2], [19], [20], [22], [24], [48], [59]–[63].

All current sensor technology measures acceleration either external to the body (sensors imbedded in a helmet) or of part of the head (i.e., mastoid process, mouth) which does not explicitly measure the acceleration that is experienced by the brain since the brain will undergo relative displacement/deformation to the head/skull [93]–[96]. This relative displacement/deformation, which is also dependent on the location of the HAE [93], [96], will contribute to the true acceleration experienced by the brain; however, measuring the acceleration of the head is within the current capabilities of the sensors and is thought to be representative of the true acceleration experienced by the brain [94]. This study reports the frequency and magnitudes of head acceleration experienced at different levels of play of

FB and GS. These measures do not, in and of themselves, entirely quantify brain trauma, but they do serve as important metrics related to asymptomatic changes in brain health [2], [19], [20], [22], [24], [48], [59]–[63]. Future work examining the translational and angular acceleration profiles along with duration, location, and type of impact may improve the current understanding of HAEs in relation to brain health.

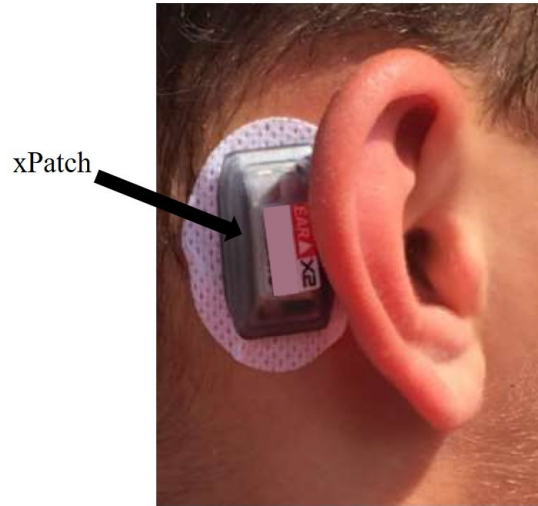
Another limitation of this study is the inability to determine if the difference between FB and GS is due to sport or sex since they are confounding factors. Collecting HAE data on boys’ soccer will help to distinguish how sport and sex individually contribute to the differences. However, the objective of this study was to examine two groups of athletes that traditionally have the highest rates of reported concussion and not determine the individual contributions of sport and sex to HAE characteristics. Players were also only designated by level of play, and although football HAE characteristics are also dependent upon position, some players in this study played multiple positions and would not have allowed for analysis by position [5], [19], [42], [85], [88], [97]–[99]. Designating players by level of play also caused unequal sample sizes for the different levels of play. This caused some of the levels of play to have small sample size which may bias or skew the results when comparing the levels of play.

2.5 Conclusion

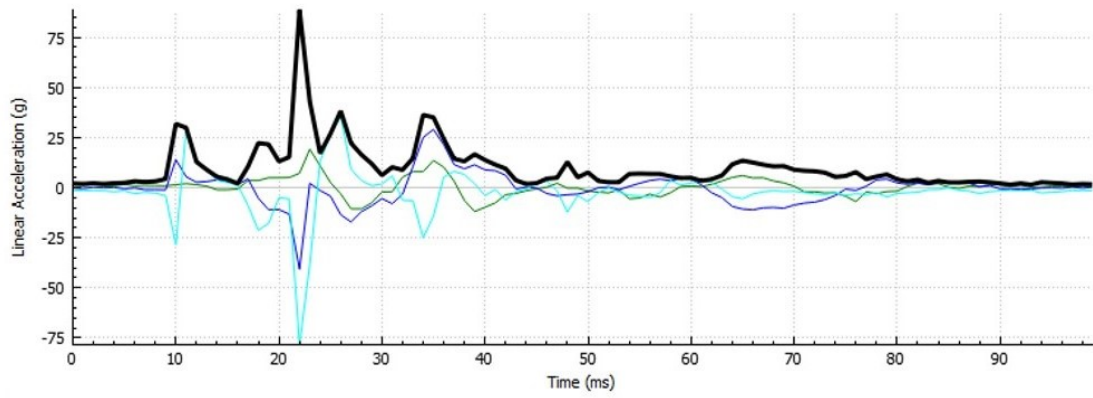
This study was designed to determine the dependency of HAEs on sports/sex (GS and FB) and levels of play to obtain a better understanding for how repetitive head traumas contribute to neurological deficits. There were significant differences between GS and FB. The differences in rules and game play readily account for FB players accumulating more HAEs than GS players, but the mechanisms by which the HAEs occur in the two groups of athletes and differences in protective equipment likely explain the differences in player average PAA per HAE for each group. Sport and sex are confounding factors in this study that are both likely to substantially contribute to the HAE metrics.

Analyzing the HAEs by level of play within each sport has revealed some concerning trends within each sport, specifically the trends seen at the JV-V level and FB MS level. For GS, JV-V players tend to have greater HAE metrics than JV players, presumably due

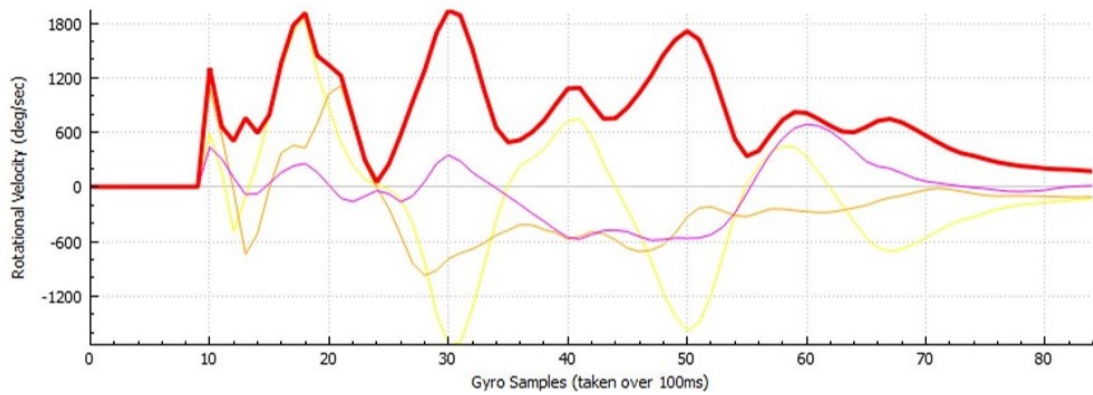
to the relative difference in skill level and increased playing time. For FB, the younger players at the MS level exhibit similar HAE characteristics to high school players but are not as developed, physically or neurologically. Reducing the number of HAEs athletes sustain during the season, be that by implementing additional rules and regulations or continuing to improve technique, will decrease the risk of changes in neurological health of contact sport athletes.



(a)



(b)



(c)

Figure 2.1. The xPatch sensor and an example of (a) placement on a player's head, (b) waveform of the translational acceleration, and (c) waveform of the angular velocity.

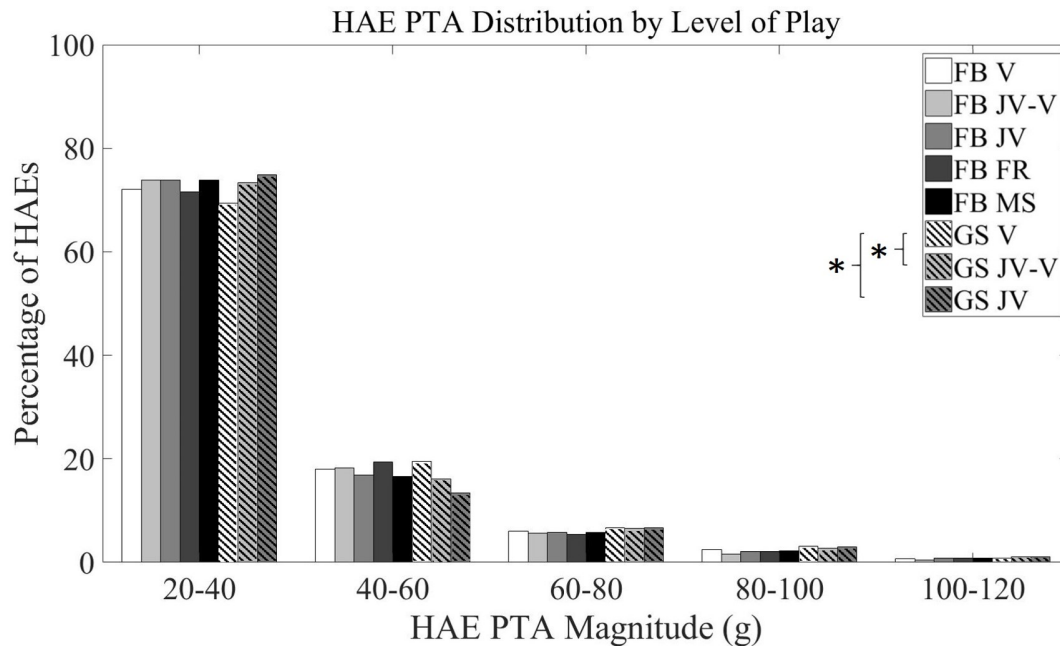


Figure 2.2. Normalized distribution of HAE PTA magnitudes by level of play. There was no statistical difference between FB levels of play ($p=.190$), and GS V differed from both GS JV ($p=.001$) and GS JV-V ($p=.006$) distributions. High school FB and GS distributions were significantly different from each other ($p=.001$). Less than 1% of HAEs occurred above 120 g for each level.

Table 2.2. Sport and level of play player medians of median HAEs per contact session, total HAEs, cumulative PTA, and cumulative PAA per season with the statistical difference noted in the column to the right of the metric of interest.

Group	n	Median Number of HAEs [†]	SG [‡]	Total Number of HAEs [†]	SG [‡]	Cumulative PTA ($\times 10^3$ g) [†]	SG [‡]	Cumulative PAA ($\times 10^5$ rad \cdot sec ⁻²) [†]	SG [‡]
FB MS	16	7.5 (4.5, 10)	A	229.5 (138.5, 322.5)	A	7.40 (4.85, 11.8)	A	13.7 (7.86, 20.0)	A
FB FR	11	5 (3, 7)	A,B	168 (138, 348)	A	6.71 (5.14, 12.0)	A	12.5 (7.47, 20.5)	A
FB JV	28	4 (3, 5)	B	224 (139.5, 287)	A	8.25 (4.90, 10.4)	A	14.6 (7.90, 17.8)	A
FB JV-V	8	5 (3.75, 8.5)	A,B	313.5 (236.5, 557.5)	A	10.5 (8.08, 19.4)	A	17.6 (12.2, 35.3)	A
FB V	48	5.5 (3.75, 10)	A,B	298 (169, 506)	A	11.8 (5.90, 18.9)	A	20.3 (8.99, 30.2)	A
GS JV	11	2 (2, 3)	E	66 (45, 107)	E	2.47 (1.64, 4.05)	E	4.59 (3.12, 7.02)	E
GS JV-V	15	2.5 (2, 4)	E	190 (67, 246)	F	7.75 (2.55, 8.10)	E	11.7 (5.46, 16.3)	F
GS V	35	2 (2, 4)	E	108 (69, 204)	E,F	4.18 (2.59, 7.61)	E	7.89 (5.15, 14.2)	E,F

[†]Each cell contains the median (1st quartile, 3rd quartile) for the metric.

[‡]Significance grouping (SG) rows with the same letter denote levels within the sport that are not significantly different ($p > .05$). A-D are used for FB and E-F are used for GS.

Table 2.3. Average number of contact sessions in a season and the percentage of sessions in a season that had contact for each sport and level with the statistical difference noted in the column to the right of the metric of interest.

Group	Average (standard deviation) Number of CS	SG[‡]	Average (standard deviation) Percent of Sessions Involving Contact	SG[‡]
FB MS	26.8 (2.67)	A	87.6 (6.88)	A
FB FR	27.5 (6.76)	A,B	76.4 (16.6)	A,B
FB JV	37.0 (9.38)	C,D	75.0 (16.3)	B
FB JV-V	45.4 (6.63)	C	87.1 (8.43)	A,B
FB V	34.2 (8.15)	B,D	77.4 (14.5)	A,B
GS JV	21.2 (6.06)	E	47.4 (13.4)	E
GS JV-V	36.1 (11.0)	F	62.7 (17.9)	E
GS V	32.8 (10.2)	F	56.5 (15.7)	E

[‡]Significance grouping (SG) rows with the same letter denote levels within the sport that are not significantly different ($p > .05$). A-D are used for FB and E-F are used for GS.

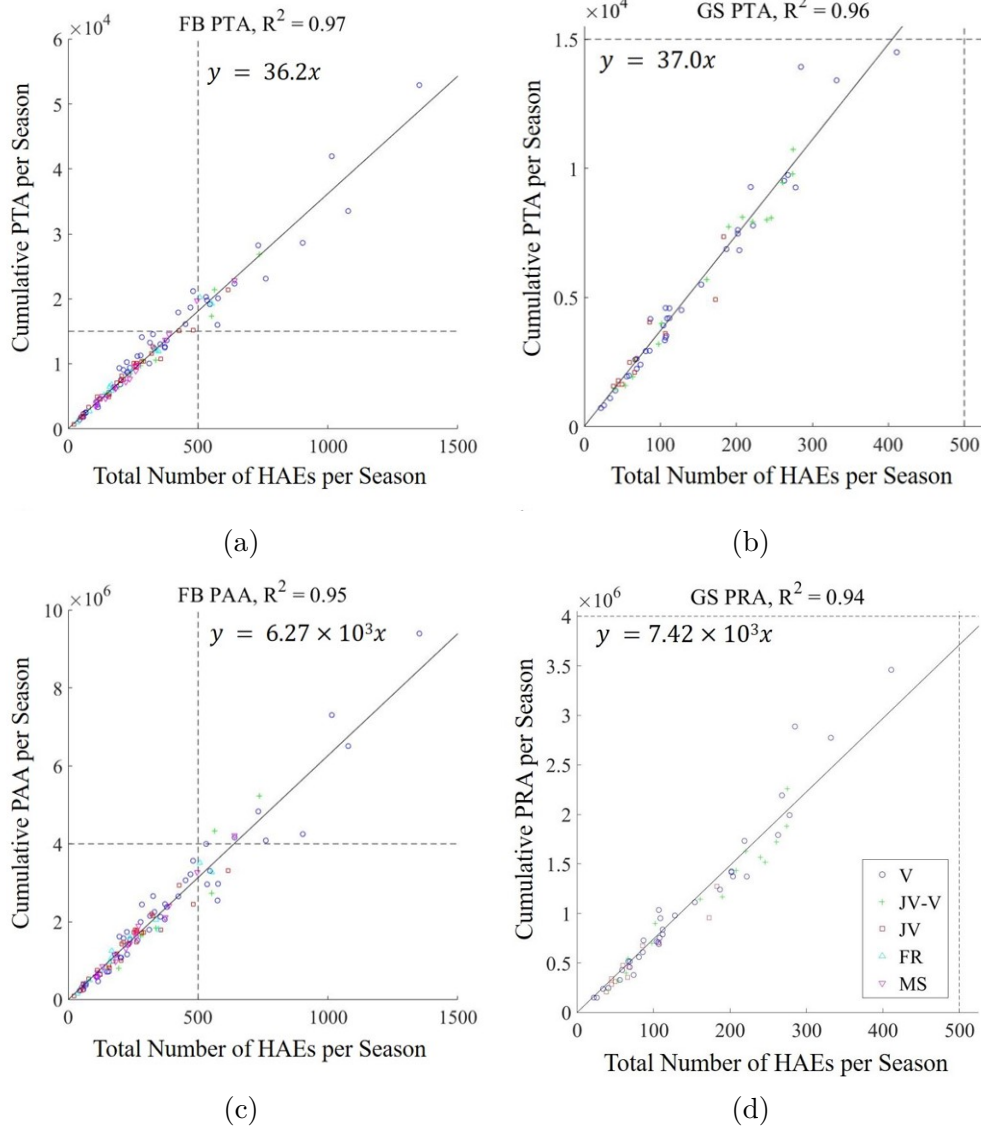


Figure 2.3. Cumulative PTA (g) for the season versus the total number of HAEs per player per season for (a) FB and (b) GS, and cumulative PAA ($\text{rad} \cdot \text{sec}^{-2}$) for the season versus the total number of HAEs per player per season for (c) FB and (d) GS. For cumulative PTA, there was no statistical difference across of the levels of play in terms of the slope (FB: $p=.367$, ANOVA; GS: $p=.615$; KW), or between high school FB and GS ($p=.702$; KW). For cumulative PAA, there was no statistical difference between any of the slopes among the different levels of play (FB: $p=.933$, KW; GS: $p=.146$, ANOVA). There was a significant difference between PAA regressions between high school FB and GS ($p<.001$, ANOVA). To demonstrate the difference in scale, the dashed lines in (a) are the same as in (b), and the dashed lines in (c) are the same as in (d).

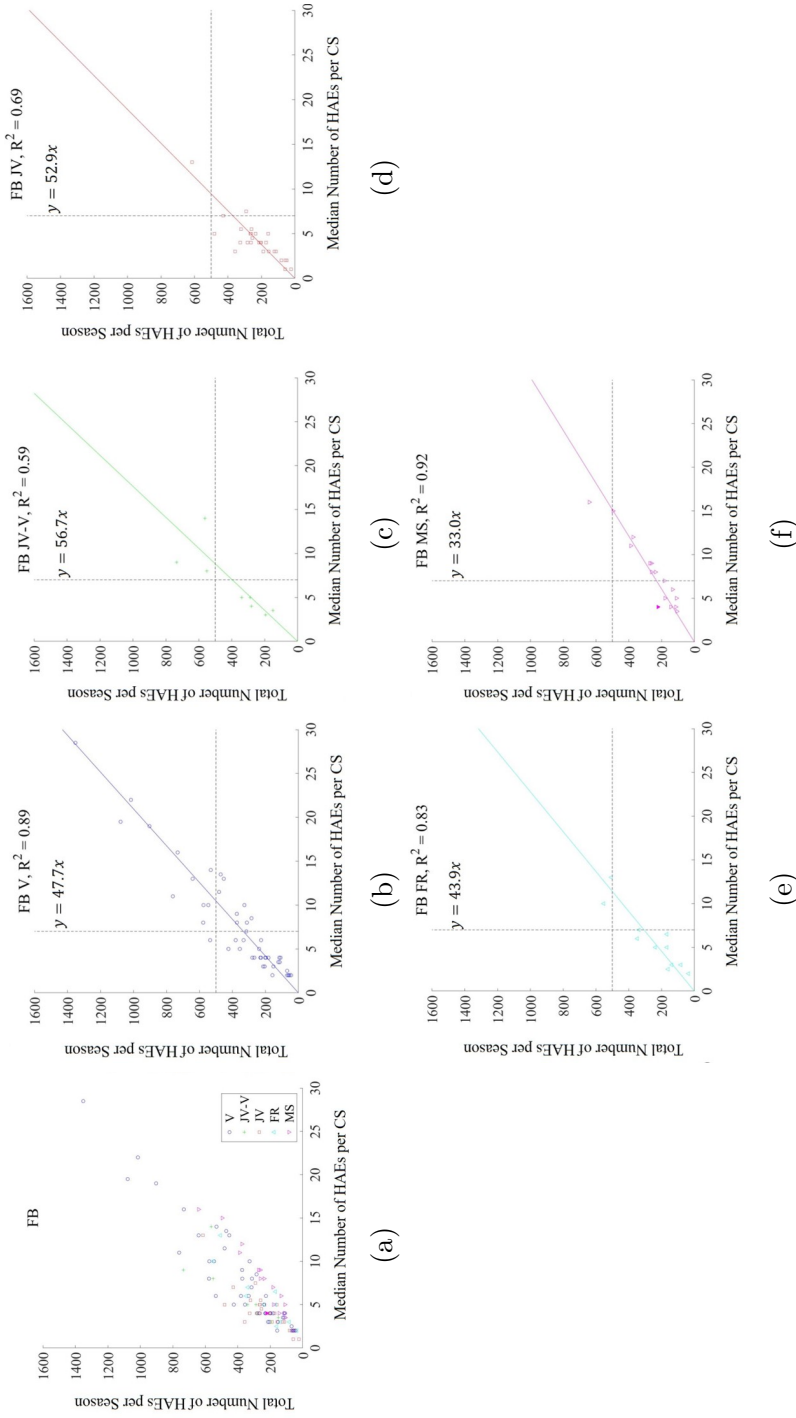


Figure 2.4. Total number of HAEs per season per FB player versus the median number of HAEs per contact session (CS). The plots have the players grouped by level of play as follows: (a) all players (b) V (c) JV-V (d) JV (e) FR (f) MS. The dashed lines on these plots are the same as those used in Fig. 2.5 to demonstrate the differences in scale. There is a significant difference in the slopes between V and MS ($p=.001$; KW), JV-V and MS ($p<.001$; KW), and JV and MS ($p<.001$; KW). The filled data point in (a) and (f) indicates a player who accumulated 40% or more of the HAEs for the season in a single session and was not included in the regression analysis.

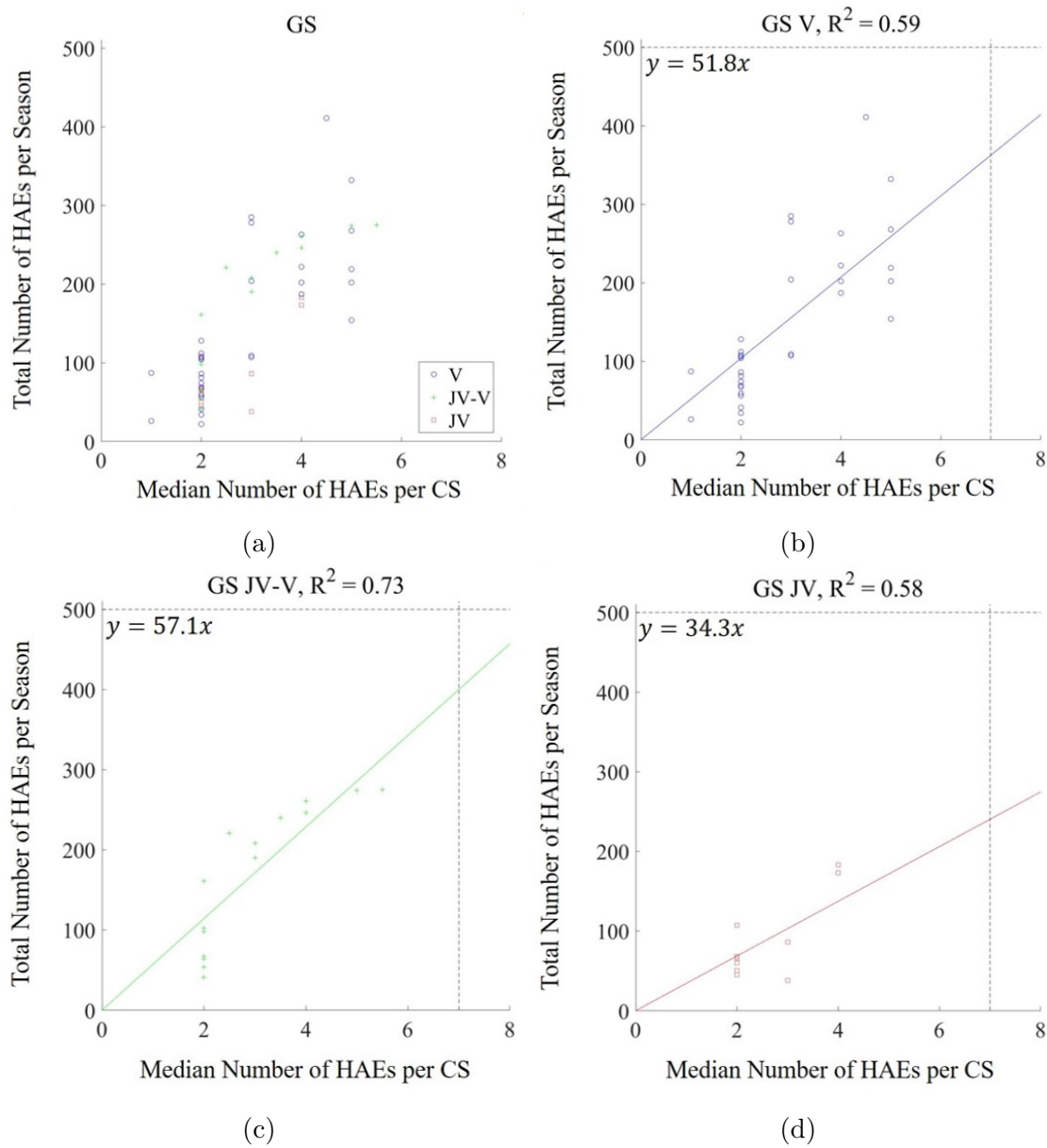


Figure 2.5. Total number of HAEs per season per GS player versus the median number of HAEs per contact session (CS). The plots have the players grouped by level as follows: (a) all players (b) V (c) JV-V (d) JV. The dashed lines on the plots are the same as the lines shown in Fig. 2.4 to demonstrate the differences in scale. There was a statistical difference between JV and JV-V ($p=.014$; ANOVA) and JV and V ($p=.048$; ANOVA).

Table 2.4. Comparison of the teams in this study to similar data that has been collected by others. All values below are calculated or estimated means.

Study		Number of HAEs per Session [†]	HAE PTA in g's [†]	Number of HAEs per Season [†]	Cumulative PTA per Season in g's [†]
	Broglia et al. [85], Eckner et al. [87], Broglia et al. [86]	16 (8)	25.5 (35.6)	549 (284)	14,009.1 (10,102.5)
	Schnebel et al. [88]	22 (10)	24.6 (37.8)	520 (250)	12,822.0 (9,439.6)
	Breedlove et al. [2], Breedlove et al. [60], Talavage et al. [19]	15 (8)	27.5 (38.8)	672 (365)	18,494.8 (14,163.1)
Current Study	FB MS	(8)	(35.9)	(257)	(9,227.4)
	FB FR	(7)	(36.5)	(249)	(9,089.8)
	FB JV	(5)	(35.8)	(230)	(8,240.6)
	FB JV-V	(7)	(34.9)	(388)	(13,528.3)
	FB V	(8)	(36.9)	(369)	(13,600.2)
	HS FB	(7)	(36.4)	(316)	(11,492.2)
	GS JV	(2)	(36.6)	(84)	(3,065.7)
	GS JV-V	(3)	(36.1)	(167)	(6,014.9)
	GS V	(2)	(37.2)	(143)	(5,304.5)
	HS GS	(2)	(36.8)	(138)	(5,075.5)

[†]Data in cell are from the publication and the number in parenthesis is estimated when HAEs with a PTA below 20 g are removed to allow for a more accurate comparison with the data from this study.

3. PLAY TYPE AND STANCE: PILOT STUDY

This is a non-final version of an article published in final form in the Clinical Journal of Sports Medicine: Taylor A Lee, Roy J Lycke, Patrick J Lee, Caroline M Cudal, Kelly J Torolski, Sean E Bucherl, Nicolas Leiva-Molano, Paul S Auerbach, Thomas M Talavage, and Eric A Nauman. Distribution of Head Acceleration Events Varies by Position and Play Type in North American Football. *Clinical Journal of Sport Medicine : Official Journal of the Canadian Academy of Sport Medicine*, 2020. DOI: 10.1097/JSM.0000000000000778. https://journals.lww.com/cjsportsmed/Abstract/9000/Distribution_of_Head_Acceleration_Events_Varies_by.98992.aspx [100]

3.1 Introduction

Traumatic brain injuries (TBIs) result from both direct head impacts and whiplash motions[1] that can result in diminished cognitive, motor, and sensory functions, and in severe cases, permanent brain damage [101]. In 2010, it was estimated the lifetime costs (direct medical and indirect) of all TBI in the United States was approximately \$76.5 billion [7]. There is growing concern about the long-term effects playing North American football can have on a player’s brain, particularly long-term cognitive health. This problem was first identified and documented in football players when former National Football League (NFL) players’ autopsies revealed they had a neurodegenerative disease known as chronic traumatic encephalopathy (CTE), previously observed only in retired pugilists [9]–[13]. Patients with CTE can exhibit short-term memory deficiency, lack of emotional stability, poor decision making, difficulty with behavioral control, and suicidal tendencies [8]. CTE has been confirmed postmortem in more than 120 former professional, 48 college, and four high school American football players, although selection bias in the studies may contribute to the high observation rate of those confirmed to have CTE [11]–[14], [37]–[39], [102]. Development of CTE does not correlate with history of diagnosed concussions [103], a type of TBI, but rather with a history of repetitive brain trauma [15], [18], [26], [104]–[106]. This suggests that continuous exposure to subconcussive impacts, or impacts that do not cause a diagnosed concussion, may be the critical aspect contributing to CTE [8], [15]–[18], [104].

This causation is consistent with the results of studies by Talavage and colleagues, who determined that over the course of a season, high school football players experience impaired neurocognitive and neurophysiological capabilities without being diagnosed with concussion or displaying any classic concussion symptoms [2], [19]. Specifically, these investigators found that subconcussive blows can have effects over an extended period of time similar to those from a concussion [2], [19]–[21], [26], [43]–[49]. It has been established that the number and locations of impacts are important factors to consider when determining whether a player is going to experience decreased neurocognitive function by the end of a season [2], [19].

Head acceleration events (HAEs) are direct blows to the head and/or whiplash motions of the head associated with blows to other parts of the body. Studies examining changes in brain function, chemistry, and structure following periods of exposure to repeated HAEs reveals that while high magnitude individual HAEs are likely to produce near-term clinical symptoms and might contribute to chronic injury, these “big hits” are not the sole major cause of later-life neurodegenerative disorders in former collision-sport athletes [15], [42].

Numerous studies have reported abnormal neuroimaging and neurocognitive measurements in athletes who experienced appreciable numbers of HAEs [20], [22]–[24], [59], [84]. Examples include within-season functional magnetic resonance imaging (fMRI) changes that are strongly associated with the number of HAEs in the preceding week [19], and post-season cognitive testing and fMRI changes predicted by average weekly number of HAEs during the season [61]. These investigations suggest that cumulative mechanical loading might result in more injury to brain tissues than can be repaired by natural processes [42], with the limit likely lying between 65 and 90 HAEs per week for high school football players [61]. The concept of a “cumulative subconcussive threshold” has been extrapolated by Alosco et al. to predict how lifetime history of exposure to HAEs might predict later-life risk of cognitive dysfunction and structural damage [107], [108]. Reducing the total number of HAEs experienced can be achieved through four strategies: (1) modify the rules of the game to limit head impacts [18], [109], (2) teach and use better techniques during practice, (3) reduce or eliminate full contact practice activities [18], which might translate to the style of play in games, and (4) develop helmets that absorb more energy [18]. Of these four, rules modification and eliminating full contact practices can be implemented immediately.

One specific rule change that has been suggested is to eliminate the three- and four-point (“down”) stances for linemen, as these stances may increase the number of collision and other head impacts sustained due to the initial weight distribution of the player and height of the head [18]. Consequently, the goal of this pilot study was to evaluate the potential for this rule change to reduce HAEs in a post-collegiate group of athletes participating in a football skills development and professional recruitment camp.

3.2 Methods

3.2.1 Subjects

The study was approved by the Purdue Institutional Review Board. Written informed consent was obtained from each subject prior to enrolling in the study. Football (FB) athletes participating in up to three practice sessions and one exhibition game as part of a post collegiate skills development camp were recruited for the study. The position of each participant was recorded and divided into the following categories: Defensive Backs (DB), Defensive Linemen (DL), Linebackers (LB), Offensive Linemen (OL), Tight Ends (TE), Running Backs (RB), Wide Receivers (WR), and Skill Players (Quarterbacks [QB], Placekickers [K], and Punters [P]).

3.2.2 Impact Data Collection and Analysis

HAEs were monitored using the xPatch (X2 Biosystems; Seattle, WA). Each practice and each game was considered a separate “session.” Sensors were placed on each participant for all practice sessions and for the exhibition game. A sensor was affixed behind the player’s right ear with an adhesive patch after cleaning the area with isopropyl alcohol [58], [64]. Each head impact was recorded as a separate “event” on the sensor when the peak linear acceleration (PLA) projected on any axis was greater than 10 g ($g = 9.81 \text{ m/s}^2$). Data were downloaded using the Head Impact Monitoring System software (X2 Biosystems) after each session. For the purposes of this study, the clack recognition algorithm (X2 Biosystems; Seattle, WA) was not used, because events caused by different mechanisms (e.g., direct impacts, whiplashes, falls and dives) were not distinguished [58], [64].

Data from the sensors were processed using a custom MATLAB (MathWorks; Natick, MA) program to include only events occurring within the valid time window of each session and registering a PLA greater than or equal to 20 g. Although the sensors were programmed to collect low acceleration events (10-20 g), these events were excluded from analysis because they can frequently result from non-impact mechanisms (eg, changing direction, kicking the ball, stopping) [58]. Data were also analyzed to remove sessions that exhibited evidence of a defective sensor or detached sensor.

3.2.3 Video Data Collection and Analysis

Video footage of the exhibition game was collected using six Sony HDR-CX160 AVCHD HD Handycam Camcorders and two Sony DCR-SX85 Handycam Camcorders (Sony Corporation; Kōnan, Minato, Tokyo). The HD cameras were set to record on Long Time with HD Quality. Three HD cameras were placed on each side of the field. During game play, one camera covered the middle of the field from one 30-yardline to the other 30-yardline, while the other two cameras per sideline each covered the area from one 30-yardline to the closest end zone. The two DCR-SX85 cameras were operated at the field level.

For each play examined, there were five OL players positioned at the line of scrimmage. Depending on the play, the TE would either be positioned at the line of scrimmage directly next to the OL, or he would be positioned further away in the slot receiver position. If the TE was positioned directly next to an OL, then the TE was considered a player on the offensive line and eligible for stance analysis.

The video footage revealed which players were on the field for each play, and the stance of players positioned as the offensive line (up [2-point] or down [3- or 4-point], Fig. 3.1). The impact data for the game were filtered to only include impacts for players that were on the field for each play. The hit rate for the players positioned as the offensive line was calculated for the i^{th} play type (run or pass) and j^{th} stance (up or down) by,

$$player\ hit\ rate_{ij} = \frac{\sum player\ registering\ HAE_{ij}}{\sum players_{ij}} \quad (3.1)$$

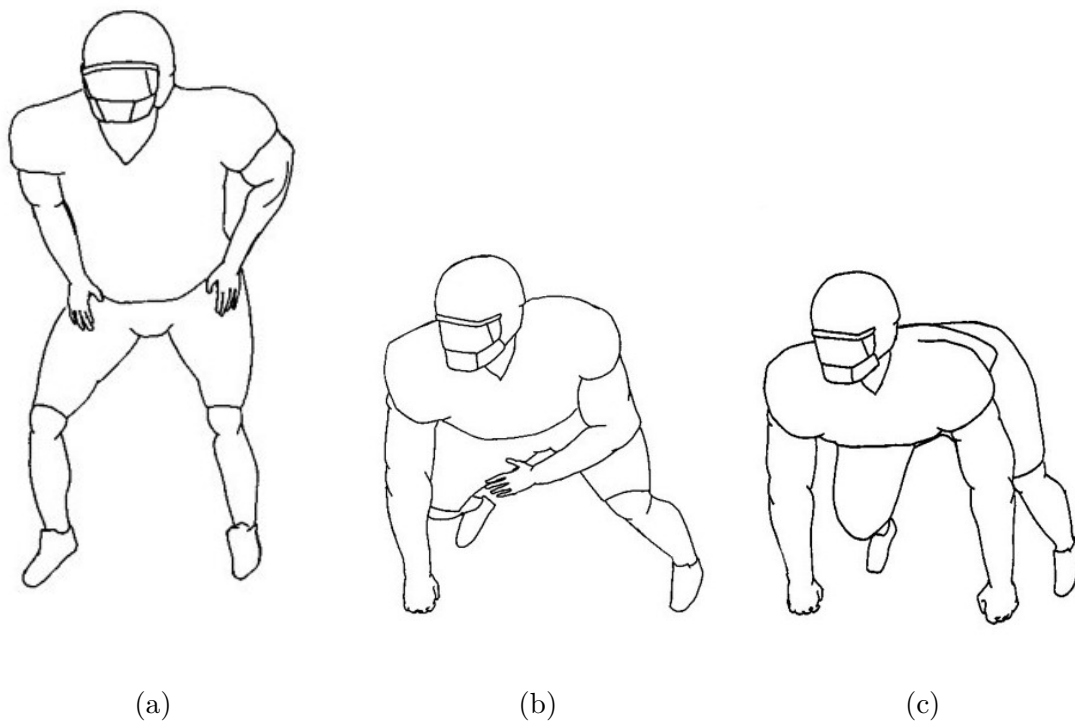


Figure 3.1. The players on the offensive line began each play in a (a) 2-point, (b) 3-point, or (c) 4-point stance. A 2-point stance was considered the “up” stance and a 3-point or 4-point stance was considered a “down” stance.

Dividing the total number of players that sustained hits for a specific combination of the play type and stance by the total number of players with that specific combination makes it possible for rates to be compared by normalizing by the respective sample sizes.

3.2.4 Statistics

Statistics were performed using Stata/SE 15 (StataCorp LLC; College Station, TX). Histograms were generated by binning the HAEs by PLA in 20 g intervals and were separated by position. They were compared using a χ^2 test, with post-hoc testing performed using pairwise χ^2 tests with a Bonferroni correction. The number of hits were compared using the Wilcoxon Rank Sum test. Hit rates for the players on the offensive line were compared using a χ^2 test, with post-hoc testing performed using pairwise χ^2 tests with a Bonferroni correction.

3.3 Results

Among the 78 participants, there was a total of 141 measured player practice sessions and 66 player game sessions (defective sensors: $n = 2$; detached: $n = 35$). A total of 437 (62%) HAEs were recorded during practices and 272 (38%) were recorded during the exhibition game (Table 3.1), 265 of which occurred during a run or pass play.

Table 3.1. HAEs by position as a function of practices (session 1, 2, 3) and game.

Position	No. of Players	Practice HAEs	Game HAEs	Total HAEs
Defensive Backs	19	22 (0, 8, 14)	36	58
Defensive Linemen	9	96 (0, 50, 46)	52	148
Linebackers	10	45 (0, 14, 31)	31	76
Offensive Linemen	10	155 (0, 76, 79)	98	253
Tight Ends	3	41 (1, 34, 6)	16	57
Running Backs	8	41 (0, 13, 28)	21	62
Wide Receivers	12	28 (3, 15, 10)	11	39
Skill	7	9 (0, 7, 2)	7	16
<i>Quarterbacks</i>	4	6 (0, 5, 1)	7	13
<i>Placekickers/Punters</i>	3	3 (0, 2, 1)	0	3

The histogram of HAEs for practice sessions (Fig. 3.2) and the exhibition game (Fig. 3.3) demonstrated significant differences between the different positions for both the practices ($p = 0.011$) and game ($p = 0.017$). For practices, there were significant differences between RB and OL ($p < 0.001$), and RB and DL ($p < 0.001$). For the game, there were significant differences between OL and LB ($p = 0.001$), and OL and TE ($p < 0.001$).

The number of HAEs that exceeded 20 g observed over the ensemble of players on the field differed appreciably between passing and running plays (Fig. 3.4). There were 46 pass plays and 23 run plays in the exhibition game. The pass plays had a total of 242 players on the offensive line (90 up, 152 down); the run plays had a total of 119 players on the offensive line (28 up, 91 down). The frequency of players in the up stance was significantly greater for pass plays than for run plays (χ^2 test, $p = 0.009$). When a play was scripted to be a run, the number of HAEs observed to exceed 20 g (5.57 ± 3.00 HAEs per play) was nearly twice that

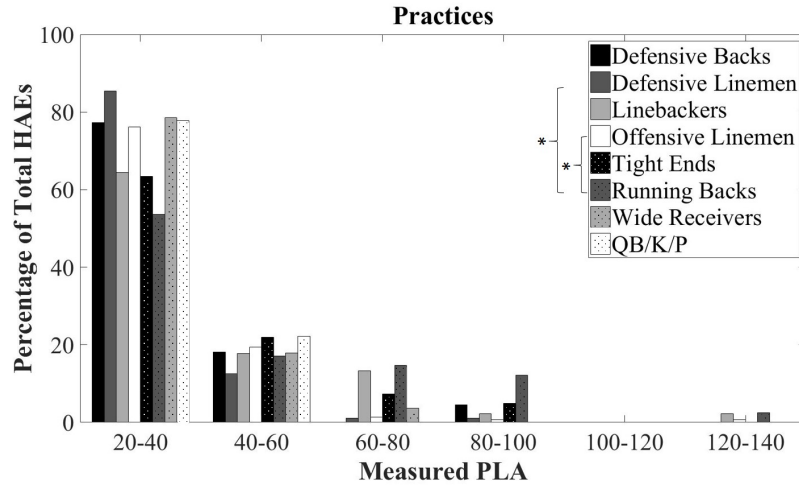


Figure 3.2. HAE distribution by position (DB, DL, LB, OL, TE, RB, WR, QB/K/P) for all three practice sessions.

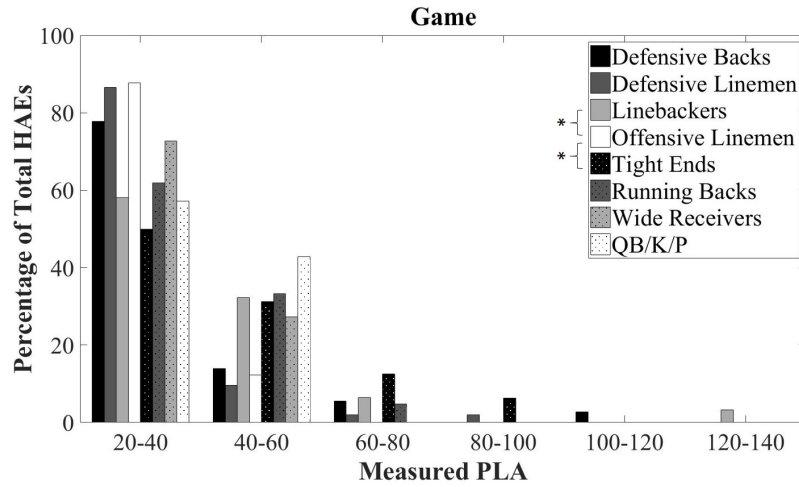


Figure 3.3. HAE distribution by position (DB, DL, LB, OL, TE, RB, WR, QB/K/P) for the exhibition game.

observed when a play was scripted to be a pass (2.98 ± 1.65 HAEs per play). The Wilcoxon Rank Sum test revealed these distributions to be significantly different ($p < 0.001$).

Regardless of play type, players in a down stance had a higher likelihood of sustaining a HAE than players starting in an up stance (Fig. 3.5; χ^2 test, $p = 0.001$). When separating by play type, players in a down stance for a run play sustained significantly more HAEs than players in an up stance (χ^2 test, $p < 0.001$) or down stance (χ^2 test, $p = 0.003$) for a pass.

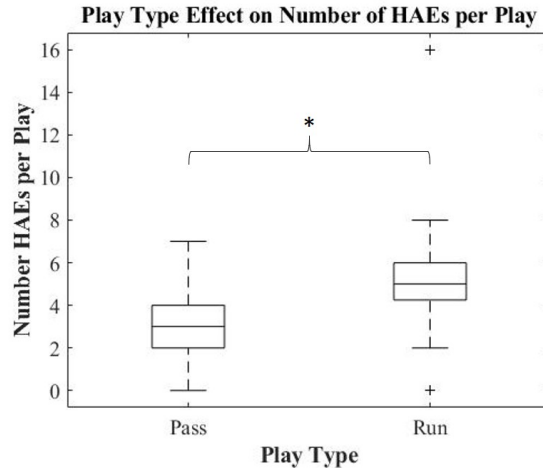


Figure 3.4. Comparison of the average number of play-related HAEs (exceeding 20 g) observed across all monitored players on the field during plays intended to be passing vs. running.

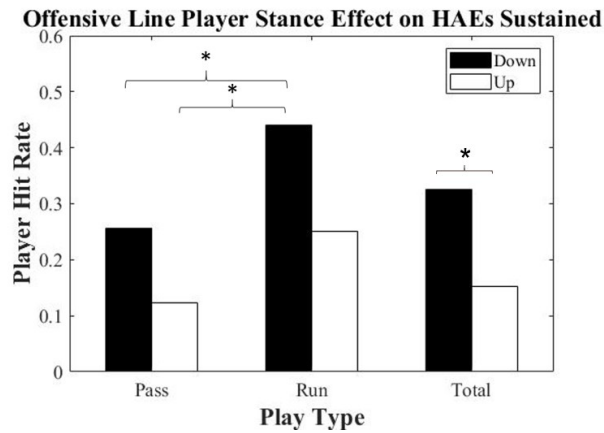


Figure 3.5. Comparison of the rate that OL and TEs sustain impacts separated by play type (pass vs. run) and stance (up vs. down).

3.4 Discussion

The purpose of this pilot study was to examine the HAE characteristics for players participating in a post-collegiate skills and recruitment football showcase. Analysis by position revealed that tight ends are of particular concern since they can act as both blockers and receivers for the same play, increasing their odds for sustaining a HAE. The starting stance of the offensive line players influences the frequency at which these players accumulate HAEs, with players starting in the down stance recording a higher hit rate than those starting in

the up stance. The findings from this study are intended to aid in developing potential technique and rules changes to decrease the accumulation of HAEs in football athletes, notably linemen.

The hit distributions in practices and in games varied by position. The LBs and TEs tended to sustain the greatest number of high magnitude impacts (above 60 g PLA; 9.68% and 18.75%, respectively, in games). Unlike linemen, linebackers have a defensive role in the game and position on the field that encourage them to collide with offensive players head on or at an oblique angle, and at a high speed of approach. Tight ends had the greatest frequency of high magnitude game hits compared to other player positions. Tight ends often function as both an OL (to block) and as a WR (to catch a pass) within the same play. Blocking generates a large number of lower magnitude HAEs [20], [110], and receiving passes followed by being tackled generates high magnitude impacts.

Offensive and defensive linemen deliver and receive the most hits during sessions, but they tend to be smaller in magnitude (20-40 g PLA). Players in these positions typically lack a running start before contact, leading to lower PLA measures. This is similar to trends seen in other studies [88], [110]. Although the impacts are smaller in magnitude, these players may still be at risk for developing neurological changes because the number of HAEs may be a factor in the severity and degree of neurological changes experienced [2], [11], [12], [19], [20], [24], [26], [60], [61]. It is possible that these less forceful HAEs are the root cause of CTE [16], [17].

The average number of HAEs (exceeding 20 g) per play was significantly lower for pass plays than run plays. This is expected for linemen because the OL are more likely to generate impacts when they act as aggressors for run plays than when they play the protector role for pass plays. This trend was generally true for players at all positions, not just linemen. So, while linemen dominate the number of impacts for both pass and run plays, pass plays in general result in less contact between opposing players at all positions.

The initial stance of the OL and TE for pass and run plays affects the hit rate. Players that began in the down stance generally were more likely to sustain HAEs, regardless of the play type. Most line players end up blocking from an up stance, so beginning play in a two-point stance has the added benefit of making the head less vulnerable to a substantial

HAE. There was a greater frequency of players in the up stance for pass plays than for run plays. Players that started in a down stance for a run play had a significantly higher hit rate than players in either the up or down stance for pass plays. During run plays, OL are tasked not only with protecting the quarterback but with moving DL to clear a path for the RB. This requires the OL to keep their center of gravity low, which puts the head in a position that can contribute to a higher hit rate.

Limitations of this paper include some nominal variability in the measurements obtained from the xPatch sensor [64]. The RMS and mean absolute errors for the xPatch are both typically 20%, which is sufficient for characterizing differences in HAE distributions and cumulative exposure [64]. In addition, this study only includes two full practices sessions and one game, resulting in a relatively small sample size. However, the results and trends documented here are sufficient to warrant a larger study to determine if the trends hold. The small sample size of players in the TE position poses an issue for the validity of the trends recorded in this study. These trends warrant further study to determine if and how HAEs can be reduced for players in this position.

3.5 Conclusion

The starting stance of the line players influences the frequency at which these players accumulate HAEs. Players starting in the down stance have a higher HAE rate than players starting in the up stance. Changing linemen stance rules and reducing the number of full contact practices will lower the number of HAEs sustained and increase player safety. Tight ends are of particular concern because they can act as both blockers and receivers for the same play, increasing the chance of sustaining impact. We plan a study of longer duration to further investigate these contentions.

4. PLAY TYPE AND STANCE: CONFIRMATION STUDY

4.1 Introduction

Although the results from the pilot study to examine how play type and stance affects the number and distribution of HAEs indicate starting offensive line players in an up stance reduces the number of HAEs sustained by these players, one of the limitations of that study was the small sample size. Only one exhibition game was examined for that study, and the exhibition game was not a true “game” in the sense that it was offense versus defense instead of team A versus team B. To determine if the trends seen in the pilot study hold, a larger, more game realistic study was conducted on a similar group of athletes.

4.2 Methods

4.2.1 Subjects

The study was approved by the Stanford University and Purdue University Institutional Review Boards. Written informed consent was obtained from each participant prior to participating in the study. All activities (practices and four exhibition games) and data collection occurred at The Spring League, a professional football developmental league. A total of 174 players consented to participate. The Spring League assigned players to one of four teams, indicated here as Team 1, 2, 3, and 4 (Table 4.1). There were two game days on each of which two games were played (four total games), with each team participating in one game per game day. Our analysis focuses on these games, which were possible to fully document (Table 4.1).

The playing position of each participant was recorded as one of the following: defensive back (DB), defensive lineman (DL), linebacker (LB), offensive lineman (OL), tight end (TE), running back (RB), wide receiver (WR), or skill (quarterback [QB], placekicker [K], and punter [P]). Twenty players for game day 1 and 24 players for game day 2 dropped from the study due to injury or personal reasons. Due to these dropped players, some athletes played for multiple teams on a single game day to ensure enough players for each team. These cases were treated as independent observations (i.e., a player who played in two games in one day is treated as two separate player observations).

Table 4.1. Number of study participants for both games for each position and team. This includes players that played on two teams in one day.

Position	Team 1		Team 2		Team 3		Team 4	
	Game 1	Game 2	Game 1	Game 2	Game 1	Game 2	Game 1	Game 2
Defensive Back	10	11	9	9	9	9	8	7
Defensive Lineman	5	6	5	4	4	4	6	5
Linebacker	3	2	3	4	4	4	5	5
Offensive Lineman	6	5	6	7	5	5	5	6
Tight End	3	3	2	2	2	2	2	2
Running Back	2	2	5	4	6	6	7	8
Wide Receiver	6	5	4	4	8	8	8	7
Skill	3	3	3	3	2	2	2	2
Quarterback	1	1	2	2	2	2	2	2
Kicker/Punter	2	2	1	1	0	0	0	0

4.2.2 Assignment of Stance

During games the stance at the beginning of each play for all of the OL (except the “center”) was dictated by the investigators and later verified with video footage. This initial stance was varied by quarter within a game. Offensive linemen were instructed to use a singular initial stance—either 2-point (“up”) or 3- or 4-point (“down”)—in quarters 1 and 3, and the alternate initial stance in quarters 2 and 4. To partially account for fatigue and order effects, “up” and “down” quarters were counter-balanced across games. Note that the “center” position was the only OL that started every play in the down stance, as this was necessary to snap the ball.

4.2.3 Modified Game Rules

This camp used modified punts and modified kick-offs during the games. In both modified play types, the punt or kick receiver must attempt to catch the punt or kick unless it goes out of bounds. For punts, there was a five-yard “halo” around the punt receiver until the ball was caught, meaning that a player on the kicking team could not be within five yards of the punt returner until they caught the ball. For kick-offs, the ball was kicked from the kicking team’s own 25-yardline and the kicking team lined up on the opposing team’s 35-yardline. All of the players on the receiving team except for the kick returner lined up on their own 30-yardline, putting them five yards away from the kick team. Players were not allowed to move until the kick returner caught the ball. This modification to the kick-off may help reduce concussions, as kick-offs have a higher concussion rates than other types of plays [111].

4.2.4 HAE Data Collection and Analysis

The impact data collection and analysis used here is very similar to the data collection and analysis procedure used in the level of play study and pilot study. HAEs were monitored using the CSx earpatch sensor (CSx Systems Ltd; Auckland, New Zealand). Each practice and each game was considered a separate “session.” Sensors were placed on each participant for practice and game sessions. A sensor was affixed behind the player’s right or left ear with

an adhesive patch after cleaning the area with isopropyl alcohol [58], [64]. Each head impact was recorded as a separate “event” on the sensor when the peak linear acceleration (PLA) projected on any axis was greater than 10 g. Data were downloaded using the CSxDataApp (CSx Systems Ltd; Auckland, New Zealand) after each session. For the purposes of this study, the shock recognition algorithm (CSx Systems Ltd; Auckland, New Zealand) was not used, because events caused by different mechanisms (e.g., direct impacts, whiplashes, falls and dives) were not distinguished [58], [64].

Raw timestamps for each event on the sensor were adjusted using calibration points. If calibration points could not be identified (i.e. the sensor memory was filled, sensor ran out of battery before post-calibration points could be put on the sensor, etc.), timestamps could not be adjusted, and the entire sensor’s session was excluded (24 instances). HAE data were processed using a custom MATLAB (MathWorks; Natick, MA) program to filter and transform the acceleration from the sensor to an approximated center of mass (CoM) of the head, as derived from a 50th percentile male Hybrid III headform (Humanetics Innovative Solutions, Inc.; Farmington Hills, MI). Data processing methods are the same as for the pilot study.

4.2.5 Video Data Collection and Analysis

Video footage of the exhibition games was collected using six Sony FDR-AX53 4K HD Video Recording Camcorders and four Sony HDR-CX160 AVCHD HD Handycam Camcorders (Sony Corporation; Kōnan, Minato, Tokyo). Three 4K cameras were placed on each side of the field. During game play, one camera covered the middle of the field from one 30-yardline to the other 30-yardline, while the other two cameras per sideline each covered the area from one 30-yardline to the closest end zone. Each of the HDR-CX160 cameras was placed at the corner of the field and angled toward the center of the field. The same approach in the pilot study to determine stance was also used in this study.

4.2.6 Offensive Linemen Stance

Several different HAE rates were calculated, but the general formula for calculating the HAE rate for the i^{th} play type and the j^{th} stance is calculated by:

$$HAE\ rate_{ij} = \frac{\sum players\ registering\ HAE_{ij}}{\sum players_{ij}} \quad (4.1)$$

Offensive lines were also analyzed for skill level due to the larger skill level range observed in the Texas camp compared to the pilot study. Game footage was examined by a former National Collegiate Athletic Association Division 1 football player (linebacker), who used determinations of speed out of stance, ability to punch with hands, footwork, and overall athleticism and agility to categorize the offensive lines as either higher or lower skill. High skill offensive lines were typically quicker out of the stance, had better use of hands, faster footwork, and overall higher athletic ability. Higher skill offensive lines were on Teams 1 and 3, while Teams 2 and 4 exhibited lower skill levels. Note offensive line skill (OLS) does not necessarily reflect the overall team skill.

4.2.7 Statistics

Statistical analyses were performed using Stata/SE 15 (StataCorp LLC; College Station, TX). Histograms and HAE rates were compared using the χ^2 test, with post-hoc testing performed using a pairwise χ^2 test with a Bonferroni correction. The number of HAEs by play type were compared using a Kruskal Wallis (KW) test, and pairwise comparisons were performed using Dunn's post-hoc test with a Bonferroni correction. A logistic regression was used to determine significant contributing factors for HAE rates of OL. The main effects of stance (up vs. down), play type (run vs. pass), OLS (high vs. low), binned score difference (BSD: number of scores [seven points] the team on offense was ahead [positive] or behind [negative] the team on defense), and match-up (matched vs. mismatched OLS) were considered. All two-way interactions between the main effects were considered for the model.

4.3 Results

The number of hits sustained by each position varies by team and by game (Table 4.2). Typically for all games, DL and OL sustained the greatest number of hits, except for Team 4, where LB sustained the most impacts among the different positions. The number of hits also varied by game. While Team 1 had about the same number of impacts in both games (110 and 117), Teams 2 and 3 both sustained more impacts in game 2 (104 and 246, respectively) and Team 4 sustained more impacts in the first game (134). For a single game, the greatest number of impacts was experienced by DL on Team 3 in game 2 (73), while the least number of hits was typically experienced by skills positions (0).

The distribution of the magnitude of HAEs sustained in games was significantly different among positions (Fig. 4.1; χ^2 test, p-value=0.001). After pairwise comparisons were performed, significant differences were observed between OL and DB (χ^2 test, p-value < 0.001), OL and LB (χ^2 test, p-value < 0.001), OL and RB (χ^2 test, p-value < 0.001), OL and WR (χ^2 test, p-value < 0.001), and OL and skill (χ^2 test, p-value < 0.001). Over 70% of the HAEs for DL, OL, and TE occurred in the 20-40 g range (74.1%, 86.6%, and 77.3%, respectively), while all of the other position HAEs occur less than 70% of the time in this range.

There were a total of 189 run plays, 268 pass plays, 35 punts and 36 modified kick-offs (Fig. 4.2). Run plays had the most HAEs per play (2.71 ± 2.26), followed by modified kick-offs (1.83 ± 1.40), pass plays (1.53 ± 1.64), and punts (1.37 ± 1.55). The number of HAEs per play varied significantly by play type (KW test, p-value < 0.001). Run plays had significantly more HAEs per play than pass plays (p-value < 0.001) and punt plays (p-value = 0.001). The modified kick-off resulted in a similar number of HAEs as run plays (p-value = 0.206).

A total of 1,329 players on the offensive line started in a down stance (735 pass, 594 run) and 919 players started in an up stance (574 pass, 345 run) for run or pass plays. The HAE rate for players on the offensive line varied by stance and play type combination (Fig. 4.3; χ^2 test, p-value < 0.001). Pass down was significantly lower than run down (p-value < 0.001) and run up (p-value = 0.001) and pass up was significantly lower than run down (p-value =

Table 4.2. Number of HAEs sustained by each position separated by team and game (G1, G2, All Games).

Position	Team 1			Team 2			Team 3			Team 4		
	G1	G2	All	G1	G2	All	G1	G2	All	G1	G2	All
Defensive Back	8	30	38	11	12	23	14	34	48	15	4	19
Defensive Lineman	10	64	74	31	41	72	39	73	112	34	5	39
Linebacker	9	18	27	15	13	28	19	28	47	36	22	58
Offensive Lineman	28	48	76	20	31	51	33	49	82	24	5	29
Tight End	32	3	35	1	3	4	10	8	18	7	2	9
Running Back	15	8	23	3	2	5	16	42	58	5	12	17
Wide Receiver	6	5	11	5	2	7	7	10	17	8	0	8
Skill	2	1	3	0	0	0	1	2	3	5	1	6
Quarterback	2	1	3	0	0	0	1	2	3	5	1	6
Kicker/Punter	0	0	0	0	0	0	0	0	0	0	0	0
Total	110	117	287	86	104	190	139	246	385	134	51	185

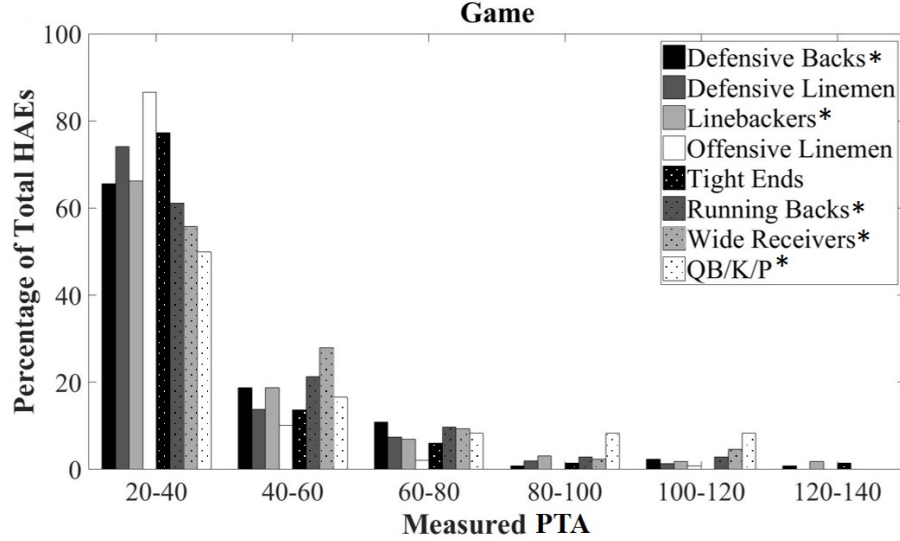


Figure 4.1. Histogram of the PLA for all hits sustained in the games. Offensive linemen had a significantly different distribution (indicated by *) than: DB, LB, RB, WR, Skill.

0.001) and run up (p-value = 0.004). Overall, there was no statistical difference between up and down stance when not accounting for the play type (p-value = 0.820).

When the teams were separated into higher and lower skill level groups, the HAE rate trends differed (Fig. 4.4). Teams of higher skill had 735 observations in a down stance (385 pass, 350 run) and 371 in an up stance (226 pass, 145 run) while teams of lower skill had 594 observations in a down stance (350 pass, 244 run) and 548 (348 pass, 200 run) in an up stance. For teams of higher skill, they had the same statistical differences when considering all of the teams. Run down and run up had significantly higher HAE rates than pass down (p-value = 0.001 and p-value = 0.002) and pass up (p-value < 0.001 and p-value = 0.001, respectively). Higher skill teams tend to have higher HAE rates for down stance than an up stance. Teams of lower skill had a significantly lower HAE rate for a down stance on a pass play compared to both an up stance on a pass play (p-value < 0.001) and an up stance on a run play (p-value < 0.001). Lower skilled teams also had a significantly higher HAE rate for an up stance than a down stance overall (p-value = 0.005).

HAE rates were calculated based on the OLS match-up (Table 4.3). Two of the four games had teams with matched OLS (both low, both high) and two of the four games had

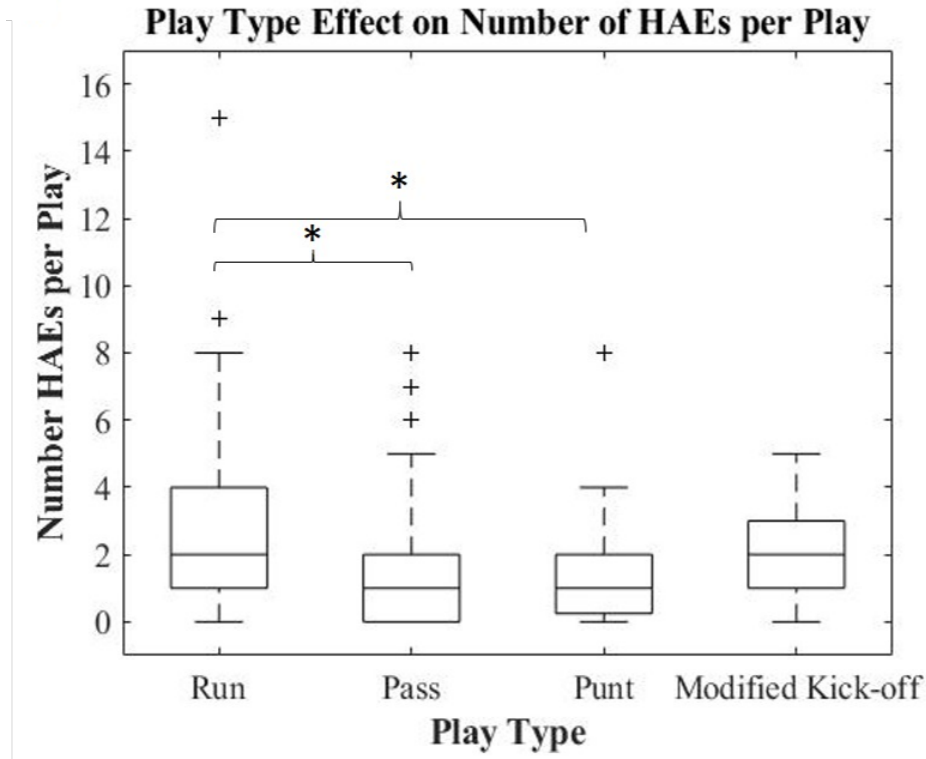


Figure 4.2. Hits sustained on each play by play type. Run plays had statistically more hits per play than pass (p-value < 0.001) and punt plays (p-value = 0.001).

teams with mismatched OLS (low vs. high). When low OLS teams played each other, HAE rates tended to be higher in the up stance than down. The opposite was observed when two high OLS teams played each other. When teams with mismatched OLS played each other, the low skill offensive lines exhibited a higher HAE rate than when they played another low skill offensive line. Conversely, there was a slight decrease in HAE rates during down stance plays for high OLS teams playing lower OLS teams.

A logistic regression revealed which variables most contributed to HAE rate (Table 4.4). Stance (p-value = 0.021), play type (p-value < 0.001), OLS (p-value < 0.001), BSD (p-value < 0.001), and match-up (p-value < 0.001) were all significant main effects. The interaction terms between OLS and BSD (p-value < 0.001), stance and OLS (p-value < 0.001), stance and BSD (p-value = 0.003), and OLS and match-up (p-value < 0.001) were all significant.

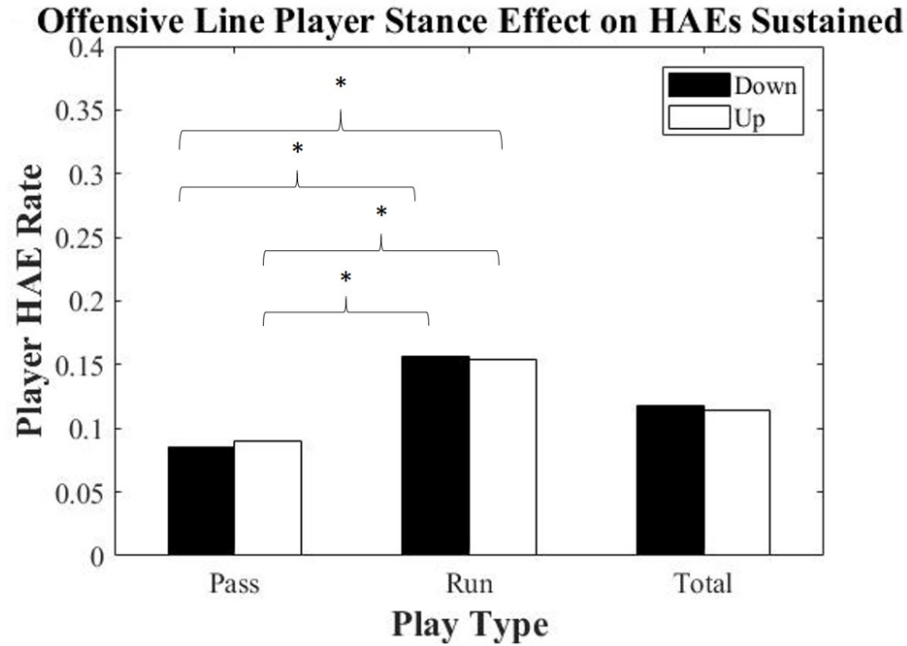


Figure 4.3. HAE rate of the players on the offensive line. The HAE rates for run down and run up were both statistically greater than pass down (p-value < 0.001 and p-value = 0.001, respectively) and pass up (p-value = 0.001 and p-value = 0.004, respectively).

Table 4.3. Head acceleration event (HAE) rates for different play/stance combinations when matched and mismatched offensive line skill (OLS; low or high) teams play each other. Note that when matched OLS teams play each other, lower OLS teams had lower HAE rates than when two high OLS teams played each other. When mismatched OLS teams played each other, the HAE rate for lower OLS team increased, but decreased for the higher OLS team for certain combinations relative to playing a team matched OLS.

Play Type	Stance	Matched OLS			Mismatched OLS		
		Game	Low Skill	High Skill	Game	Low Skill	High Skill
Pass	Down	0.09	0.01	0.17	0.08	0.04	0.11
	Up	0.08	0.06	0.12	0.10	0.10	0.11
Run	Down	0.13	0.03	0.22	0.18	0.12	0.22
	Up	0.13	0.09	0.18	0.21	0.21	0.21
All	Down	0.11	0.02	0.19	0.13	0.07	0.17
	Up	0.10	0.07	0.14	0.14	0.14	0.15

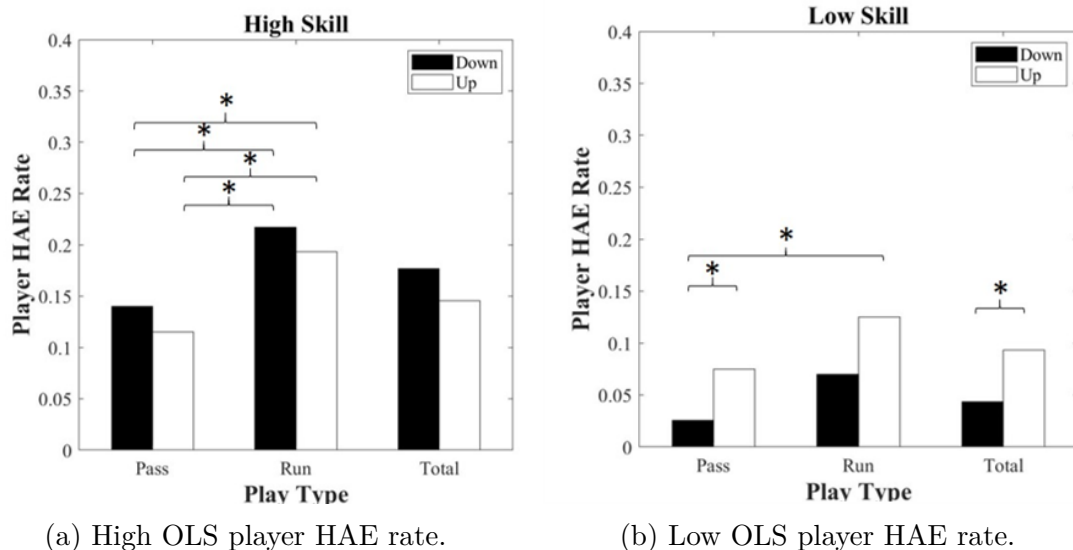


Figure 4.4. HAE rate for players on the offensive line separated by skill level. For (a) higher skill level, both pass up and pass down stances had significantly lower HAE rates compared to run up (p-value = 0.001 and p-value = 0.002, respectively) and run down (p-value < 0.001 and p-value = 0.001, respectively). For (b) lower skill, pass down had a significantly lower HAE rate than pass up (p-value < 0.001) and run up (p-value < 0.001). Lower skill players also had a significantly higher HAE rate when up compared to down (p-value = 0.005).

Table 4.4. Variables and coefficients from logistic regression analysis. Main effects were included in the model if interaction effect with the variable was significant (p-value < 0.05 noted by *).

Variable	Coefficient
Stance*	0.19
Play Type*	-0.31
OLS*	0.35
BSD*	0.23
Match-up*	-0.37
OLS, BSD Interaction*	-0.22
Stance, OLS Interaction*	-0.37
Stance, BSD Interaction*	0.11
OLS, Match-up Interaction*	0.39
Constant*	-2.06

4.4 Discussion

The purpose of this study was to determine how HAEs depend on position, play type, and the starting stance of the players on the offensive line in this post-collegiate skills development

and recruitment camp. Examining rule changes in the games and the starting stance of the players on the offensive line can lead to rule changes and technique recommendations that may potentially reduce the number and severity of HAEs sustained by players. By studying this group of players, recommendations can be made at younger levels of play to implement these potentially safer rule changes and techniques at the beginning of players' careers.

4.4.1 Effect of Position on HAEs

The distribution of HAEs by position revealed players along the line of scrimmage (OL, DL, and TE) tend to have a greater frequency of HAEs in the 20-40 g range than players in other positions. The OL and DL typically engage with each other on every play. These players lack a running start prior to their collision, leading to lower magnitude HAEs. Likewise, TEs can act as an additional OL, so it is reasonable that these positions exhibited similar HAEs. While our previous work [100] observed TEs had a different HAE distribution from OL (with a higher percentage of HAEs exceeding 40 g), that was in an offensively-oriented scrimmage setting, and it is likely that the dominant role played by a TE—acting either as OL or WR—meaningfully affects the HAE distribution.

4.4.2 Factors Affecting the HAE Rate

The play type affects the number of HAEs sustained per play. Run plays result in more HAEs per play than pass plays, consistent with prior work [100], [112]. The current study also included rule changes for punts and modified kick-offs. These changes may have helped reduce the number and magnitude of HAEs sustained on these plays, based on the fact that punts had fewer HAEs per play than run plays, and modified kick-offs were similar to run plays regarding number of HAEs. A five-yard “halo” around the punt receiver protects the punt returner from being hit immediately after catching the ball. This can potentially allow the player enough time to maneuver, possibly reducing the number and magnitude of HAEs. With the modified kick-off, having players start five yards apart might reduce the peak relative velocity between two colliding players, which can reduce the number and magnitude

of HAEs. However, without data from traditional punt and kick-off rules/formations, we cannot say whether these alterations make these play types safer.

Interpreting how the starting stance of players on the offensive line affects the HAE rate of these players was more complex than in our previous study [100]. In the current study, the simple evaluation of stance and play type (run/pass) did not lead to a clear difference in HAE rate. However, when the OLS of the teams were considered, stance and play type had an effect. For teams with higher OLS, it tended to be advantageous to start in an up (vs. down) stance, and vice versa for lower OLS teams. For lower OLS players, this “advantage” may represent a competitive disadvantage. These players generally do not react as quickly to the snap of the ball, and the delay in getting out of a down stance and into a position to engage the DL, possibly missing contact entirely. Thus, the higher HAE rate for the up stance in lower OLS players may be related simply to being able to engage the DL more often from the up position. In contrast, it is likely that the up stance does offer protection to higher OLS players. These players are generally faster out of their initial stance, and able to engage the DL on more plays. For higher OLS players, the down stance may keep the head at a lower height for a longer period, increasing susceptibility for HAEs.

There was also an interesting trend when looking at the match-ups between teams of similar and differing OLS. When two teams of low OLS played each other, the HAE rates were lower than when a low OLS team played a high OLS team. The reverse trend was also observed for the higher OLS teams (lower HAE rates when facing a team with lower OLS). Therefore, given that the offensive lines do not face one another, it is highly probable that the skill of the defensive line contributes to the HAE rate. Note that this outcome is consistent with the idea that, within this setting, the OLS was representative of the overall team skill level. This indicates that having mismatched OLS teams play each other would be harmful for low OLS as the HAE rate increases when playing a high OLS team compared to a low OLS team. Future research should further examine the defensive line and consider how aspects of this position (starting stance, initial line-up, scheme, etc.) affect the HAE rate for players on the offensive line.

In contrast to our prior work, this study represented true game scenarios. The previous study involved an exhibition scrimmage with a set number of plays, representing only

“offense” against “defense.” The current study consisted of four teams that were coached separately, and competed in true game scenarios. The element of competition affected the HAE rate, based on the logistic regression. As a main effect in the model, when the team on offense is winning, the HAE rate increases. This could be due to the fact that the team on defense is losing and attempting to regain possession of the ball, making them play more aggressively and collide with the players on the offensive line more frequently. This relationship is also true when accounting for different play types, proscribed stances, OLS, and match-ups. The exception is high OLS teams in down stances. For this group, if the team is losing, the HAE rate will increase. The players might be working harder to score, causing them to play more aggressively and increase the HAE rate.

4.4.3 Limitations

HAEs are likely not an “all or none” phenomenon with identical thresholds of injury for all individuals. More likely, there is a gradation of injury corresponding to the magnitude of the HAE and brain anatomy of the player. Further, it is unclear if ten 10 g HAEs have the same detrimental cumulative effect as five 20 g HAEs [113]. Several functional MRI studies have observed experimental thresholds at which there are correlations between HAEs and changes in brain health [22], [114], [115]. However, how each individual HAE or HAEs at the same PTA range contribute to the changes observed in functional MRI is not well understood. Understanding how each HAEs translate to microstructural and functional changes in the brain remains a key research target.

There remain challenges associated with current sensor technology and its application [64], [75], [89], [113], [116]. For example, because timestamps required adjustment for each sensor and the difference between the video timestamp and the adjusted sensor timestamp might be several seconds, the HAE rate for the offensive line players was calculated to include any HAE that happened over the course of the play, not just HAEs that occurred directly after the ball was snapped. As this technology improves, more precise measurements of HAEs will become available.

This study only evaluated professional level football players. The effects of beginning stance in OL may differ at different development levels of football, from youth to professional,

presumably due to each individual player’s previous experience. Because OL were mandated to be in specific stances for each quarter, this might have made some players uncomfortable for certain plays. HAE rate could increase if the OL decided to lead with his head from an unfamiliar stance, or could decrease if he was unable to engage with an opponent.

It is apparent that addressing the target of reducing HAEs through changes in stance is more complex than hoped. Skill level, familiarity with the stance, and competitive environment interact with one another in complex ways, and do not lead to simple relationship between play type and stance regarding HAE rate. Future studies should augment analysis to include the defensive linemen, coaching techniques, and explore other rule interventions (e.g., starting offensive and defensive lines further apart) to better discern how stance affects HAE accumulation.

4.5 Conclusion

For higher OLS players, starting in an up stance will help reduce the number of HAEs sustained by players on the offensive line. For lower OLS players, although the HAE rate is lower when starting in a down stance, these players may not be able to play the sport effectively from this stance. Therefore, it still may be reasonable to also start lower OLS players in an up stance because overall, these HAE rates are about the same as that for higher OLS players in an up stance.

More generally, the approach to preventing concussions and difficult-to-detect brain trauma might include rule changes that lessen the occurrence of concussive and subconcussive HAEs [109], [117]. More studies should be done to determine which modifications of the game of football in the categories of policy, rule changes, equipment, and playing technique can be made to lessen brain injury rates while preserving the values of competition that are deemed essential for the athletes and spectators.

5. WHITE MATTER

5.1 Introduction

MRI is a non-invasive method to evaluate soft tissue health and has been used in numerous studies to evaluate the neurological health of contact sport athletes. Many studies have indicated that participation in contact sports causes significant changes in blood flow, chemistry, and the default mode network [2], [19]–[23], [59], [118]. White matter is another brain health biomarker that can be evaluated using a tensor-based analysis of MR diffusion weighted images, known as diffusion tensor imaging (DTI) [24], [63], [114], [119]. DTI has been used to evaluate white matter health post-concussion and demonstrated advanced aging in retired athletes with a history of concussion [120]–[126].

Previous studies found head injuries cause changes in white matter and they are typically characterized by two metrics: fractional anisotropy (FA) and mean diffusivity (MD) [24], [63], [114], [118], [119], [121], [122], [127]–[161]. FA describes the directionality of the water diffusion in the white matter and MD describes the water’s average ability to freely diffuse [162], [163]. These values are calculated from the eigenvalues ($\lambda_1 \geq \lambda_2 \geq \lambda_3$) of the diffusion matrix for the voxel (Eq. 5.2, Eq. 5.1).

$$FA = \sqrt{\frac{(\lambda_1 - \lambda_2)^2 + (\lambda_1 - \lambda_3)^2 + (\lambda_2 - \lambda_3)^2}{2(\lambda_1^2 + \lambda_2^2 + \lambda_3^2)}} \quad (5.1)$$

$$MD = \frac{\lambda_1 + \lambda_2 + \lambda_3}{3} \quad (5.2)$$

The health of brain white matter is of specific interest because it has been linked to strokes, development of dementia, traumatic brain injury, and post-concussive syndrome [121]–[126], [164]–[171]. Cubon et al. found that MD increased in certain brain regions in concussed varsity level college athletes [122]. They also postulated that MD is better able to detect mild brain injury, but that FA is better at detecting and evaluating severe injury [122]. Further work found that substantial white matter changes can be induced by repetitive head acceleration events without a diagnosed concussion [24], [63], [114], [119]. The changes in FA and MD in the brain are associated with different physiological responses within the

white matter (Table 5.1). Decreased FA and with increased MD is thought to indicate compromised structural integrity of the white matter and myelin sheath [128], [129], [139], [141], [144]–[147], [150], [151], [156], [160]. Conversely, increased FA and decreased MD is associated with swelling or inflammation of the white matter [121], [131], [137], [138], [147], [150], [152], [153], [157]. However, the physiological changes associated with homogeneous changes in FA and MD in either direction have received considerably less attention, but increases in both are thought to indicate selective sparing or degeneration of crossing fibers and decreases in both are thought to indicate neuronal degeneration or cell death [133], [134], [154], [172], [173].

Table 5.1. Combinations of DTI metrics and their biological meaning [121], [128], [129], [131], [133], [134], [137]–[139], [141], [144]–[147], [150]–[154], [156], [157], [160], [172], [173].

		FA Change	
		Increase/Higher	Decrease/Lower
MD Change	Increase/Higher	Selective Sparing/ Degeneration of tracts [133], [134], [154]	Tissue Degeneration [128], [129], [139], [141], [144]–[147], [150], [151], [156], [160]
	Decrease/Lower	Swelling or Inflammation [121], [131], [137], [138], [147], [150], [152], [153], [157]	Cell Death [172], [173]

The aim of this work is to extend the analysis of the data in Jang et al. and examine the change in each white matter voxel as a paired measurement of FA and MD [114], [128]. Instead of examining FA and MD separately, joint analysis of these two metrics allows for each voxel in the white matter to be sorted into one of the four categories corresponding to physiological relevant interpretations (Table 5.1). Three analyses were conducted to compare football players to non-contact control athletes. The first analysis compared pre-season data

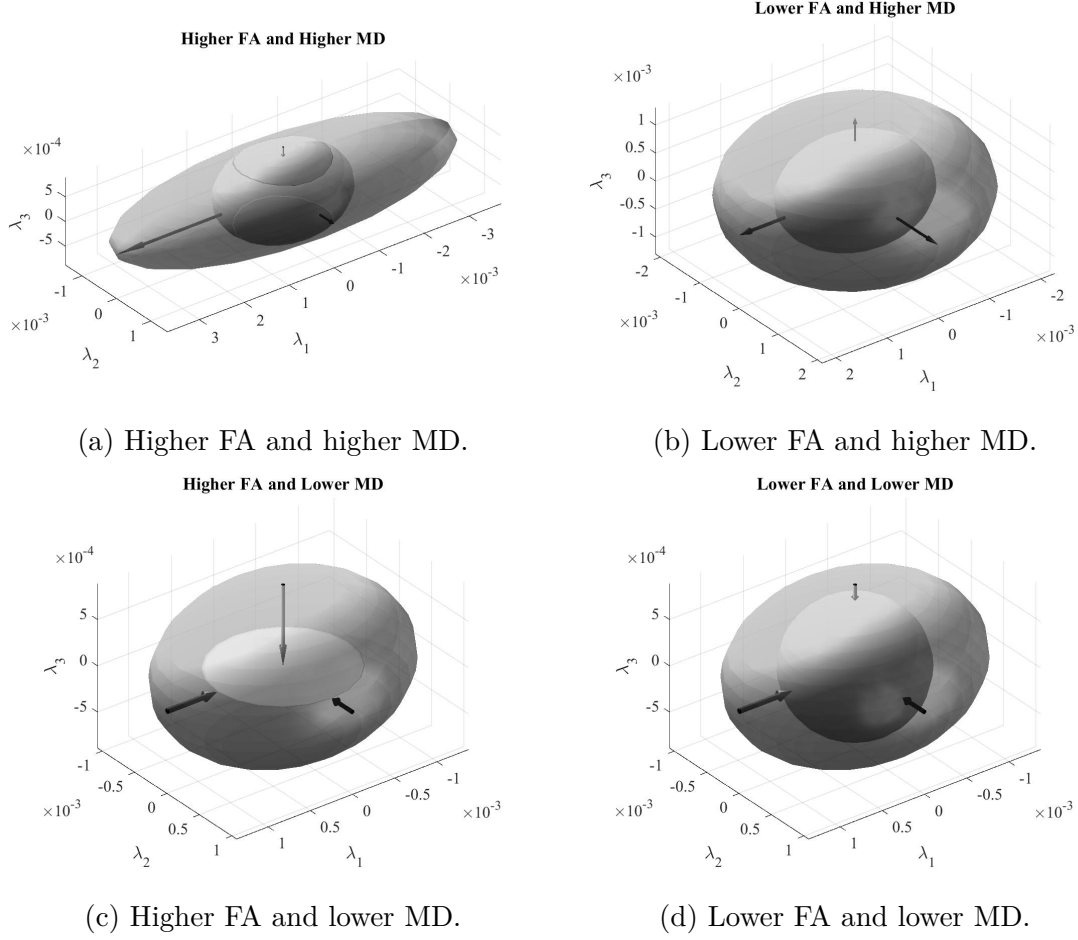


Figure 5.1. Ellipsoid representations of changes in eigenvalues such that a) FA+/MD+, b) FA-/MD+, c) FA+/MD-, and d) FA-/MD-. The direction of the arrows indicates the change in the eigenvalue with respect to the original eigenvalues [174].

from football players to that of the controls to determine if there are differences in white matter health due to prior seasons of competition that have accumulated over time, with the hypothesis being football athletes are significantly different from control athletes. The second analysis examined how FA and MD change due to participation in a single season of football compared to control athletes, with the hypothesis that football athletes will experience a greater percentage of white matter voxels exhibiting changes due to sustaining rHAEs. The third analysis compared post-season data from football players to control data to determine if the white matter changes that occurred over the course of the season result in absolute differences in the white matter, with the hypothesis being football athletes are significantly

different from control athletes more at the post-season than the pre-season. These analyses are specifically focused on white matter that has congruent changes in FA and MD as these have not been examined in detail in athletes.

5.2 Methods

5.2.1 Subjects

All research methods involving human participants were approved by an Institutional Review Board. Participant consent was obtained for those 18 years or older and participant assent and parental/guardian consent was obtained if under the age of 18. Data were collected from 162 male high school football athletes and 19 age-matched, non-contact male athletes to serve as a control group. After quality control assessments and removal of partial data sets, only 61 football players (ages 15-18) and 15 non-contact athletes (ages 14-18) were used for analysis.

5.2.2 Magnetic Resonance Image Acquisition and Data Processing

The full MRI data acquisition and pre-processing methods may be found in Jang et al. [114], and are described only briefly herein.

Data Acquisition

All of the participants were scanned with a 16-channel head coil (Nova Medical; Wilmington, MA) on a 3 Tesla General Electric (Waukesha, WI) Signa HDxt MRI. Football players were scanned four times throughout the season (once before, twice during, and once after the season). Control athletes were imaged twice for test-retest purposes at an interval of 5-18 weeks (average = 7.7 weeks). At each session, DWI scanning (TR/TE = 12000/83.6 ms) was conducted to acquire 46 axial slices with 30 diffusion encoding directions per subject. Scans from all of the sessions were used to generate the white matter skeleton, but only data from scans prior to the beginning of the season and 3-6 months after the season ended (26.4-43.1 weeks between scans; average = 34.8 weeks) were analyzed for the purpose of this study.

Data Pre-Processing

FSL was used to segment brain tissues, correct for motion and eddy current distortions, and replace slices with signal dropout. Original data were upsampled and non-linearly registered to 1 mm isotropic resolution prior to generation of the white matter skeleton such that all of the data were transformed to a standard space. FA and MD were calculated from the fitted diffusion tensor model of each voxel. The white matter skeleton was defined using a threshold of 0.2 on the mean FA image generated from all of the scans, resulting in 110,939 voxels as white matter.

DTI Metric Session Value Comparison

The values from the first scan for the control athletes were used to generate confidence intervals for FA and MD. For each voxel in the white matter skeleton, the 95% and 99.9% confidence intervals (t-distribution, mean $\pm t_{critical} \times$ standard deviation) were calculated for FA and MD using the control values from the first scan session. These confidence intervals were compared to the controls and football players. If the FA or MD value fell outside the 99.9% confidence interval, the voxel-level property likely reflected a spurious measurement and was discarded from further analysis. If the FA or MD value fell outside the 95% confidence interval, but within the 99.9% confidence interval, the voxel was considered to have “primary deviant” behavior (measure₁^{+/-}). When a voxel was found to be primary deviant for FA or MD, the other measure (i.e., MD or FA) was examined to see if the corresponding value was at least one standard deviation from the mean in the control athletes, which was considered to be “secondary deviant” behavior (measure₂^{+/-}). Voxels that exhibited primary and secondary deviant values (double-deviant) were considered for further analysis. Double-deviant voxels were sorted into one of the following categories relative to the mean FA and mean MD values for the control athletes: higher FA, higher MD (FA+/MD+); lower FA, higher MD (FA-/MD+); higher FA, lower MD (FA+/MD-); lower FA, lower MD (FA-/MD-). Each of these categories is the union of two primary/secondary deviant combinations (i.e. FA+/MD+ is the union of FA₁⁺/MD₂⁺ and MD₁⁺/FA₂⁺). Voxels that exhibited primary deviant behavior for both FA and MD were only considered once in the analysis.

DTI Metric Difference Comparison

A procedure similar to that described above compared changes in FA and MD values accrued over activities between the sample points (e.g., retest vs. test; post-season vs. pre-season). The inter-session changes in FA (ΔFA) and MD (ΔMD) values for control athletes were computed and used to generate confidence intervals for ΔFA and ΔMD . As before, 95% and 99.9% confidence intervals were constructed for all of the voxels in the white matter skeleton, here based on the distributions ΔFA and ΔMD (t-distribution; $\Delta \pm t_{critical} \times \text{standard deviation}$) for the control subjects. If the ΔFA or ΔMD value fell outside the 99.9% confidence interval, the voxel likely reflects a spurious measurement, and was discarded from further analysis. If the ΔFA or ΔMD value fell outside the 95% confidence interval, but within the 99.9% confidence interval, the voxel was considered a “primary Δ deviant” voxel ($\Delta \text{measure}_1^{+/-}$). When a primary Δ deviant voxel was observed, the other change measure was examined to see if the corresponding value was at least one standard deviation from the mean in the control athletes (“secondary Δ deviant” voxel [$\Delta \text{measure}_2^{+/-}$]). Voxels that exhibited primary and secondary Δ deviant values (double- Δ deviant) were considered for further analysis. Again, these double- Δ deviant voxels were then sorted into one of the following categories based on ΔFA and ΔMD relative to control athlete session differences: increased FA, increased MD ($\Delta FA+/\Delta MD+$); decreased FA, increased MD ($\Delta FA-/\Delta MD+$); increased FA, decreased MD ($\Delta FA+/\Delta MD-$); decreased FA, decreased MD ($\Delta FA-/\Delta MD-$). Each of these categories is the union of two primary/secondary Δ deviant combinations (i.e. $\Delta FA+/\Delta MD+$ is the union of $\Delta FA_1^+/\Delta MD_2^+$ and $\Delta MD_1^+/\Delta FA_2^+$). Voxels that exhibited primary Δ deviant behavior for both FA and MD were only considered once in the analysis.

5.2.3 Football Athlete Relative Region of Interest Change Factor Visualization

To determine if any regions of interest (ROIs) evidenced a propensity for a type of change more so than other ROIs, visualizations of white matter ROIs were generated for football athletes. This obtained white matter was matched to the JHU White Matter Tractography Atlas (maxprob_thr0, 20 unique ROIs) to categorize each voxel as corresponding to one ROI specified by the atlas [175]. For the i^{th} athlete, the double-deviant or double- Δ deviant

voxels in the j^{th} FA/MD group (FA+/MD+, FA-/MD+, etc.) considered for analysis were sorted into the appropriate (k^{th}) ROI.

$$n_{ijk}^{athlete\ group} = \# \text{ voxels considered for analysis for the athlete}_i \text{ in group}_j \text{ in ROI}_k \quad (5.3)$$

The average number of voxels considered for analysis in the j^{th} FA/MD group for the k^{th} ROI was then calculated for the control athletes.

$$\bar{n}_{j,k}^{control} = \frac{\sum_{i=1}^{15} n_{ijk}^{control}}{15} \quad (5.4)$$

Each ROI for the i^{th} football player was then divided by ($\bar{n}_{j,k}^{control}$) to produce a relative change factor.

$$Relative\ ROI\ Change\ Factor_{ijk}^{football} = \frac{n_{ijk}^{football}}{\bar{n}_{j,k}^{control}} \quad (5.5)$$

The relative ROI change factor characterizes the number of voxels in the specified FA/MD category and ROI that the i^{th} football athlete had, relative to the number of voxels the average control athlete had for the same FA/MD and ROI combination. The median relative ROI change factor for all football athletes was then calculated for each ROI and the entire ROI was then color-coded based on the calculated factor.

Statistics

The number of double-deviant or double- Δ deviant voxels that fell into each FA/MD category was converted to a percentage of the brain white matter by dividing each by the number of voxels (110,939) in the obtained white matter skeleton generated from this group of athletes. A two-sample Wilcoxon rank-sum test ($\alpha = 0.05$) was performed to compare control to football athletes for each FA/MD group. A permutation test (trials = 1,000,000) using the Wilcoxon signed-rank test was performed to compare pre-season ROI likelihood factors to the post-season ROI likelihood factor for each ROI and FA/MD group. Only significant ($\alpha = 0.05$) ROI and FA/MD group combinations were reported.

5.3 Results

5.3.1 Comparison of Football vs. Control Athlete at Pre-Season

Control athletes had a relatively low volume of white matter that exhibited double-deviant values at the pre-season scan (2.04% average). Football players exhibited a higher volume of white matter with double-deviant values than controls at the pre-season scans (5.00% average). Football players exhibited significantly more double-deviant voxels in each category (see Fig. 5.2): FA+/MD+ ($p < 0.001$), FA-/MD+ ($p = 0.002$), FA+/MD- ($p < 0.001$), FA-/MD- ($p < 0.001$).

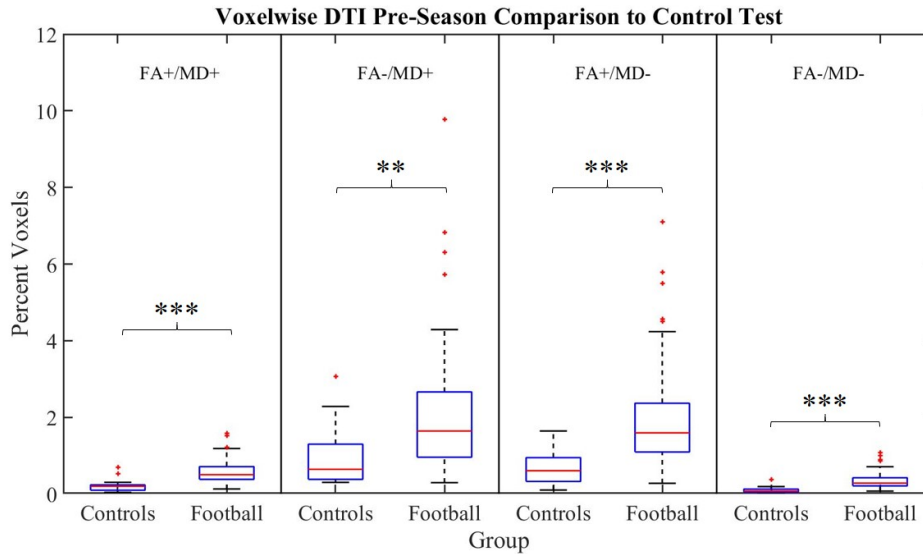


Figure 5.2. Football players have a significantly higher percentage of voxels in each of the categories compared to controls indicating football athletes are different from controls in pre-season.

The pre-season ROI likelihood factor maps for football athletes (Fig. 5.5, top row in subfigures) demonstrate that the football athletes tended to exhibit ROIs categorized as FA+/MD+ (Fig. 5.5a, top row) and FA+/MD- (Fig. 5.5c, top row) fairly homogeneously throughout the brain between 2-3.5 times more likely than control athletes in the specified ROIs. Most of the obtained white matter exhibits less than twice the number of voxels with FA-/MD+ than controls (Fig. 5.5b, top row). The FA-/MD- group (Fig. 5.5d) was concentrated in the inferior portion of the brain (cf., coronal and sagittal planes).

5.3.2 Comparison of Football vs. Control Athlete Over a Season

Control athletes also had a lower volume of white matter that exhibited double- Δ deviant values from retest-test (2.55% average) when compared to the change in football players after a single season of play (6.98% average). As with the pre-season values, football players exhibited significantly more double- Δ deviant voxels categorized as Δ FA+/ Δ MD+ ($p < 0.001$), Δ FA-/ Δ MD+ ($p < 0.001$), Δ FA+/ Δ MD- ($p < 0.001$), and Δ FA-/ Δ MD- ($p < 0.001$; Fig. 5.3).

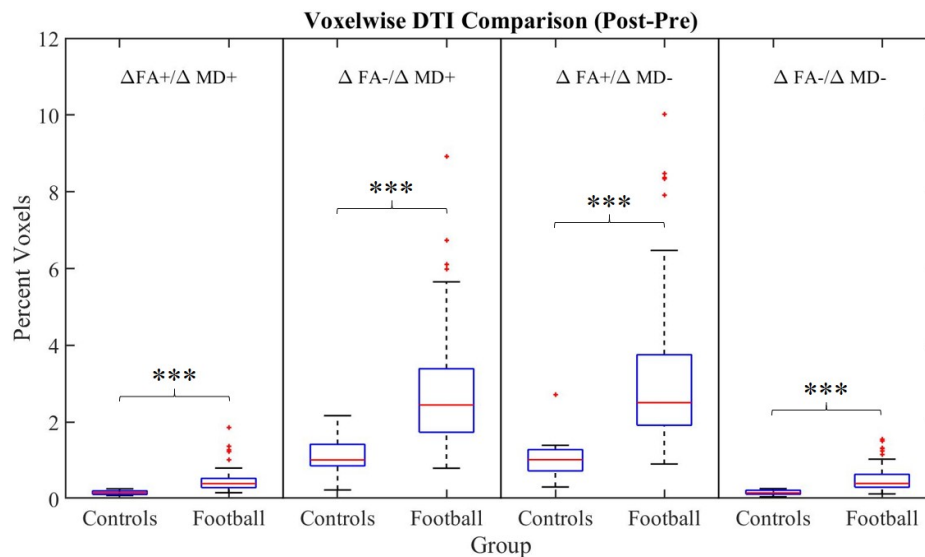


Figure 5.3. Percentage of control and football athletes' voxels that are considered significantly different in either difference in FA or difference in MD at post-season sorted into the four different groups compared to the difference in controls (retest-test).

The ROI likelihood factor maps for football athletes reveal interesting patterns for the different categories of analysis. The change in values after a season of play for football athletes indicates football athletes have ROIs in the Δ FA+/ Δ MD+ (Fig. 5.5a, middle row) category that have changes throughout the brain between 2-5 times more often than controls. While Δ FA+/ Δ MD- occurs homogeneously throughout the brain between 2-3.5 times more than controls (Fig. 5.5c, middle row), Δ FA-/ Δ MD+ (Fig. 5.5b, middle row) occurs more on the left side of the brain while Δ FA-/ Δ MD- (Fig. 5.5d, middle row) occurs more on the right side of the brain.

5.3.3 Comparison of Football vs. Control Athlete at Post-Season

Football athletes also had a greater percentage of white matter voxels at post-season that exhibited double-deviant values from test (4.97% average). As with the pre-season values, football players exhibited significantly more double-deviant voxels categorized as FA+/MD+ ($p < 0.001$), FA-/MD+ ($p = 0.004$), FA+/MD- ($p < 0.001$), and FA-/MD- ($p < 0.001$; Fig. 5.4).

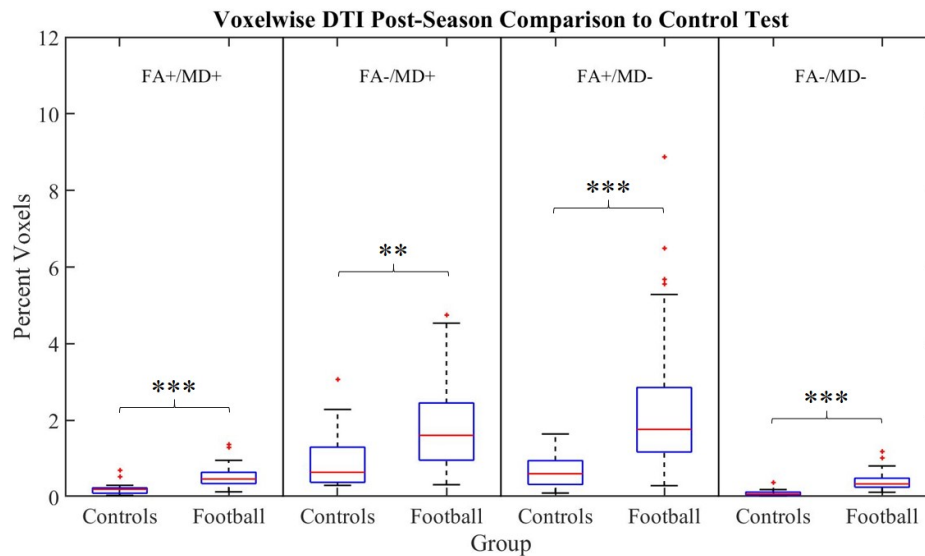


Figure 5.4. Football players have a significantly higher percentage of voxels in each of the categories compared to controls indicating football athletes are different from controls in post-season.

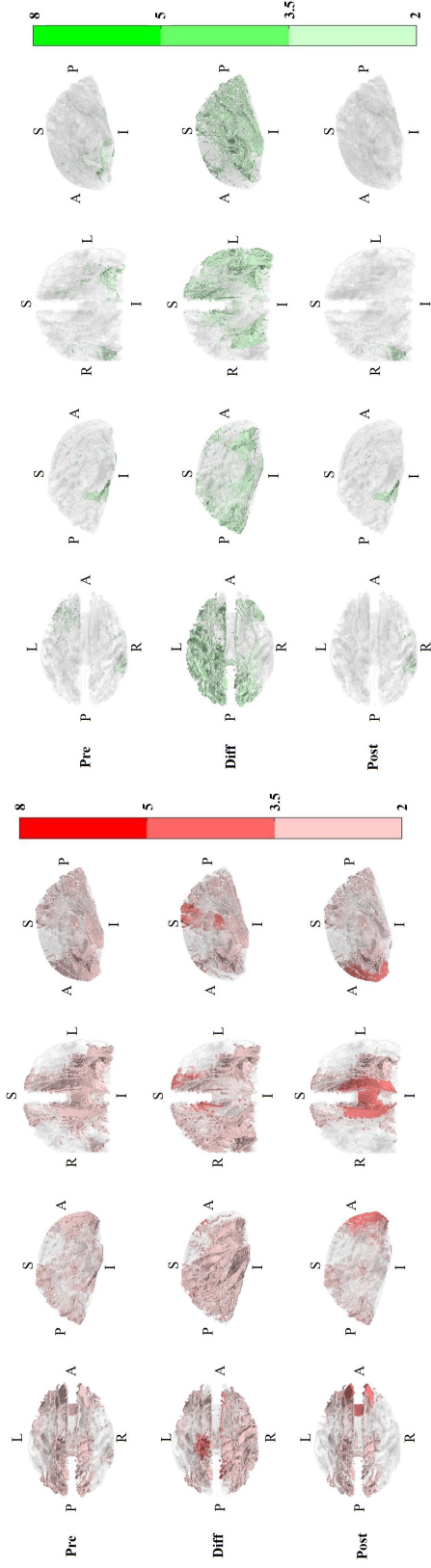
The post-season ROI likelihood factor maps for football athletes (Fig. 5.5, bottom row in subfigures) demonstrate that the football athletes tended to exhibit ROIs categorized as FA+/MD+ (Fig. 5.5a, top row) more in the left anterior portion of the brain (cf., transverse plane). Most of the obtained white matter exhibits less than twice the number of voxels with FA-/MD+ than controls (Fig. 5.5b, bottom row). The FA+/MD- category (Fig. 5.5b, bottom row) at the post-season occurs more on the left posterior part of the brain (cf., coronal and transverse planes). Both the left and right inferior, distal portions of the brain experience higher factors of FA-/MD- (Fig. 5.5d, bottom row).

5.3.4 ROI Likelihood Factor Analysis

There were several ROIs that exhibited significantly different ROI likelihood factors at the post-season assessment compared to the pre-season (Table 5.2). Of interest is that significant ROIs for the FA+/MD+ group was greater at the pre-season than the post-season in one ROI (right corticospinal tract). Conversely, the significant ROIs for the FA+/MD- and FA-/MD- groups were larger at the post-season relative to the pre-season in numerous ROIs. The FA-/MD+ group was not significantly different between pre-season and post-season for any ROI. The left side of the brain also exhibited more ROIs with significantly different likelihood factors than the right side of the brain.

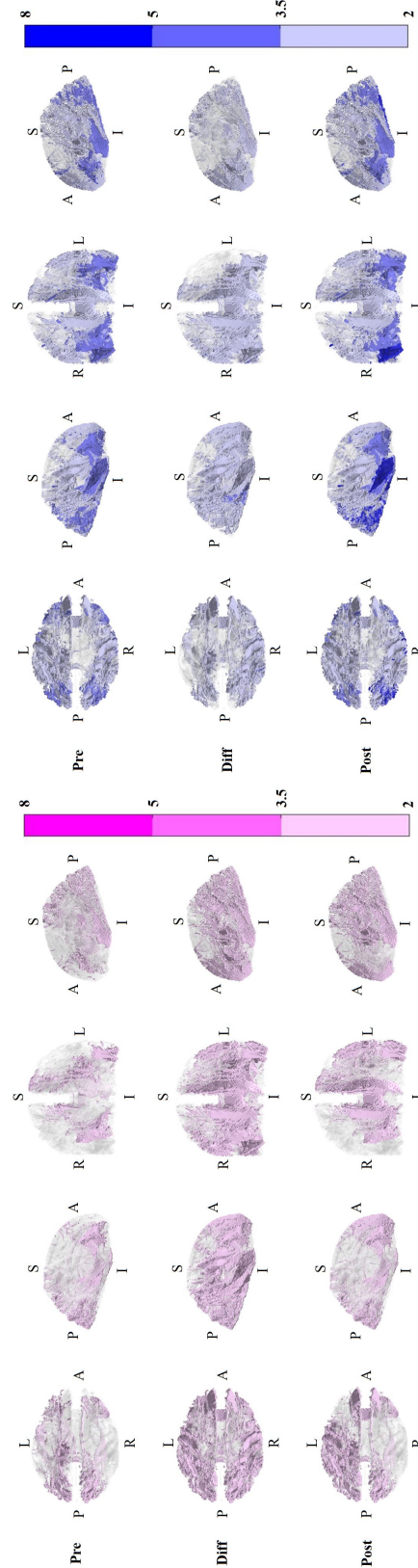
Table 5.2. Comparison between pre-season and post-season likelihood factors for each ROI (L/R: Left-Right hemisphere) and FA/MD category, along with which session was significantly greater than the other. P-values are derived from the distribution generated from permutations ($n = 1,000,000$) of the Wilcoxon signed-rank.

ROI	FA	MD	p-value	Order
Anterior thalamic radiation L	Low	Low	0.018	Post > Pre
Corticospinal tract R	High	High	0.021	Pre > Post
Cingulum cingulate gyrus L	High	Low	0.006	Post > Pre
Cingulum hippocampus R	Low	Low	0.024	Post > Pre
Superior Longitudinal Fasciculus L	Low	Low	0.025	Post > Pre
Uncinate fasciculus L	High	Low	0.048	Post > Pre
	Low	Low	0.024	Post > Pre



(a) Increase FA and increase MD.

(b) Decrease FA and increase MD.



(c) Increase FA and decrease MD.

(d) Decrease FA and decrease MD.

Figure 5.5. Relative ROI change factor maps in the coronal, sagittal and transverse planes for a) FA+/MD+, b) FA-/MD+, c) FA+/MD-, and d) FA-/MD- for pre-season and post-season values compared to control test values. Shade of the color indicates the median factor by which football athletes have more voxels in the ROI/obtained white matter intersection that fell into the respective group than control groups. Note that the darkest shades (width = 3) represent a range twice that of the other shades (width = 1.5).

5.4 Discussion

This study examined differences in white matter health between control and football athletes prior to the beginning of the season to examine if participation in previous seasons of football lead to chronic changes in white matter and over the course of a season to assess whether a single season of football causes more voxel changes in white matter health than is seen in control athletes. Instead of examining FA and MD on a tract-based analysis, a voxel-wise analysis was used to effect a volumetric analysis of changes in diffusivity, comparable to that used in Jang et al. [114]. This analysis sorted significant voxels based on their combination of changes in FA and MD as opposed to using just one metric. Football athletes exhibited greater percentage of double- Δ deviant white matter voxels in all of the different categories of changes in FA and MD compared to control athletes. Similar results were observed when pre-season football athlete white matter values were compared to controls suggesting that repetitive HAEs sustained due to participating in football cause both acute (within a season) and chronic (season to season) changes in white matter.

A majority of the differences in the white matter between football and control athletes at pre-season, post-season, and over a season of play are associated with compromised axon integrity (FA-/MD+, Δ FA-/ Δ MD+) and inflammation (FA+/MD-, Δ FA+/ Δ MD-). The patterns of these persistent differences in football players are most likely a function of their head impact history (location, frequency, and magnitude). Although these two types of changes occur most frequently in the brain (Figs. 5.2, 5.3, 5.4) they are not concentrated to a certain ROI or area (Fig. 5.5). Specifically, the FA+/MD- category is associated with maturation in adolescents which may be why this category, although making up a considerable portion of the obtained white matter for both controls and athletes, is dispersed throughout the brain [176]–[187].

The changes in FA and MD observed between football athletes over the course of the season can most likely be contributed to the repetitive HAEs sustained during the season. The football players were scanned 3-6 months after the end of the season, a period which would theoretically allow healing processes to occur and return the athletes' data back to baseline values. However, the changes in FA and MD persisted even several months after the

end of the season (Figs. 5.3, 5.4), which may indicate that the amount of voxels that change was much larger than the healing processes could fix in that time period. This is consistent with the pre-season results observed which indicated that changes in prior seasons carry over to the next season.

It was also observed that prior to, after, and over the course of a season, football athletes had a significantly greater percentage of voxels with congruent changes in FA and MD (FA+/MD+, Δ FA+/ Δ MD+; FA-/MD-, Δ FA-/ Δ MD-) when compared to control athletes. Although these FA/MD groups make up a small percentage of the white matter (no football athlete exhibited these changes in more than 2% of the white matter), the percentage of voxels are still significantly greater than in the control athletes and could have neurobiological significance. These groups are also more concentrated than the opposing FA/MD categories (Fig. 5.5). Although the overall percentage of voxels in the obtained white matter is less for congruent changes than opposing changes in FA and MD, the fact that they are more concentrated in certain ROIs demonstrates that these groups may be the better indicator for finding commonalities across football athletes in general. FA-/MD- and Δ FA-/ Δ MD- may indicate decreases in both directionality and overall diffusivity, which may be a preceding biomarker to cell necrosis [172], [173].

Differences in the pre-season and post-season ROI likelihood factor revealed an interesting trend in for the different FA/MD groups. Since FA+/MD- and FA-/MD- groups were always greater at the post-season compared to the pre-season, it can be inferred that the rHAEs over the course of a season cause inflammation/swelling in the brain along with a potential increase in neuronal cell death. The left side of the brain also experienced more ROIs that had changes in FA/MD groups than the right side of the brain. This may indicate that the location of rHAEs may lead to a concentration of white matter changes either by coup injury (sustain rHAEs to the left side of the head), countercoup injury (rHAEs to the right side of the head), or as the result of a common biomechanical reaction to rHAEs from the front and back (i.e. common had motion among players that result in more white matter changes on the left side of the brain) [98].

5.4.1 Monte Carlo Simulation to Investigate Trends

An interesting trend revealed in the analysis was that the percentage of voxels in groups with congruent changes in FA and MD are less than the percentage of voxels in groups with opposite changes in FA and MD, even for the control athletes. Based on probability, it could be argued that there should be similar percentage of voxels for each group if it is thought that each voxel has the same probability for FA/MD to increase or decrease. However, FA and MD are related as they are both calculated from the eigenvalues of the diffusion tensor. Therefore, the changes in FA and MD are not independent and their relationship was investigated using a Monte Carlo simulation on the eigenvalues.

The data collected from the 15 non-contact male athletes were used as a basis for the simulation. The eigenvalues ($\lambda_1 \geq \lambda_2 \geq \lambda_3$) were extracted from the diffusion tensor in each voxel for each participant. Voxels that had all zero eigenvalues or any eigenvalue less than zero were removed. The mean and standard deviation for all of the eigenvalues were calculated considering all participants. For each eigenvalue (i), 1 million samples were taken from a Gaussian distribution [$N_i \sim (0, \text{standard deviation}_i)$] and were added to the respective mean eigenvalues to generate 1 million sets of three simulated eigenvalues. The simulated sets were checked to ensure that $\lambda_1 \geq \lambda_2 \geq \lambda_3$ and that all of the eigenvalues were positive. If these conditions were not met, that set of simulated points was removed and another set of simulated points was generated. This process continued until 1 million eigenvalue sets satisfied these conditions.

The FA and MD values were calculated for all 1 million simulated eigenvalue sets. The 95% and 99.9% confidence intervals (t-distribution; $mean \pm t_{\text{critical}} \times \text{standard deviation}$) were calculated for FA and MD. The same approach used to sort the FA and MD values for the football and control athletes was applied to the simulated data. A similar trend was seen in terms of the percentage of voxels that fell into each group (Fig. 5.6). In the simulation, more voxels will have double-deviant behavior expressed as opposing changes in FA and MD rather than changing in the same direction (Fig. 5.6).

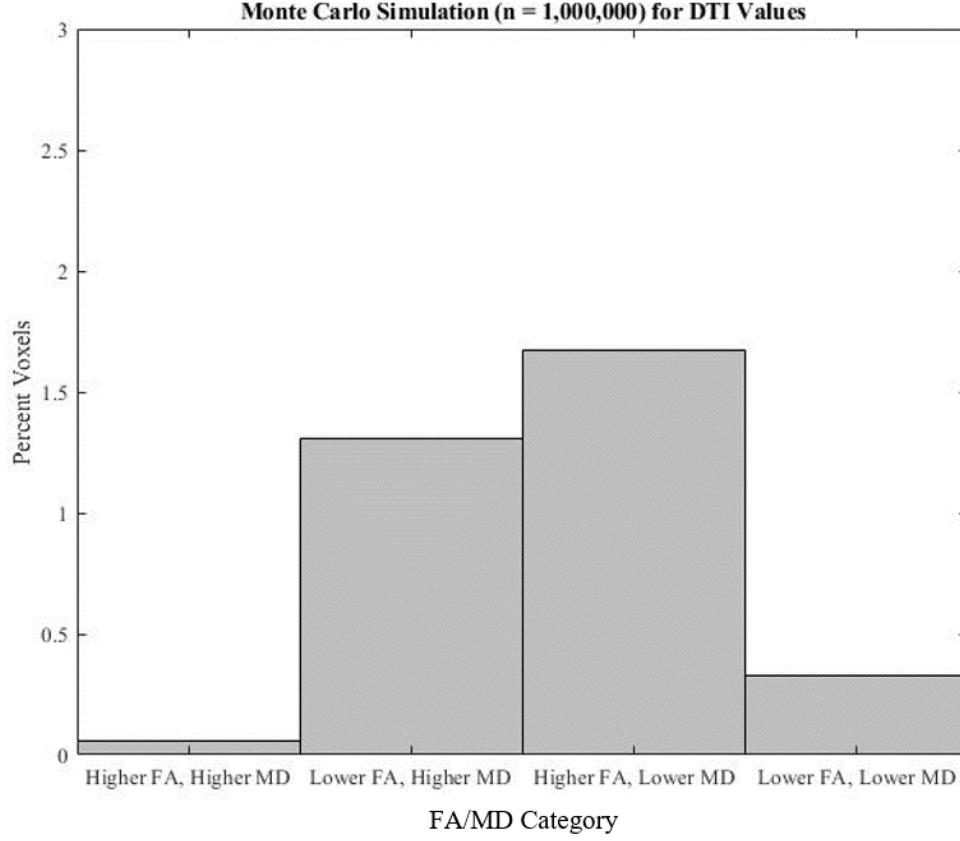


Figure 5.6. Results from a Monte Carlo Simulation of eigenvalues to quantify the effect of noise on FA and MD sorted values. The simulation reveals a similar trend seen in both controls and football athletes with opposing changes in FA and MD occurring more frequently than concurrent changes.

5.4.2 Limitations

Limitations of this work include the difference in scan time for the football athletes compared to the control athletes. While minimal effect is anticipated, future work should scan these athletes at similar time intervals. Also, football athletes may have competed in other activities between the end of football season and their post-season scan where they sustained HAEs (i.e. wrestling) that could have affected their DTI measures. Each of the four categories for double-deviant and double- Δ deviant voxels is a combination of two sub-groups (i.e. FA+/MD+ is the union of primary FA+/secondary MD+ and secondary FA+/primary MD+). An argument could be made that there should be eight different groups of compar-

ison, taking into account which of the white matter metrics was the primary deviant and which was the secondary deviant measure. While we are confident the voxels we have identified as double-deviant are meaningfully altered from normal, we are not confident that either measure's change is necessarily more important than the other. Due to this uncertainty, the sub-groups were collated to represent a single double-deviant or double- Δ deviant category. There is also a limitation of the atlas used for correlating the obtained white matter to known white matter tracts and ROIs. There may be misalignment between the obtained white matter and the defined ROIs in the atlas, but both utilized Montreal Neurological Institute (MNI) space as a basis for alignment and approximately 70% of the obtained white matter can be categorized by the ROIs in the atlas.

5.5 Conclusion

The percent of white matter metric differences/changes in football players is greater than control athletes, likely the result of rHAEs. White matter metrics should be analyzed jointly instead of separately as this provides a better indication of what is happening on a cellular level. Future work will examine the time course of FA and MD changes and whether there are genetic risk factors as well as imaging or blood-based biomarkers that can presage them.

6. RUGBY HAE STUDY

6.1 Introduction

With all of the research that has been performed on American football (football for the remainder of the chapter) athletes, other contact sports have not yet been studied to the same extent. Rugby is a sport that is very similar to football in terms of physicality and overall objective. However, there are marked differences in protective equipment, with football players wearing mouthguard, helmet, shoulder pads, and leg pads, and rugby players have optional protective equipment, with mouthguards only required for certain levels depending upon the country [188]. These differences in protective equipment result in different tackling rules and styles between the two sports that may influence the effect repetitive HAEs can have on neurological health. Despite all of the studies that have been conducted on football athletes and that fact that CTE has confirmed in a former rugby athlete, the affect of repetitive head trauma on rugby athletes has yet to be fully examined and few studies have been able to quantify the magnitude of the repetitive head impacts [189]–[191]. Therefore, this study aims to characterize HAEs experienced over the course of the season by New Zealand collegiate (ages 12-18) rugby athletes to allow for a comparison between rugby and football.

6.2 Methods

6.2.1 Participants

All research methods involving human participants were approved by the Auckland University of Technology Ethics Committee prior to the beginning of the study. Participants were recruited from one New Zealand high school/college rugby program (ages 12-18). All of the participants were 16 years or older and were able to self-consent to the study. A total of 34 male rugby athletes enrolled in the study. Participants were categorized by position as either a forward or back for each game.

6.2.2 HAE Data Collection

Head acceleration events were monitored using custom-fit Nexus A9 Smart Mouthguards (hitIQ Pty Ltd; South Melbourne, Australia; precision and accuracy testing performed by company). There were approximately three months between fitting the mouthguard and deploying the mouthguards for the study. During this time, dentition changed for five of the enrolled participants (i.e. braces), causing the previously fitted mouthguards to be unusable for these players in the study, reducing the number of participants with HAE data to 29. Rugby participants wore the smart mouthguards for 14 contact practices/trainings, six games/matches and two scrimmages/pre-season matches during the season. Each HAE was recorded as a separate “event” on the sensor. Data were downloaded by hitIQ and sent to researchers (hitIQ Pty Ltd; South Melbourne, Australia).

There were four sessions (two games and two practices) where the mouthguards were deployed, but technical issues occurred which resulted in no HAE data from those sessions. This reduced the total number of monitored contact practices to 12 and games to four.

6.2.3 HAE Data Analysis

For games, a similar Matlab program to what was described in Ch. 2 was used to analyze the HAEs. However, for games, outlier analysis was disabled since the HAEs were confirmed via video analysis. Also, a PTA threshold of 10 g was used to examine the effect of a changing threshold on the data analysis. Data points were removed if the mouthguard was suspected it was not in the mouth but was recording events (i.e. stored in the sock; five consecutive seconds of events being recorded when player was running for four seconds and involved in a collision event for one second).

6.2.4 Video Analysis

Rugby games were recorded by team personnel and viewed by researchers via Hudl (Agile Sports Technology, Inc.; Lincoln, Nebraska). The video was used to verify HAEs caused by a rugby match action, determine possession of the ball, calculate playing time for each player to determine individual athlete exposure, and classifying the cause of HAE. The video was

examined at the HAE time stamp acquired from the mouthguard (within a window of 10 seconds, 5 seconds on each side of the HAE time stamp to allow for variation between the HAE time stamp and the video time stamp). Possible causes of HAEs were: tackle (or attempted tackle), ruck (either as a direct participant or as the player underneath the ruck), scrum, maul, and other. For tackle designations, instead of the designation being “tackled” or being the “tackler” (initiating the tackle), possession of the ball was noted at the time (i.e. if their team had possession of the ball [offense] or not [defense]). Even though players on defense typically initiate the tackle and engage with an offensive player, if the offensive player is well prepared for the collision, they may be considered the “tackler” and initiating contact. Therefore, to avoid ambiguity on who had initiated the tackle, possession of the ball was noted as the team to last have controlled possession of the ball. Video and sensor data were only available for four games, so only these data were considered in the analysis.

6.2.5 Statistics

Statistics were calculated using IBM SPSS Statistics 26 (IBM; Armonk, NY) to determine if metrics were significant ($\alpha = 0.05$). The number of HAEs per game was calculated by counting the number of HAEs above a the specified PTA threshold and dividing by the percent of playing time for each specific player for that game (Eq. 6.1).

$$n_{HAEs \text{ per Game}} = \frac{n_{HAEs \text{ sustained}}}{\text{fraction of game played}} \quad (6.1)$$

Comparison by position was performed using a two-sample t-test if normality (Shapiro-Wilk) and equal variance (Levene’s Test) assumptions are satisfied or a Mann-Whitney (MW) test if they were not. Possession and HAE cause/type comparisons were performed using either a two-sample t-test/ANOVA (if normality and equal variance assumptions are satisfied) or a MW/Kruskal-Wallis (KW) test (if assumptions not satisfied). Post-hoc testing consisted of Tukey’s test or pairwise MW tests with a Bonferroni correction to determine pairwise differences for significant ANOVA and KW tests, respectively.

6.3 Results

A total of 254 HAEs were considered for analysis. Forwards sustained 151 HAEs in the games and backs sustained 103. While in possession of the ball, 108 HAEs were sustained and 146 were sustained while on defense. With respect to the type of HAE, 133 were sustained during a tackle, 92 during a ruck, 1 during a scrum, 14 during a maul, and 14 during some other type of event. Due to the vast differences in sample size, analysis of HAE type will only consider HAEs by tackle and ruck.

From the four games, a total of 24 player observations (11 forwards, 13 backs) were considered for analysis as these players a) participated in the game and b) had a functioning mouthguard for that game. One player observation (forward) was not considered for the number of HAEs per game analysis since he played in less than 10% of the game. There were no significant differences between forwards and backs at the 10 g (t-test, $p = 0.050$), 20 g (t-test, $p = 0.123$), or the 50 g threshold (MW test, $p = 0.284$), although the trend at each level was that forwards sustained more HAEs than backs per game (Table 6.1).

Threshold	Forwards	Backs	All Players
10 g	19.5, 19.3 (13.0, 27.5)	12.0, 11.5 (4.8, 15.4)	15.2, 13.0 (8.8, 21.7)
20 g	10.0, 10.2 (8.0, 12.0)	6.4, 7.0 (2.3, 9.9)	7.9, 8.1 (3.3, 11.2)
50 g	2.1, 2.3 (0, 4.0)	1.3, 0 (0, 3.0)	1.6, 1.0 (0, 3.4)

Table 6.1. The estimated number of HAEs per game sustained by each position and all players. Values in the cell are the mean, median (lower quartile, upper quartile). There were no significant differences between the number of HAEs sustained by forwards and backs at any of the different threshold levels.

When a threshold of 20 g was applied to the data (Fig. 6.1), 130 HAEs were considered in the analysis, with 56 sustained while on offense and 74 sustained while on defense. The forwards accounted for 76 of the HAEs over 20 g and the backs accounted for 54 of them. For HAE type, 70 were the result of a tackle, 46 from a ruck, one from a scrum, seven from a maul, and six caused by other mechanisms (due to differences in sample size, only compared PTA between tackle and ruck). There were no significant difference for the PTA of a HAE between forwards and backs (Fig. 6.1a; MW, $p = 0.992$), offense and defense (Fig. 6.1b; MW, $p = 0.232$), or between a tackle and a ruck (Fig. 6.1c; MW, $p = 0.391$). However, there was

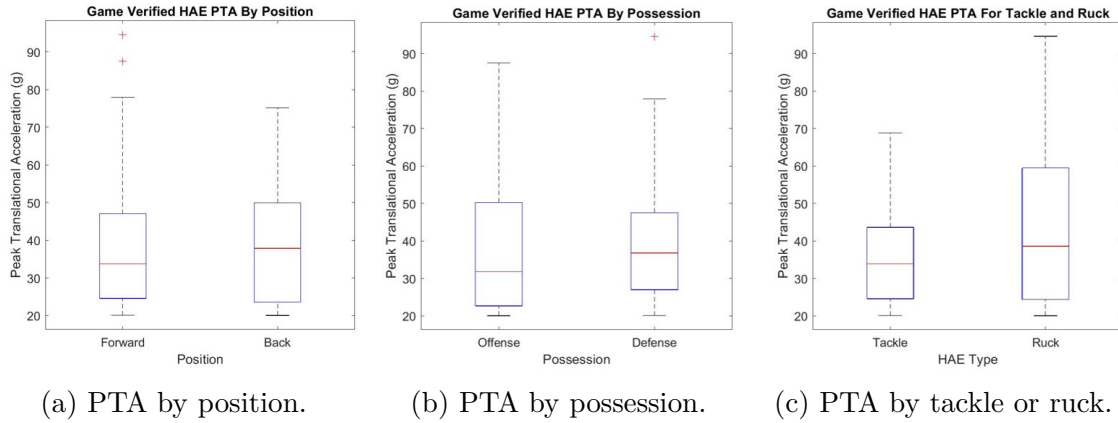


Figure 6.1. When HAE PTA is analyzed by a) position (MW, $p = 0.992$), b) possession (MW, $p = 0.232$), or c) mechanism (tackle or ruck; MW, $p = 0.391$), there are no differences between the different groups.

a significant difference in PTA of a HAE when considering both possession and cause of the HAE (KW, $p = 0.031$; Fig. 6.2). There was a significant difference for the PTA between a defensive ruck and an offensive ruck (MW, $p = 0.008$).

6.4 Discussion

This study aimed to characterize the HAEs of young adult male New Zealand rugby players to better understand the mechanical load sustained by the brain during play and to compare the results to similar previous studies performed on football players. Asymptomatic changes in brain health due to repetitive HAEs in contact sport athletes is concerning due to their potential to lead to chronic neurological health issues later in life. Specifically in rugby where there is no mandated protective head gear, these athletes need to be examined to understand the HAEs sustained during rugby and to see if there are potential interventions that can be shared between similar sports (i.e. football) to improve player safety for all athletes.

6.4.1 Difference by Position

Although there was no statistical difference at any of the three thresholds, forwards tended to sustain more HAEs than backs during games. A previous study found that linemen

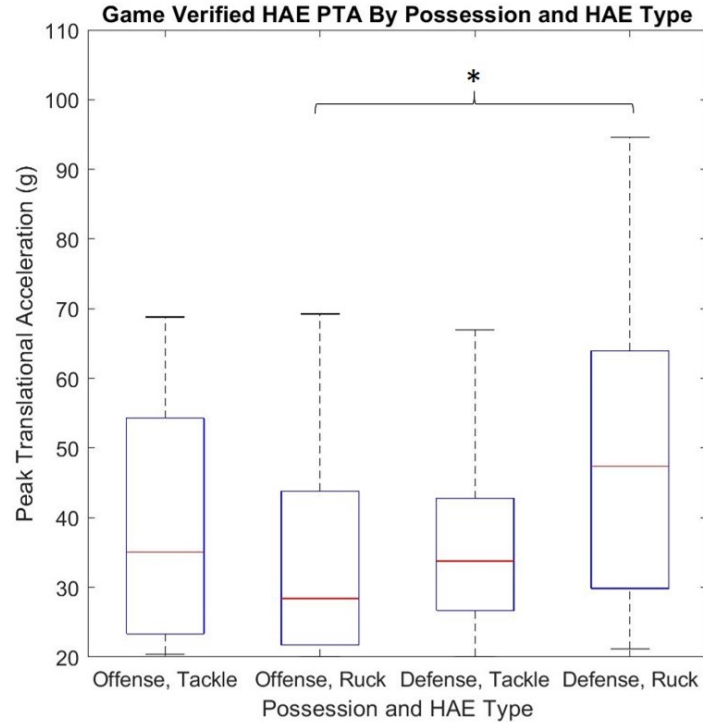


Figure 6.2. Differences in the PTA of a HAE when considering possession and cause of the HAE (KW, $p = 0.031$). There was a significant difference between a defensive and offensive ruck (MW, $p = 0.008$).

in football sustain more HAEs than other positions (most likely due to their engagement with opponents on almost every play), which would make forwards in rugby similar to linemen in football [192]. Forwards are involved in open field tackles, the scrum, and, typically, the ruck, putting them in situations where they can accumulate more HAEs than backs. The small sample size may be limiting the statistical power of the analysis.

6.4.2 Difference by Possession

There were no differences in the PTA of a HAE if the team was in possession of the ball or not. Every player in rugby plays both offense and defense due to the continuous nature of the game. Therefore, a player may have similar biomechanics during a collision event regardless of whether they are on offense or defense. Rugby also requires the ball to be passed backwards and that each team must (typically) be on their respective side of the

offside line at the beginning of each play, leading to tackles that involve players that are facing each other which may reduce the vulnerability of players during collisions and the frequency of the blindside tackle. These fundamental rules of rugby may make it so there is not a difference in HAEs by possession.

6.4.3 Difference by Cause of HAE

Although not main effect, the difference between defensive ruck and offensive ruck reflects, at least for this study, the aggressive nature of the players and willingness to get the ball back. During a ruck, a play is momentarily paused until the offense picks up the ball again unless the defense breaks through the gate to regain possession of the ball. There is usually an offensive player over the player on the ground and in order to win back possession, a defensive player must engage with that offensive player. The results indicate that when on defense, players may be more willing to do whatever it takes to regain possession of the ball and engage in higher magnitude collision events. Another scenario in a defensive ruck is if a defensive player is engaged with the ruck or trying to poach the ball, an offensive player may come in and drive the defense off the ball in order to protect it and maintain possession. If unaware of the incoming offensive player, the defense may be caught unaware of the eminent collision if focused on the ball, which may result in the higher PTA observed. A defensive ruck may be a place to work on proper technique to keep the head out of the way to lower/reduce HAE readings.

6.4.4 Comparison to Previous Rugby Studies

The trends from this study are consistent with previous rugby studies conducted in other age groups. In junior league (11 years old and younger) and premier amateur senior rugby players (mean age of 22 years), it was also seen that forwards tended to sustain more HAEs than backs in games [190], [191]. This indicates that the use of forwards and backs in play may be consistent across different levels of play and adjustments that can be made to protect forwards can be instituted and effective at all levels. Two ways that can help reduce the

HAEs for forwards may be to require substitutions for forwards during games or to limit the HAEs sustained by these players during practice to limit overall HAEs during the week.

6.4.5 Sport Comparison: Rugby vs. Football

Rugby and football have a similar level of physicality in their games, with players on teams using their bodies to bring an opposing player to the ground in the hopes of regaining possession of the ball. However, there are some key differences between the two sports that merit further discussion.

There are differences in the equipment for the two sports, with football players wearing a mouthguard, helmet, shoulder pads, and leg pads, and rugby sometimes requiring a mouthguard. These differences can lead to different tackling mechanisms and techniques. The helmet worn by football players provides a reduction in the PTA and PAA of a HAE, but can also provide a false sense of security that a player will be “safe” if they hit their head or use it as a weapon [75]. Conversely, since there is no required protective head gear in rugby and a high tackle (above the shoulders) is illegal, this forces the players to engage with the body of an opposing player as opposed to using their head. Players in rugby can still hit their head against the ground or in ruck or scrum, but the rules limit direct head contact during tackles. When using a threshold of 20 g, the mean player PTA mean for a HAE in rugby (38.8 g) is comparable to that in football (36.2 g). This may indicate that there are offsetting effects of the helmet; although it does reduce the PTA of a HAE, since it is legal to hit the head (as long as it is not deemed a dangerous hit), this could result in higher accelerations of the head so that rugby and football are similar. This means that implementing a high tackle rule in football similar to that in rugby may help to reduce the PTA of a HAE in football.

Game play is also different between rugby and football that can cause differences in HAE characteristics. Most of the rugby game consists of passing the ball from player to player to move the ball up the field, although kicking the ball down field is used as well. For passing, rugby requires that the ball must be passed backwards to a player and that opposing players typically must be behind the offside line. Football consists of both run and pass plays, but pass plays often occur when a receiver is down field and they must turn backwards to catch

the ball, so they may have their back to opposing players, which may be the reason pass plays result in higher magnitude HAEs [112]. Being able to see an incoming opponent may help a player to better prepare for a collision and reduce the PTA of a HAE. Designing plays in football that will reduce the vulnerability of receivers may help to better protect these players.

6.4.6 Limitations

Due to the small sample size of the study, there were few significantly different results, and some groups were excluded from analysis due to the small sample size. A larger sample size in future studies should be considered to determine if trends found in this study are significant. This analysis also only examined rugby games. A future study should also use video analysis to look at practices and see if there are any drills or training habits that can be further improved upon using data from a study similar to the one conducted here. The video system used to classify HAEs was a separate system from the instrumented mouthguards. Because of this, the time stamp in the video and the time stamp for a HAE recorded on the mouthguard may be off by several seconds and with the fast paced nature of a rugby game, can make it difficult to classify HAEs. Future work may develop a single system such that the video and the mouthguards run on the same clock. The comparisons between this study and other rugby and football studies are limited because of the use of different sensor systems and PTA thresholds. A future study that uses one type of sensor will help to provide a better comparison.

6.5 Conclusion

Rugby players sustain repetitive HAEs that may be detrimental to their acute and chronic neurological health. Forwards sustain more HAEs than backs during games and HAEs sustained in a defensive ruck result in higher PTAs than other collision situations. Improving technique and awareness in a defensive ruck could help to reduce the severity of HAEs sustained in these situations. Future work should aim to gather a full season of data from a complete team.

7. INSTRUMENTED HELMET

7.1 Introduction

Based on the previous studies and the work described thus far, it has been observed that HAEs are the likely culprit for inducing asymptomatic neurological changes in contact sport athletes. Much of this work has utilized accelerometers and/or gyroscopes to measure the linear and angular accelerations of the head during a contact event. While this information is extremely useful in quantifying the mechanical load on the brain, the acceleration of the head is influenced by the force and location of the impact, protective equipment worn, and neck muscle activation and strength. A current gap in the field is quantification of the head impacts during contact events. Obtaining a better understanding of the forces during direct head impacts will provide insight to the muscle forces of individual players during a contact event, can be used to better design the helmets for different levels of play, and may be used to automatically call illegal head-to-head tackles.

Previous work has examined the frequency response of the helmet during impacts to better understand head contact in football, but were only able to examine the response during low force events (100-200 pound-force) [193]. Other work has used nano-composite foam to measure impact characteristics [194], but this work only consisted of 20 different drop tests and correlated the foam data to accelerometer, not impact force, data. Also, foam between the helmet shell and head can be compressed by the head without any external impact to the helmet resulting in false readings. In order to capture high force events (1000+ pound-force), strain gauges are the proposed alternative to capturing the force during in-play contact events. This method has been previously proposed and patented [195], but no data can be found on the helmet described in the patent. The hypothesis is that adhering strain gauges to the inside shell of a football helmet and testing it in a laboratory setting will produce an instrumented helmet capable of measuring the impact force and location during play. The objectives of this project are to: (1) determine if strain gauges are an appropriate sensor for this application and (2) find a method that can use the strain gauge data to accurately predict impact location and force. Meeting these objectives will inform future design considerations for a deployable instrumented helmet.

7.2 Methods

7.2.1 Circuitry Components and Design

The circuit to capture the strain measurements had five main components: the strain gauge, the multiplexer, the Wheatstone bridge, the differential operational amplifier (op amp), and development board (Fig. 7.1).

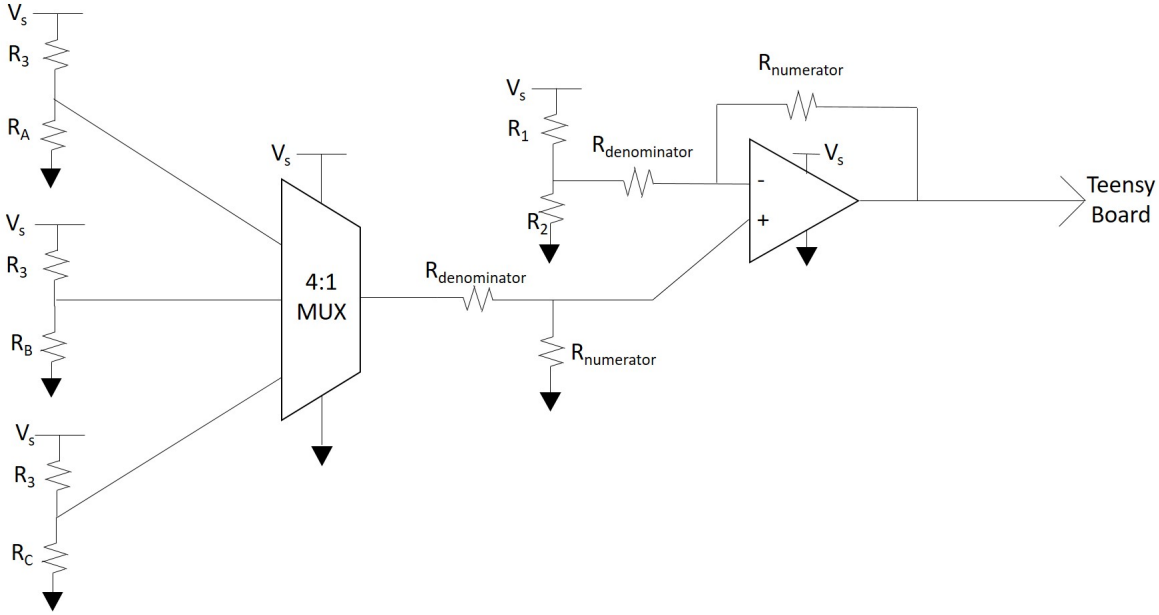


Figure 7.1. Schematic of the circuit and its components. The voltage above the strain gauge was fed to a multiplexer to iterate through multiple inputs. That voltage was then fed into one input of the op amp and the other op amp input was the second half of the Wheatstone bridge. The configuration of the op amp magnified the difference between the voltage difference at the inputs before sending the data to the development board. Abbreviation and values can be found in Tables 7.1 and 7.2.

Strain Gauges

The strain gauge sensor selected for testing was the 1-RY93-6/350 stacked rosette style strain gauge from HBK (Hottinger Baldwin Kjaer Inc.; Darmstadt, Germany; nominal values listed in Table 7.1; Fig. 7.2). These strain gauges were selected due to their high flexibility ($\pm 5\%$) since the strain change in a helmet during a collision are currently unknown. After

laboratory testing, it may be revealed that a lower flexibility range will be sufficient to adequately capture the strain. This would also reduce the overall power consumed by the circuit as lower flexibility strain gauges are available at higher resistances.

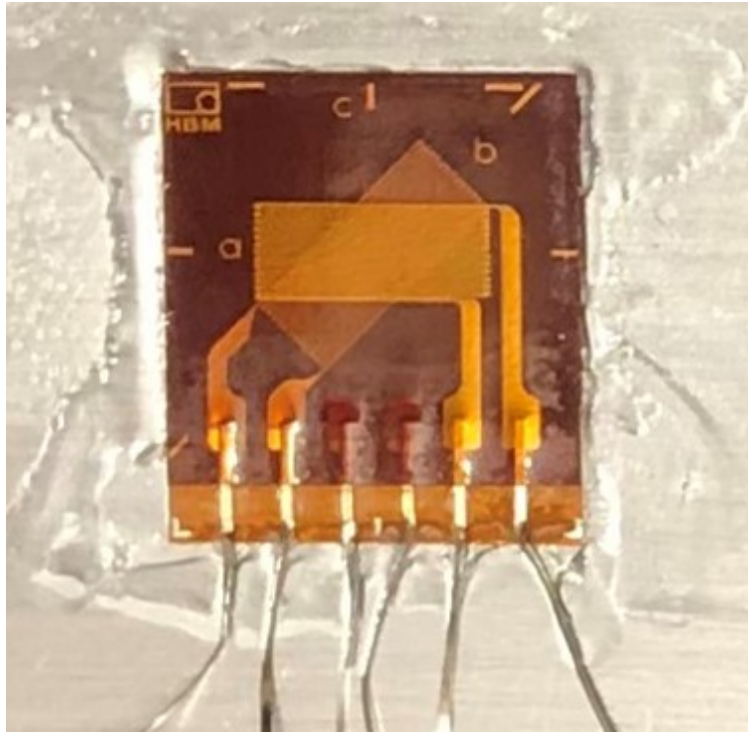


Figure 7.2. Image of the HBM rosette. The three strain gauges are stacked where the A and C strain gauges are orthogonal to each other and the B strain gauge is angled half way so that it is offset 45° from both axes (necessary values found in Table 7.1).

Multiplexer

The signal from the strain gauges were fed through a multiplexer and op amp before being input into the development board (Fig. 7.1). In order to read in 60 signals, a multiplexer was used to reduce three strain gauge readings to be read into a single input for the development board. The MAX4618 CMOS 2 channel, 4:1 multiplexer was used (Maxim Integrated; San Jose, CA). Only three channels on one channel of the multiplexer were used. The switching time is on the order of nanoseconds. Each multiplexer read in the signals from one rosette (three strain gauges).

Table 7.1. Strain gauge nominal values and ranges (if applicable). The subscript i represents the value for all of the strain gauges in the rosette (A, B, or C). Specific values for individual strain gauges are provided if necessary.

Property	Symbol	Value
Nominal Resistance	$R_{i,nominal}$	$350 \Omega \pm 0.50\%$
Gauge Factor	k_A	$2.11 \pm 1.0\%$
	k_B	$2.10 \pm 1.0\%$
	k_C	$2.12 \pm 1.0\%$
	k_{poly}	2
Transverse Sensitivity	q_A	-0.1%
	q_B	-0.4%
	q_C	-0.5%
Gauge Factor Temperature Coefficient	α_k	$101 \times 10^{-6} \text{ K}^{-1}$
Calibrating Poisson's Ratio [196]	ν_0	0.285
Lead Length	L	30 mm
Thermal Expansion Coefficient [197]	α_{SG}	$23 \times 10^{-6} \text{ K}^{-1}$

Wheatstone Bridge and Differential Amplifier

After the multiplexer selected one signal, the selected signal was then input to the differential amplifier as part of the Wheatstone bridge. The differential amplifier was used to increase the voltage difference across the Wheatstone bridge to an appropriate level for the development board (Fig. 7.3). The op amp used was a MCP6004 (Microchip Technology Inc.; Chandler, AZ). The values for the resistors in the Wheatstone bridge and for the differential op amp can be varied to affect the voltage difference and gain (selected values in Table 7.2). Resistor values for the differential op amp were chosen assuming a nominal resistor values for the Wheatstone bridge if the maximum strain is reached by the strain gauge ($\pm 5\%$) so that the voltage fed to the development board will not rail out. After the calculations, a gain factor of 15 was selected.

Development Board

A Teensy 4.1 development board (PJRC; Sherwood, OR) was used to read in the analog signal from the differential op amp and converting to digital signals. The Teensy 4.1 board had an Arm Cortex-M7 core, which had a 600 MHz CPU. The development board had

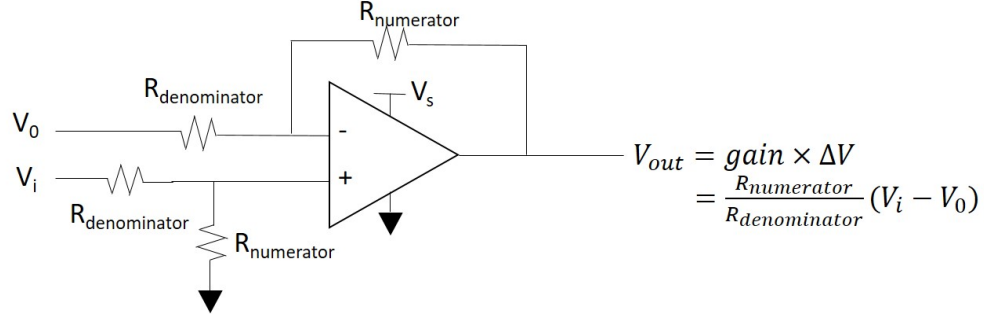


Figure 7.3. Schematic for how a differential op amp works.

Table 7.2. Wheatstone bridge and differential op amp values.

Property	Symbol	Value
Voltage Source	V_s	3.3 V
Control Upper Resistor Resistance	R_1	560 Ω
Control Lower Resistor Resistance	R_2	300 Ω
Pull-up Resistor Resistance	R_3	560 Ω
Numerator Gain Resistor Resistance	$R_{numerator}$	10 k Ω
Denominator Gain Resistor Resistance	$R_{denominator}$	150 k Ω

18 analog input pins, but only 10 were used, with one rosette feeding into each input. The development board had two 16-channel analog-digital-converters (ADCs). The Teensy board was required to: read in the amplified analog voltage difference of the Wheatstone bridge, convert the analog signal to a digital signal, and write the data to a SD card. Once data collection was complete, data were downloaded from the SD card and formatted to a csv file containing the amplified voltage difference of the Wheatstone bridge.

In order to achieve the desired sampling rate of 2 kHz for each strain gauge, a maximum of 30 strain gauges (10 rosettes, 10 analog inputs) were possible for one Teensy board to manage. Because of this, two Teensy boards were used to collect data from the instrumented helmet which contained a total of 20 rosettes, or 60 strain gauges (Fig. 7.4).

Time Sync Data Processing

Since two development boards were used to collect the data, a way to align the data in the time domain became necessary. This was done by having one board serve as the “parent”

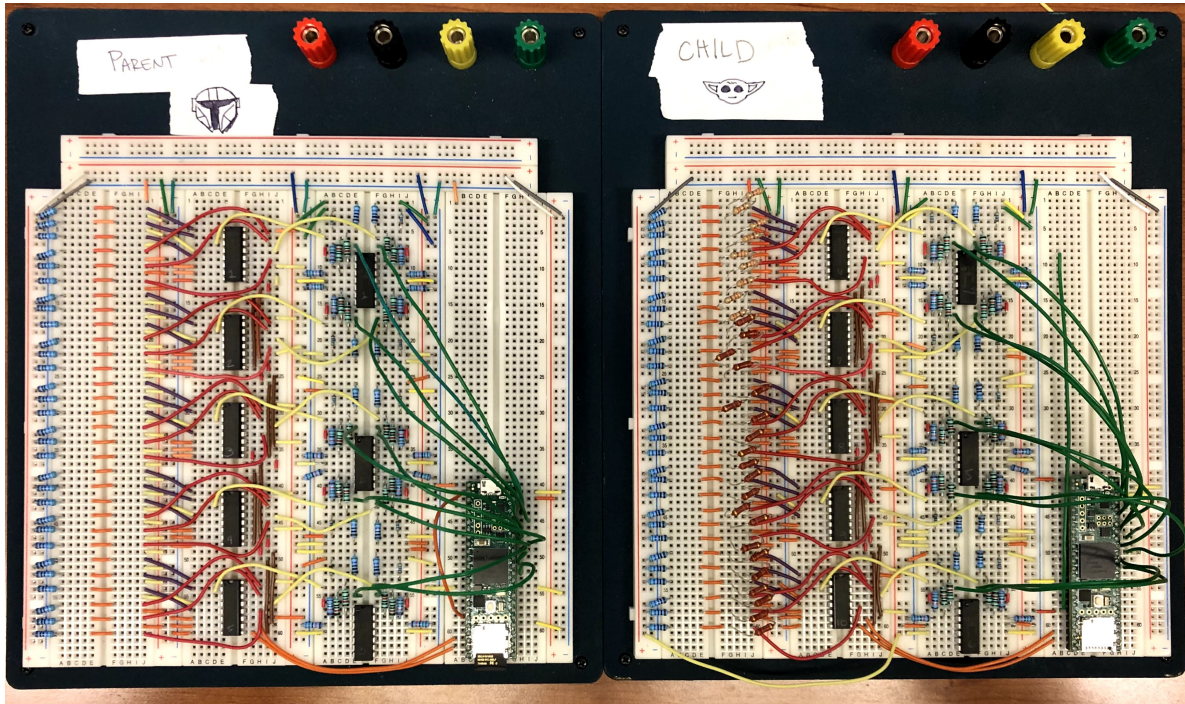


Figure 7.4. Both boards completely wired up for data collection.

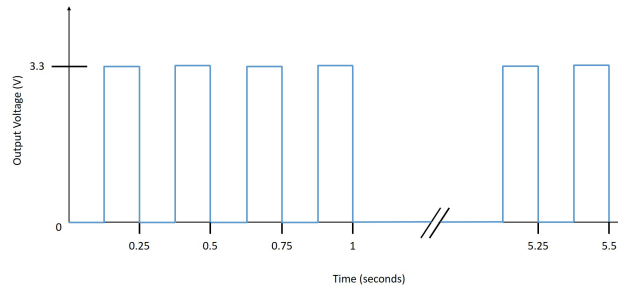


Figure 7.5. The theoretical signal used to time sync the strain gauge and hammer data.

board and one as the “child” board. The parent board output a 0 V signal for 125 ms, 3.3 V for 125 ms, and this cycle repeated three more times (four down cycles and four up cycles for a total of one second; Fig. 7.5). There was then four seconds of 0 V output from the parent board before entering the four down cycle/up cycle again. This signal was relayed to the child board, the Data Acquisition (DAQ; National Instruments; Austin, TX) system (used to collect impact force and location data), and back into the parent board so all three collected data sets had the data necessary to time sync.

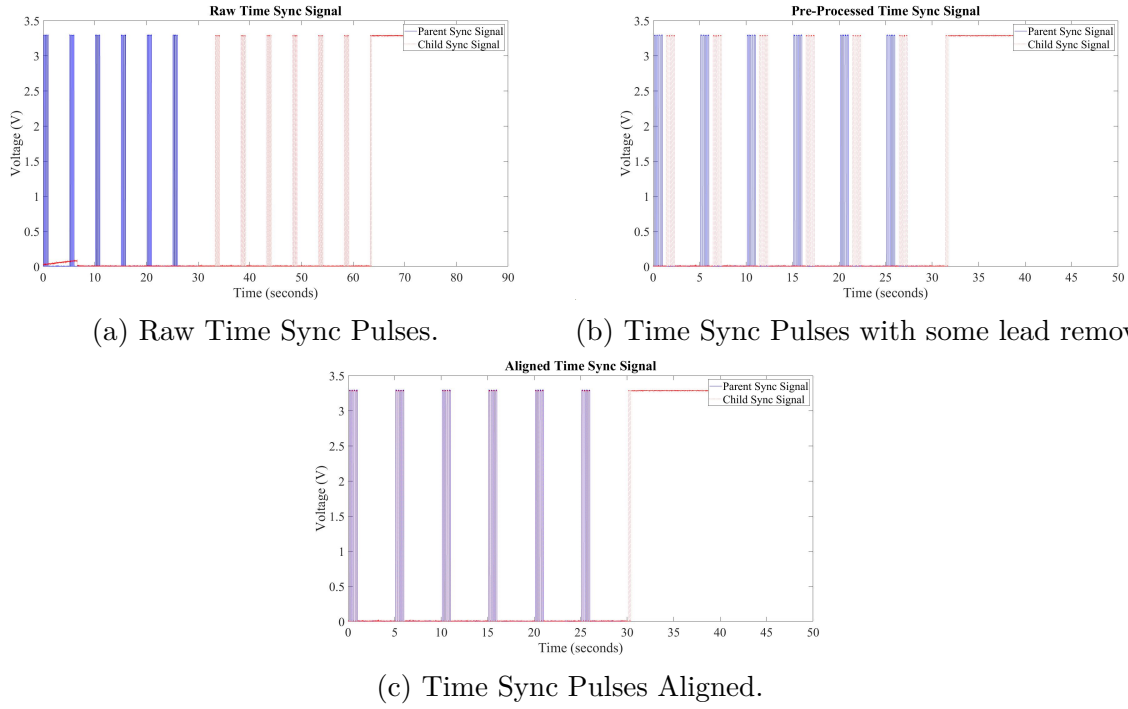


Figure 7.6. An example of how to use the pulse wave to sync the parent board and child board signals. Starting with the (a) raw pulse waves, the pulses were then (b) pre-processed to remove samples collected by the child board before the parent board is turned and then, (c) the delay between the two signals is found and removed to align the pulses.

The child board started collecting data before the parent board, so the time stamps were not aligned in the raw data that was collected (Fig. 7.6a). After some pre-processing of the data (Fig. 7.6b), the time delay between the pulse signal on the parent board and the child board was determined. After adjusting for the delay, the pulses could be aligned (Fig. 7.6c) which allowed for the strain gauge data from the boards to also be aligned. A similar process was also done to align the data acquired by the DAQ.

7.2.2 Bench Top Bending Test

Bending Test Sample

To test the circuit design and processing, two rosettes (one on the top in compression and one on the bottom in tension) were adhered to a rectangular 6063-T5 aluminum sample (Fig. 7.7). The sample was degreased with an isopropyl alcohol wipe and then wet sanded with

180 and 320 grit sand paper, respectively. The sanded surface was then wiped to remove any remaining debris. The rosettes were then affixed to the aluminum sample with M-Bond 200 strain gauge adhesive approximately at the center of the sample. The rosettes were oriented such that one strain gauge is aligned along the length of the sample (A), one along the width of the sample (C, orthogonal to A), and one 45° offset from A and C (B). Two rosettes were used for testing to test both the parent and child boards. For the coordinate system, the x-direction was defined as along the length of the sample (parallel to gauge A) and the y-direction was along the width of the sample.

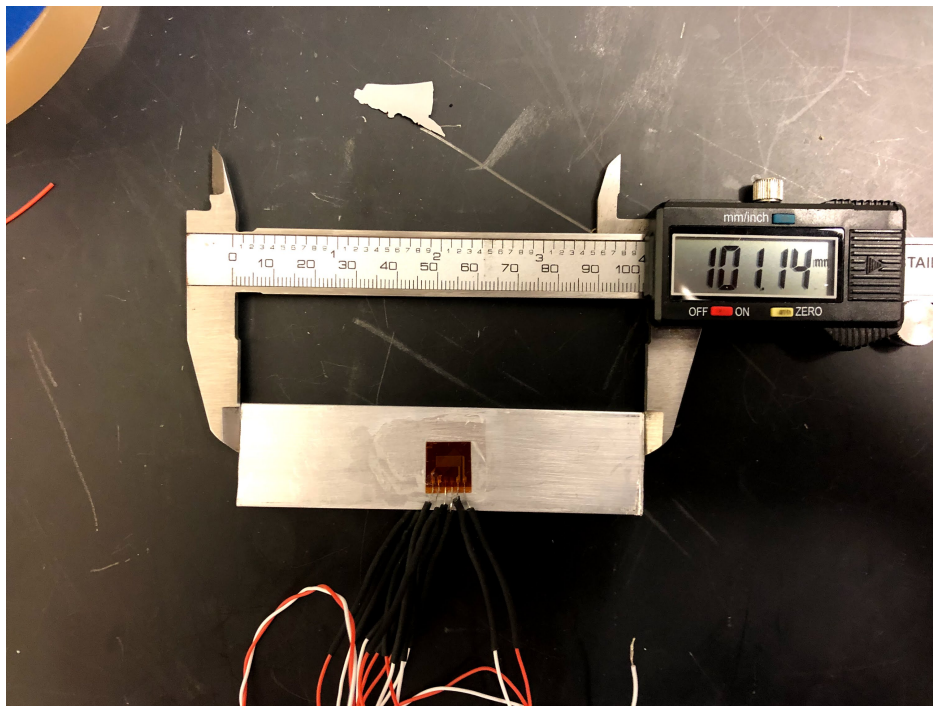


Figure 7.7. The rosette strain gauge adhered to the bending test sample.

Bending Test Set Up

The test sample was then placed inside the ME-8236 Materials Testing Machine (PASCO scientific; Roseville, CA; Fig. 7.8). The machine was connected to a workstation and data were captured using the PASCO Capstone Software (PASCO scientific; Roseville, CA) with a sampling rate of 500 Hz. The software was configured to record the time (in seconds), the

applied load (in Newtons, N), depth of the applied load (in meters, m), and speed of the applied load (in meters/second, m/s). Data were exported to a csv file.

Table 7.3. Test specimen and bending test set up values used to calculate the Euler’s stress and strain and the strain from the designed circuit [197], [198].

Property	Symbol	Value
Sample Width	b	25.4 mm
Sample Thickness	t	3.175 mm
Sample Second Moment of Inertia	I	$\frac{1}{12}bt^3$
Sample Young’s Modulus [198]	E	69 GPa
Sample Poisson’s Ratio [198]	ν	0.33
Sample Yield Stress [198]	σ_{yield}	188 MPa
Length Between Support Loads	l	66 mm
Length Between Support and Applied Loads	a	16.5 mm
Sample Thermal Expansion Coefficient [197]	α_T	$23 \times 10^{-6} \text{ K}^{-1}$

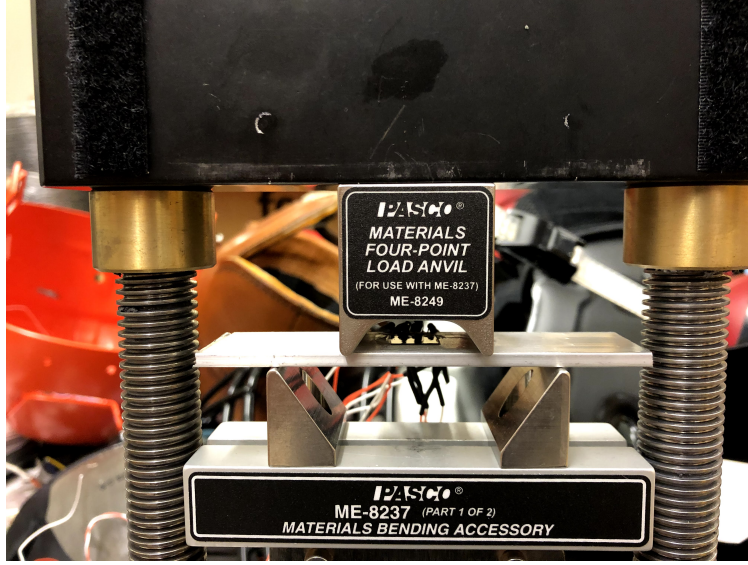
Bending Test Data Processing

A custom Matlab program (MathWorks; Natick, MA) was used to analyze the strain gauge data and PASCO output. The PASCO machine data were imported into the program and Euler’s beam bending equations were used to calculate stress (Eq. 7.1) and strains (Eq. 7.2) at the location of the strain gauge from the force data from the PASCO machine, F (N; other necessary values for calculations in Table 7.3).

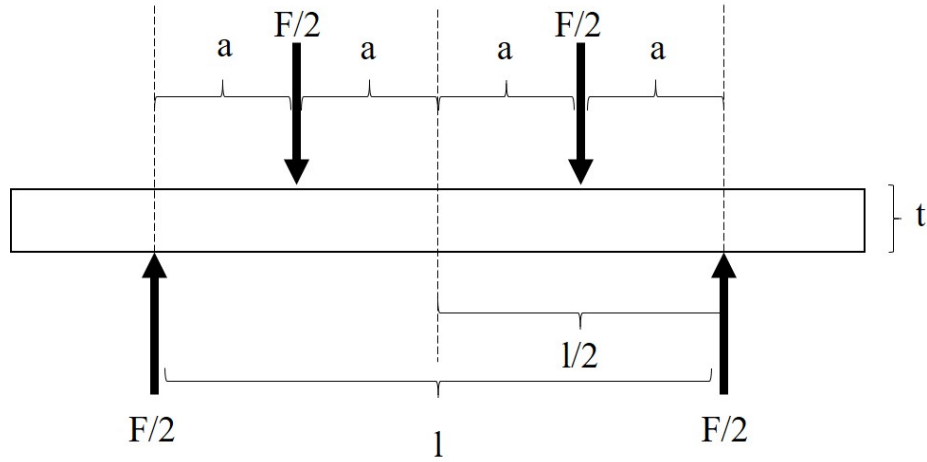
$$\sigma_{bending} = \sigma_{11} = \pm \frac{Fta}{4I} \quad (7.1)$$

$$\begin{bmatrix} \epsilon_{11} \\ \epsilon_{22} \\ \gamma_{12} \end{bmatrix} = \frac{1}{E} \begin{bmatrix} 1 & -\nu & 0 \\ -\nu & 1 & 0 \\ 0 & 0 & 2 + 2\nu \end{bmatrix} \begin{bmatrix} \sigma_{11} \\ 0 \\ 0 \end{bmatrix} \quad (7.2)$$

The strain gauge data were also imported and processed in Matlab. The imported data were the voltage difference of the Wheatstone bridge with the gain factor of the op amp ($V_{measured} = Gain \times \Delta V_i$). Strain gauge data were passed through a 7th order median filter.



(a) Materials testing machine set up for four point bending test.



(b) Free body diagram of the four point bending test.

Figure 7.8. The four point bending test (a) set up and (b) free body diagram. The rosettes were adhered to the aluminum sample and placed at approximately the middle of the sample.

The true voltage difference of the Wheatstone bridge was calculated ($\Delta V_i = \frac{V_{measured}}{Gain}$) and then resistance change of the strain gauge (ΔR_i) was then calculated (Eq. 7.3).

$$\Delta R_i = \frac{R_3[V_s R_2 + \Delta V_i(R_1 + R_2)]}{V_s R_1 - \Delta V_i(R_1 + R_2)} - R_{i,nominal} \quad (7.3)$$

In order to convert the change in resistance to strain, temperature (T, in °C) effects were accounted for in the calculation. The strain due to the thermal expansion of the strain gauge substrate (aluminum; Eq. 7.4) was calculated [199], [200].

$$\epsilon_{i,T,poly} = \frac{k_{poly}}{k_i(1 + \alpha_k \Delta T)} (-1.53 + 0.74T - 3.82 \times 10^{-2}T^2 + 2.02 \times 10^{-4}T^3) \times 10^{-6} \quad (7.4)$$

The change in resistance was then converted to the measured strain values while accounting for the temperature effect on the gauge factor (approximated T = 21.1 °C; Eq. 7.5) [199].

$$\begin{bmatrix} \hat{\epsilon}_A \\ \hat{\epsilon}_B \\ \hat{\epsilon}_C \end{bmatrix} = \begin{bmatrix} \frac{1}{k_A(1+\alpha_k \Delta T)} & 0 & 0 \\ 0 & \frac{1}{k_B(1+\alpha_k \Delta T)} & 0 \\ 0 & 0 & \frac{1}{k_C(1+\alpha_k \Delta T)} \end{bmatrix} \begin{bmatrix} \frac{\Delta R_A}{R_{A,nominal}} \\ \frac{\Delta R_B}{R_{B,nominal}} \\ \frac{\Delta R_C}{R_{C,nominal}} \end{bmatrix} - \begin{bmatrix} \epsilon_{A,T,poly} \\ \epsilon_{B,T,poly} \\ \epsilon_{C,T,poly} \end{bmatrix} \quad (7.5)$$

The properties of the strain gauge were then applied to account for the temperature effect of the leads from the manufacturer's data sheet (Eq. 7.6), transverse effects on the measured strain (Eq. 7.7), and the temperature effect on the materials [199], [200].

$$\epsilon_{T,leads} = L \times \Delta T \times 0.0114 \times 10^{-6} \quad (7.6)$$

$$\begin{bmatrix} \epsilon_A \\ \epsilon_B \\ \epsilon_C \end{bmatrix} = \begin{bmatrix} \frac{1-\nu_0 q_A}{1-q_A q_C} & 0 & \frac{-q_A(1-\nu_0 q_C)}{1-q_A q_C} \\ \frac{-q_B(1-\nu_0 q_A)(1-q_C)}{(1-q_A q_C)(1-q_B)} & \frac{1-\nu_0 q_B}{1-q_B} & \frac{-q_B(1-\nu_0 q_C)(1-q_A)}{(1-q_A q_C)(1-q_B)} \\ \frac{-q_C(1-\nu_0 q_A)}{1-q_A q_C} & 0 & \frac{1-\nu_0 q_C}{1-q_A q_C} \end{bmatrix} \begin{bmatrix} \hat{\epsilon}_A \\ \hat{\epsilon}_B \\ \hat{\epsilon}_C \end{bmatrix} - \epsilon_{T,leads} - (\alpha_T - \alpha_{SG})\Delta T \quad (7.7)$$

From here, the strain of each strain gauge was converted to strain in the x-direction ($\epsilon_{xx} = \epsilon_A$), y-direction ($\epsilon_{yy} = \epsilon_C$), and the shear strain ($\gamma_{xy} = 2\epsilon_B - \epsilon_A - \epsilon_C$). The strain values were then used to calculate the principal strains (Eq. 7.8), which were then plotted against the strain calculated from the PASCO outputs.

$$\begin{aligned}
\epsilon_{1,2} &= \frac{\epsilon_A + \epsilon_C}{2} \pm \frac{1}{2} \sqrt{(\epsilon_A - \epsilon_C)^2 + (2\epsilon_B - \epsilon_A - \epsilon_C)^2} \\
&= \frac{\epsilon_{11} + \epsilon_{22}}{2} \pm \frac{1}{2} \sqrt{(\epsilon_{11} - \epsilon_{22})^2 + \gamma_{12}^2}
\end{aligned} \tag{7.8}$$

To quantify the difference between the two methods, the percent error for the strain along the sample was calculated at each time point, using the strain from the Euler's equations as the reference. Due to the different sampling rates used to collect the data, the data from the development board were down sampled and interpolated at the time points from the PASCO machine. With the interpolated data points, the percent error was calculated.

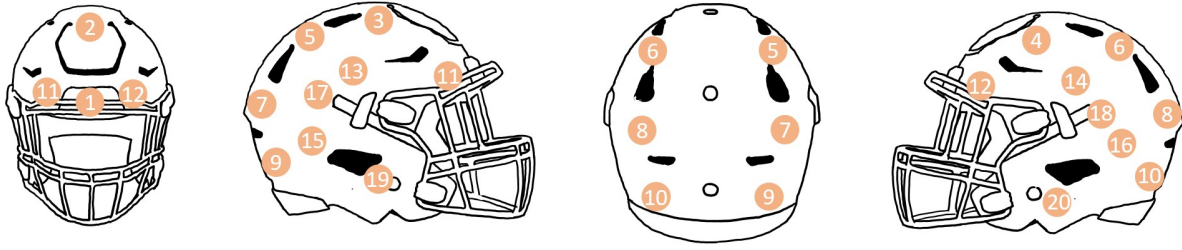
7.2.3 Strain Gauge Testing on Hybrid III Headform

Manufacturing Process

The rosettes were adhered to the interior part of a Large 2019 Riddell (Riddell Sports Group, Inc.; Elyria, OH) Speedflex football helmet shell (Fig. 7.9, $\alpha_T = 65 \times 10^{-6} \text{ K}^{-1}$ [197]). The helmet was degreased with an isopropyl alcohol wipe and then sanded with 180 and 320 grit sand paper, respectively. The sanded surface was then wiped to remove any remaining debris. The rosette was then affixed to the helmet with M-Bond 200 strain gauge adhesive. For the full array, an approximately four foot long 30 AWG wire was attached to each lead on the strain gauge to connect the strain gauge to the circuit. Heat shrink tubing was used to isolate the exposed wiring and epoxy was used to adhere the ends of the heat shrink tubing to the helmet shell.

Data Acquisition

The helmet was mounted onto a 50th percentile male Hybrid III headform (H3H; Humanetics; Farmington Hills, MI) that was instrumented with a 3-2-2-2 linear accelerometer mount to measure translational and angular acceleration. A modal impulse hammer (PCB Piezotronics, Inc.; Depew, NY) was used to impact the helmet-H3H system at different lo-



(a) Approximated location of the rosettes.



(b) Riddell Speedflex helmet with strain gauges.

Figure 7.9. Strain gauge rosette location on the Riddell Speedflex.

cations and impulse ranges (Fig. 7.10). The data from this system were recorded using a Data Acquisition (DAQ) system (National Instruments; Austin, TX).

A custom LabVIEW (National Instruments; Austin, TX) program was developed to continuously capture the data from the modal impulse hammer, the accelerometers inside the H3H, and the sync wave from the Teensy board (Fig. 7.10). A rate of 2 kHz was set as

the sampling frequency, although the actual sampling frequency was slightly faster (~ 2049 Hz).



Figure 7.10. H3H testing set up consisted of: the instrumented helmet on the H3H (left), modal hammer (on top of yellow foam), both wired boards (in front of yellow foam), DAQ (right of the boards), laptop to control the boards, and workstation running LabVIEW (right) to collect hammer and accelerometer data.

The helmet was tested at four locations (front, right side, left side, and back) and impulse ranges (2-5, 5-8, 8-11, 11+ Ns). For analysis, 15 hits with the most functioning rosettes for each location and impulse combination were considered (a total of 240 hits; loss of 9% of rosettes). The testing was performed such that all of the locations were tested at the lowest impulse range first before progressing to the next highest impulse range. This was done in an attempt to minimize the likelihood of dislodging a rosette in the middle of a testing session.

Data Post-Processing

Data from the Teensy boards and the H3H set up were analyzed using a custom Matlab program (MathWorks; Natick, MA). All data were imported and then aligned in the time domain. Corrections were made for discrepancies in sampling rates between samples so all of the observations were 500 μs apart. The strain gauge data were filtered using a 7th order median filter and the H3H data were passed through a low-pass Butterworth filter with a cutoff frequency of 750 Hz (consistent with previous works [75]). Strain gauge data were also passed through other quality control parameters: manual inspection of the signal; during the hit, the imported voltage difference of the Wheatstone bridge had to be lower than 2.6 V; the median value of the strain gauge during the first five ms of data collected had to be between 315-360 Ω ; and the strain gauge had to settle within one Ω of the starting resistance. The change in resistance, measured strain, true strain, and principle strains were all calculated using the appropriate equations (Eqs. 7.3, 7.5, 7.7, 7.8). The equivalent strain [201], [202] was also calculated to represent the strain state at each rosette (i), for each hit (j) at every time point (Eq. 7.9), assuming incompressibility of the helmet shell [$1 = (1 + \epsilon_1)(1 + \epsilon_2)(1 + \epsilon_3)$]. The impulse was calculated over a 30 ms window that captured the hit with 10 ms of data before the hammer force passed the 20 lbf. threshold.

$$\epsilon_{EQ,i,j}(t) = \frac{1}{3} \sqrt{2[(\epsilon_{1,i,j}(t) - \epsilon_{2,i,j}(t))^2 + (\epsilon_{1,i,j}(t) - \epsilon_{3,i,j}(t))^2 + (\epsilon_{2,i,j}(t) - \epsilon_{3,i,j}(t))^2]} \quad (7.9)$$

7.3 Results

7.3.1 Four Point Bending Test

It was seen that the strain gauge values were able to be correctly aligned in the time domain and that they were opposite and approximately equal (Fig. 7.11). The values from the strain gauges closely resemble the strain values calculated using the Pasco data and Euler's equations (Fig. 7.11). The typical (measurements taken between 4-13 s in the test) percent error between the strain calculated from the strain gauges and that calculated using

Euler's equations was within about $\pm 20\%$. This test indicated the circuit, time sync, and post-processing methods were valid and can accurately measure the strain of the system.

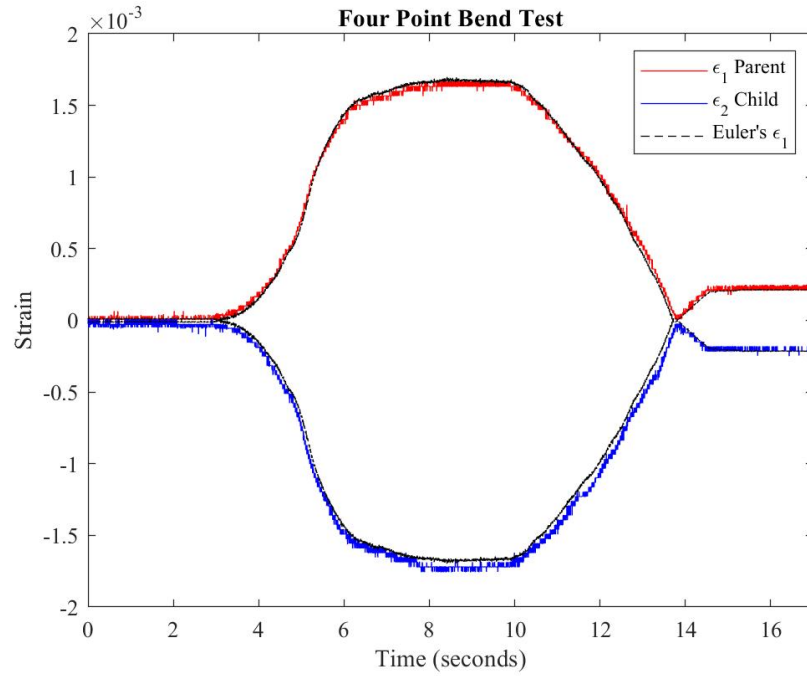
7.3.2 Strain Gauge Testing on Hybrid III Headform

Single Rosette

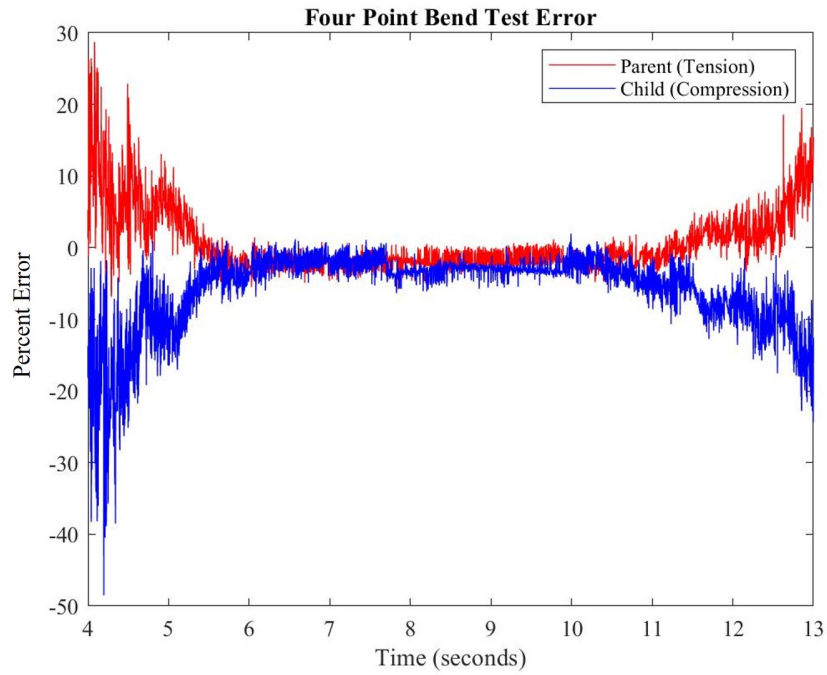
A single rosette was first adhered to the inside of a Riddell Speedflex helmet shell at the hinge to test the system at a location on the helmet likely to strain (Fig. 7.12). The rosette was oriented so the A strain gauge pointed anterior-posterior and the C strain gauge pointed left to right. The helmet was then struck on the flap of the Speedflex to induce bending at the hinge and was struck at the hinge itself with a hit impulse greater than 14 Ns (Fig. 7.13). Again, due to the fragility of the leads, one of the leads broke (strain gauge B), so only two of the three strain gauges on the rosette recorded data (strain gauges A and C). The circuit was designed to handle changes in resistance of about $35\ \Omega$ on any given strain gauge. The unfiltered resistance values were calculated to ensure that the circuit had the correct specifications (Fig. 7.12). This test indicated that the circuit values were properly assigned and the output follows initial assumptions. Striking the Speedflex flap was similar to a point load on a cantilever beam, so compression at the hinge in the direction of the beam was expected (Fig. 7.13a). Conversely, when striking at the hinge where the rosette was located, it was similar to a point load, so tension was expected beneath the point load (Fig. 7.13b).

Full Array

Boxplots were generated to examine the effective $\epsilon_{EQ,i,j}$ for each rosette as a function of hit location and magnitude (observations with no data for a specific rosette were not considered; Fig. 7.14). It was seen that for different rosettes, the effective $\epsilon_{EQ,i,j}$ was dependent on the hit location and magnitude. For rosette 4 (Fig. 7.14a), it was seen that this rosette only strained for hits on the left side of the helmet and increased in effective $\epsilon_{EQ,i,j}$ as the hit impulse increased. Similarly for rosette 10 (Fig. 7.14b) which was located near the back, the rosette strained for back hits and increased with increasing hit impulse.



(a) Principal strains from a four point bending test.



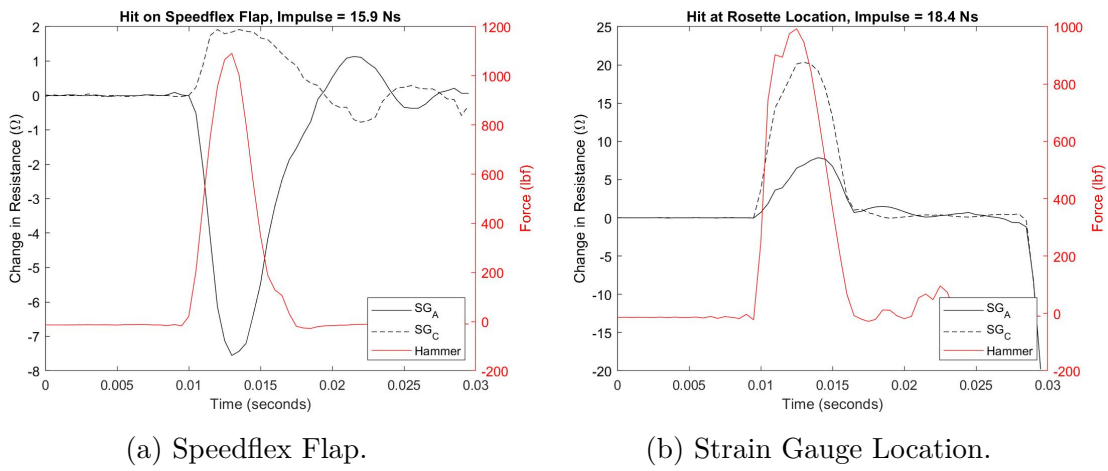
(b) Percent error in principal strains.

Figure 7.11. The (a) principal strains and (b) percent error from a four point bending test to evaluate the strain gauge circuit, data alignment method, and calculations.



(a) Rosette on the Speedflex hinge. (b) Close up of rosette on the Speedflex hinge.

Figure 7.12. The unfiltered signal from a single rosette fixed to the Speedflex hinge.



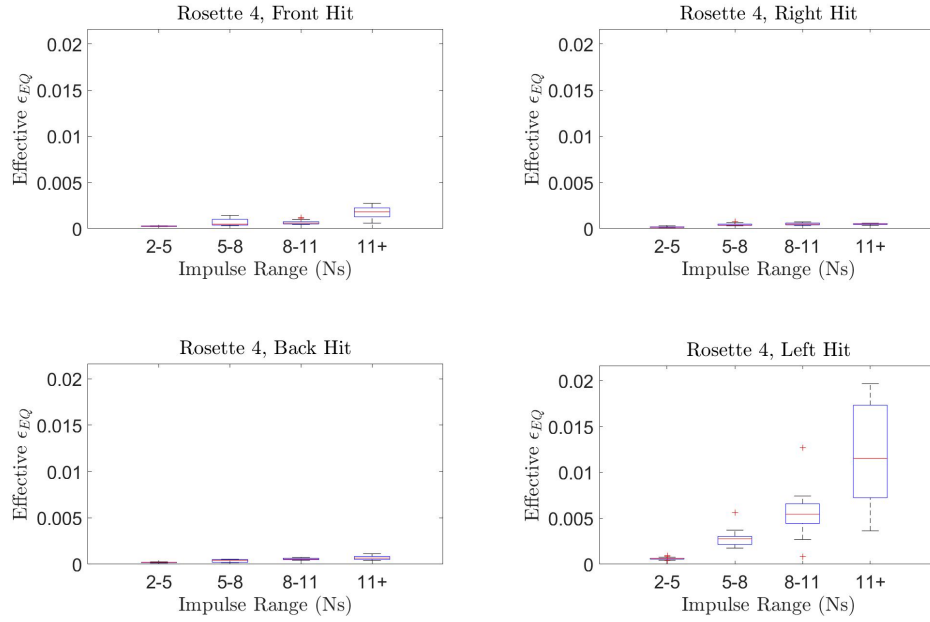
(a) Speedflex Flap.

(b) Strain Gauge Location.

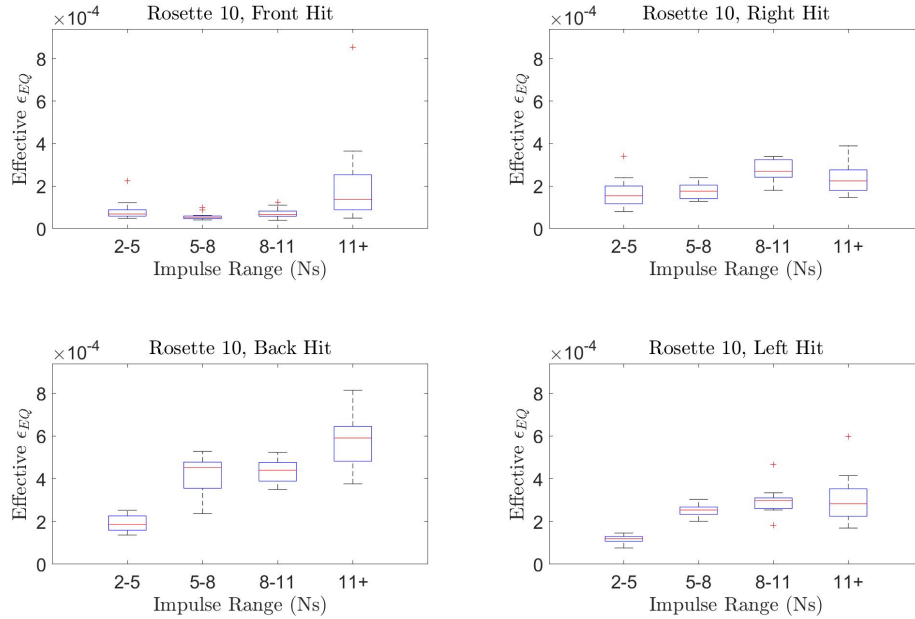
Figure 7.13. A single rosette tested on the H3H set-up indicated the values of components in the circuit were correctly assigned.

From the boxplots, the expected result was confirmed - rosettes close to where the hit was administered registered a non-zero strain during the hit while distal rosettes mostly did not. However, not all of the hit locations induced the same strain magnitude for rosettes in the nearby area (Fig. 7.15a). For example, rosettes 13 and 14 registered equivalent strain values around 5×10^{-3} for their respective side hits, but rosettes 9 and 10 were closer to 1×10^{-3} on back hits. Because of this, a universal threshold to determine which rosettes were “activated” would most likely be unable to identify back hits.

Therefore, a unique threshold for each rosette was used to appropriately normalize each rosette. For each rosette (i), the effective equivalent strain value (Eq. 7.10) was calculated



(a) Boxplots for rosette 4 by hit location.



(b) Boxplots for rosette 10 by hit location.

Figure 7.14. Boxplot for (a) rosette 4 and (b) rosette 10. Rosette 4 was located on the left side of the helmet at the front and rosette 10 was located on the left side of the helmet at the back.

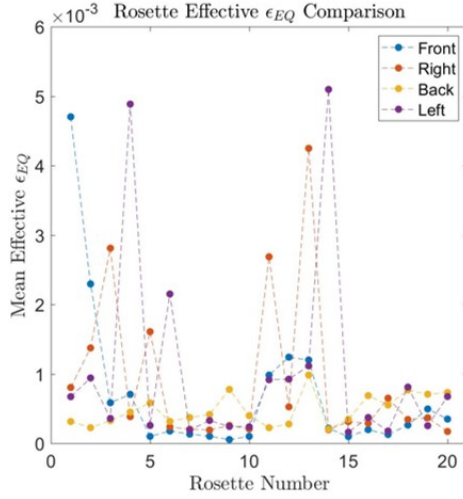
for each hit (j) and was defined as the mean of the equivalent strain values while the hammer force was greater than 20 lbf (Eq. 7.11).

$$effective \epsilon_{EQ,i,j} = mean[\epsilon_{EQ,i,j}(t)u(Hammer Force_j(t) - 20 lbf)] \quad (7.10)$$

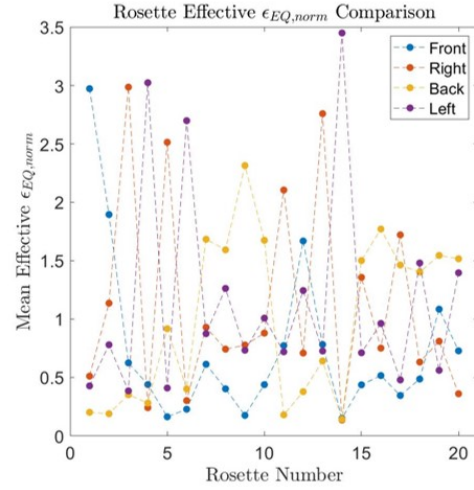
$$u(Hammer Force_j(t) - 20 lbf) = \begin{cases} 1 \text{ if } Hammer Force_j(t) > 20 lbf \\ 0 \text{ else} \end{cases} \quad (7.11)$$

The mean of the effective $\epsilon_{EQ,i,j}$ was then calculated across all hits for each rosette (effective $\bar{\epsilon}_{EQ,i}$). This value represented each rosette's ability to strain for a hit at any location, since it was observed that some rosettes were sensitive to hit location (higher effective $\epsilon_{EQ,i,j}$), but others were not (lower effective $\epsilon_{EQ,i,j}$). The i^{th} effective $\bar{\epsilon}_{EQ,i}$ served as the normalizing factor for the corresponding rosette to produce the normalized effective equivalent strain value for the i^{th} rosette, on the j^{th} hit (effective $\epsilon_{EQnorm,i,j} = \frac{effective \epsilon_{EQ,i,j}}{effective \bar{\epsilon}_{EQ,i}}$). The mean was calculated for each hit location (effective $\bar{\epsilon}_{EQnorm,i}$). Using the normalized effective equivalent strain value as the metric of interest revealed a subset of rosettes that do strain more for back hits than hits at other locations (Fig. 7.15b).

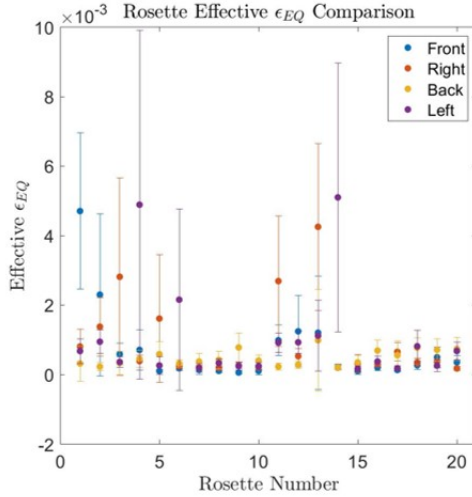
Based on the normalized values, it was determined that only a subset of rosettes would be used for further analysis to identify location then relationship to impulse/peak force since there were certain rosettes that only strained for one hit location, indicating independence of these rosettes. These rosettes were selected based on the normalized effective equivalent values by location (Fig. 7.15d) as: (1) not having an overlap between a mean and a standard deviation bar of different locations and (2) being symmetric between the left and right sides of the helmet. Rosettes 1 and 2 represented the front location; rosettes 3, 5, and 13 represented the right; 9 and 10 represented the back; and 4, 6, and 14 represented the right side. For each hit, the effective $\bar{\epsilon}_{EQnorm,location,j}$ for the appropriate rosettes was calculated for each location (i.e. effective $\bar{\epsilon}_{EQnorm,front,j} = \frac{effective \epsilon_{EQnorm,1,j} + effective \epsilon_{EQnorm,2,j}}{2}$, rosettes that were broken were ignored for the calculation). Each hit was classified at whichever location had the highest effective $\bar{\epsilon}_{EQnorm,location,j}$ among all four averages for that hit. This approach



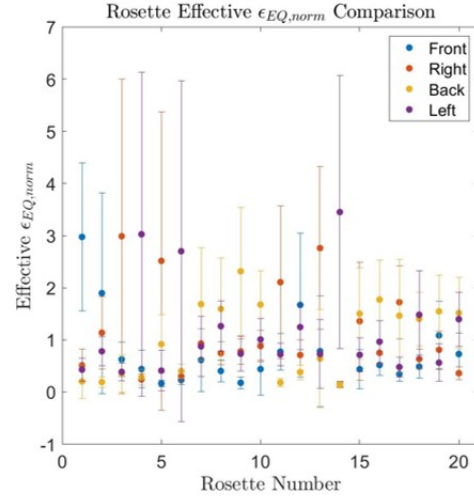
(a) Mean effective equivalent strain for each rosette by hit location.



(b) Mean normalized effective equivalent strain for each rosette by hit location.



(c) Mean effective equivalent strain for each rosette by hit location.



(d) Mean normalized effective equivalent strain for each rosette by hit location.

Figure 7.15. The (a) mean effective equivalent strain and (b) mean normalized effective equivalent strain for each rosette by hit location. This demonstrated the advantage to normalizing each rosette by it's own value. Standard deviation bars were included for the (c) mean effective equivalent strain and (d) mean normalized effective equivalent strain for each rosette by hit location to determine which rosettes should represent each hit location.

accurately classified the location for 229 out of 240 hits (95.4%; Table 7.4). Seven of the 11 hits that were not correctly classified did not have any working rosettes at that location.

Table 7.4. Location classification accuracy.

		Actual Location			
		Front	Right	Back	Left
Classified Location	Front	59	4	0	0
	Right	1	55	2	1
	Back	0	1	58	2
	Left	0	0	0	57

After the location had been determined, the relationship between the rosette strains and the hit impulse and peak force were determined. Based on the determined location of each hit, the appropriate rosettes were used to generate the independent variables for a multiple regression in Matlab (MathWorks; Natick, MA) with incomplete observations excluded from the model (i.e. if there was no data from rosette 10 for a classified back hit, the observation was not included in the regression). The model included the effective $\epsilon_{EQnorm,i,j}$ values. After a regression was performed for each location, outliers were determined using studentized residuals. Outliers then had their hit location reclassified as the next highest ranking hit location previously determined. The regressions were rerun using the new location classifications and this process continued until there were no more outliers in the plots or after four cycles (all locations had been attempted for outliers and returns back to the initial estimate). Using the peak force as the dependent variable caused two left hits to be incorrectly reclassified as front hits. However, if using the impulse, this method did not alter the classification accuracy. Both the peak force (Fig. 7.16, Table 7.5) and the impulse (Fig. 7.17, Table 7.6) though were correlated to the rosette measurements.

The regression coefficients for the different multiple linear regressions for peak force had different trends depending upon the location, but all of the rosettes were significant in the respective models ($p < 0.05$; Table 7.5). However, there were differences for left and right hits in terms of contributions for symmetric rosettes.

The regression coefficients for the different multiple linear regressions for impulse had different trends than those found for the peak force regressions (Table 7.6). Rosette 5 did not significantly contribute to the model for right hits and rosette 9 did not significantly contributed to the model for impulse for back hits.

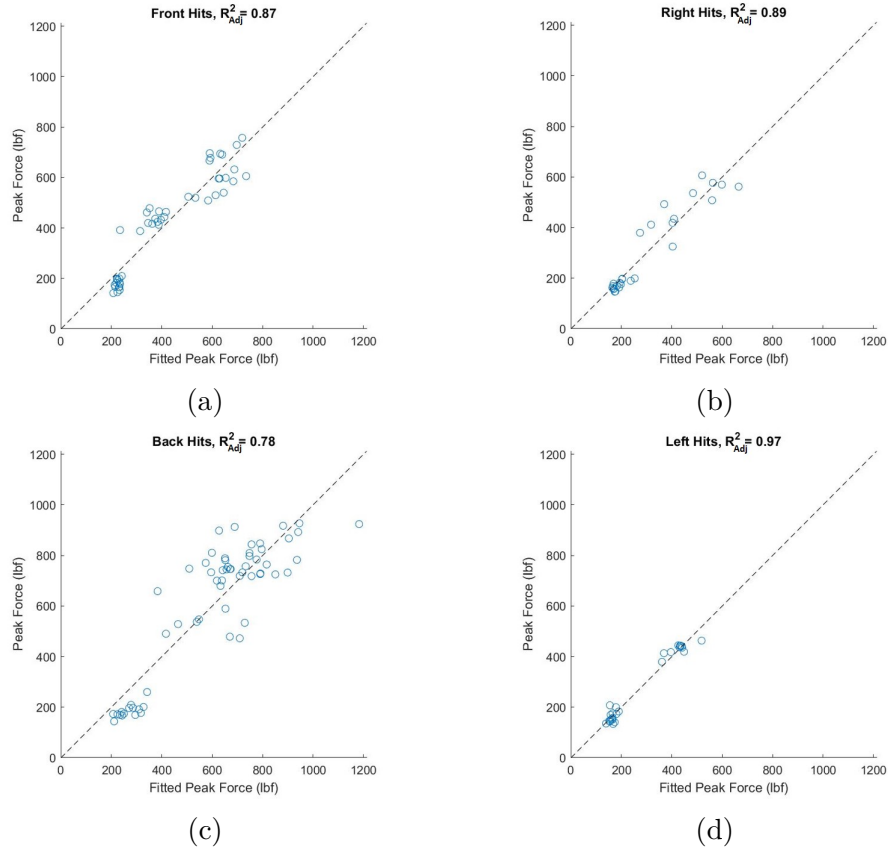


Figure 7.16. Multiple linear regression for (a) front, (b) right, (c) back, and (d) left classified hits and the peak force of the hit.

Table 7.5. Multiple linear regression coefficients for model correlating rosette effective $\epsilon_{EQnorm,i}$ to hit peak force.

Classified Location		Dependent Variable			
Front	X_i	Constant	eff $\epsilon_{EQnorm,1}$	eff $\epsilon_{EQnorm,2}$	
	β_i	18.8	77.4*	176.5*	
Right	X_i	Constant	eff $\epsilon_{EQnorm,3}$	eff $\epsilon_{EQnorm,5}$	eff $\epsilon_{EQnorm,13}$
	β_i	60.7*	26.2*	27.1*	54.2*
Back	X_i	Constant	eff $\epsilon_{EQnorm,9}$	eff $\epsilon_{EQnorm,10}$	
	β_i	23.2	68.3*	254.4*	
Left	X_i	Constant	eff $\epsilon_{EQnorm,4}$	eff $\epsilon_{EQnorm,6}$	eff $\epsilon_{EQnorm,14}$
	β_i	86.5*	145.2*	-117.6*	47.0*

* indicates a significant variable in the model ($p < 0.05$).

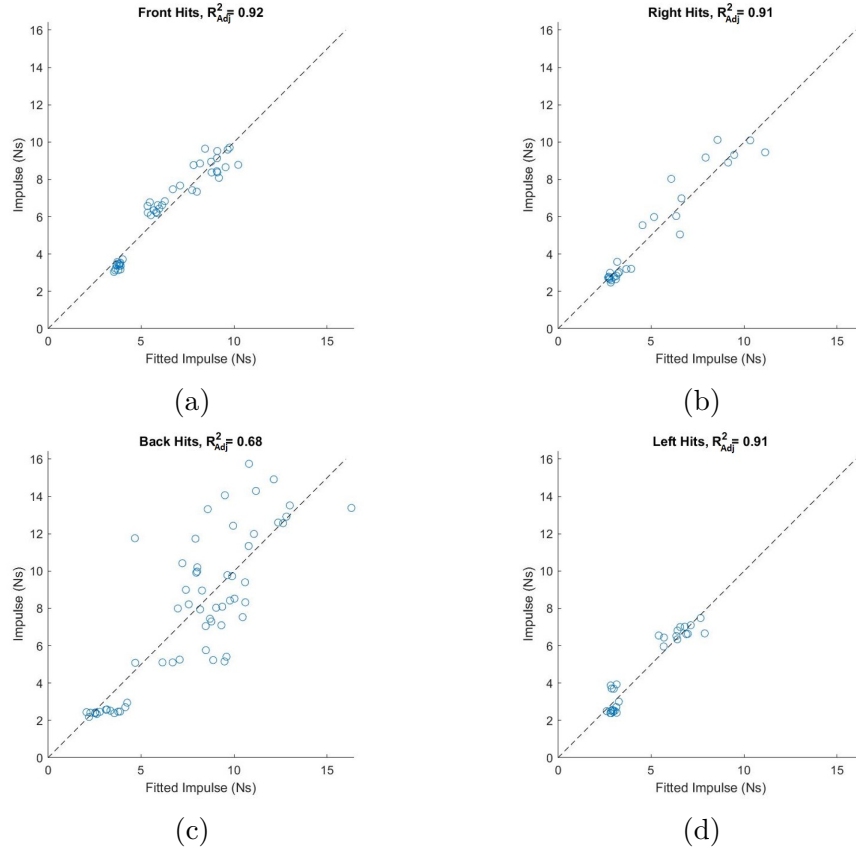


Figure 7.17. Multiple linear regression for (a) front, (b) right, (c) back, and (d) left classified hits and the impulse of the hit.

Table 7.6. Multiple linear regression coefficients for model correlating rosette effective $\epsilon_{EQnorm,i}$ to hit impulse.

Classified Location		Dependent Variable			
Front	X_i	Constant	eff $\epsilon_{EQnorm,1}$	eff $\epsilon_{EQnorm,2}$	
	β_i	0.9*	1.1*	2.1*	
Right	X_i	Constant	eff $\epsilon_{EQnorm,3}$	eff $\epsilon_{EQnorm,5}$	eff $\epsilon_{EQnorm,13}$
	β_i	1.1*	0.5*	0.4	0.8*
Back	X_i	Constant	eff $\epsilon_{EQnorm,9}$	eff $\epsilon_{EQnorm,10}$	
	β_i	-0.7	0.5	4.3*	
Left	X_i	Constant	eff $\epsilon_{EQnorm,4}$	eff $\epsilon_{EQnorm,6}$	eff $\epsilon_{EQnorm,14}$
	β_i	1.9*	1.7*	-1.5*	0.7*

* indicates a significant variable in the model ($p < 0.05$).

7.4 Discussion

Developing a system that can measure the helmet deformation to correlate to impact force/impulse and location would provide the input information for a collision. Most current

sensor technology measures the acceleration during the head impact, which is a function of the force and location of the hit, protective equipment, and athlete muscle activation. Although the acceleration can provide information about the motion of the head and is correlated to changes in brain health, impact force and location can provide information to aid in modeling these impacts, design better protective equipment, and provided feedback to players about technique and safety.

Strain gauges attached to the inside of the helmet shell were an appropriate choice for measuring the deformation of the helmet to determine location and peak force/impulse of an impact. It was observed that during the hit, strain gauges near the hit location were able to measure the deformation of the helmet shell while distal gauges were not activated during the hit. When considering four categorical locations as this project, the number of rosettes can be reduced from 20 down to 10, which would remove the need for one of the breadboards in the analysis. If more categorical locations want to be considered, more rosettes than the 10 main ones identified here may be needed to accurately classify hits at the new locations.

Also as predicted, the degree of helmet deformation was dependent on the magnitude of the hit, which the strain gauges were able to capture ($R^2 \geq 0.68$). There were some hits in this analysis for which no rosette data for a specific location were available due to either (a) a broken electrical connection between the rosette and the circuit or (b) the data were removed by the signal quality criteria. Improving the robustness of the electrical connection between the rosette and the breadboard could help improve the fit of the regressions. The unique relationship between the strain gauge measurements and the hit force/impulse at each location may be due to the geometry of the helmet shell and/or foam padding properties between the helmet shell and the H3H head. Simulating the hits with finite element analysis (FEA) and validating with the collected data set could further illuminate the relationship between strain and hit characteristics.

Although this project was able to achieve its objective, there were several limitations of the study. Only four categorical locations were considered in the analysis. Future work should explore continuous or spacial mapping of the hit location based on the measurements from the rosettes to more accurately determine the hit location. The regression analysis considers peak force and the impulse of the hit, but future work could employ sequence-to-

sequence neural networks to train and obtain a time series of the force of the hit. This would provide a more detailed input for FEA of the helmet. During the testing, several rosettes had their wires broken at the base of the rosette, resulting in no data available for that rosette for the remaining hits. The rosettes were adhered to the helmet with superglue and the wires were epoxied to the helmet at both ends of the heat shrink tubing used to electrically isolate the wires. After testing, the helmet was dismantled and it was found that most the wires at the epoxied end proximal to the rosette had broken off. It could be due to the extra weight and the plastic material of the helmet that caused the rosettes to break off at this point. Future work should consider more robust methods for wire attachment. Also, each wire connected to a strain gauge was approximately four feet long and due to the testing set up, wires coming from the right side of the helmet were passed along the helmet shell, over the H3H head, which could have resulted in extra noise in the system. Future work should optimize wire lengths and paths to reduce noise. The 20 rosette design required 120 individual wires to come out of the helmet, which is not realistic for use during an athletic event. From neural network analysis and FEA, the optimal number and placement of strain gauges could be determined to make this a deployable helmet.

This system could, ideally, be deployed in any helmet model by any helmet manufacturer. However, this poses the challenge of calibrating the rosettes for each unique helmet model and accounting for how weather and aging of the helmets would affect the strain measures. Laboratory testing and modeling could be performed to account for how these factors would affect the strain values that could then be implemented into the data processing.

7.5 Conclusion

Creating an instrumented helmet with strain gauges can provide more information about collision events in football. Measuring impact location and magnitude can supplement data collected on accelerometers worn by players, which would provide data to more accurately model what happens to the head during in impact. Data can then be used to validate FEA models, provide player specific feedback on technique, and improve overall player safety in football.

8. SUMMARY

8.1 Level of Play

Football and girls' soccer have similar PTA characteristics, but different PAA characteristics which may be due to differences in protective equipment and cause of the HAE. Football players also accumulate more HAEs than girls' soccer players likely due to the frequency at which these players are involved in collision events. Protocols need to be put in place that will protect overexposed players, either those that play offense and defense in football, or those that play on multiple teams for both football and soccer. These players are at risk of accumulating HAEs faster than if they were to only play one position or on one team.

8.2 Stance Analysis

Starting in an up stance may help players on the offensive line reduce the number of HAEs they sustain. Future work should further examine how lower skill players may be able to safely start in an up stance. Also, run plays typically result in more HAEs per play than pass plays, but modifications to traditional punts and kick-offs may be a unique approach for reducing the severity and/or number of HAEs on these play types.

8.3 White Matter

Repeated exposures to HAEs are correlated with alterations in white matter health. Fractional anisotropy (FA) and mean diffusivity (MD), two metrics used to assess white matter structural integrity, can exhibit four possible change combinations: increased FA, increased MD; decreased FA, increased MD; increased FA, decreased MD; decreased FA, decreased MD. After a season of participation, football athletes exhibited a significantly greater percentage of deviant voxels in each of the four categories than were observed from test-retest of non-contact athletes. Even prior to a season of participation, football athletes exhibited significantly more voxels in each of the categories, relative to controls. Of particular concern is that voxels exhibiting jointly decreased FA and MD—a change typically associated with cell death—were observed at a significantly higher rate within football athletes than

non-contact athletes. This finding suggests that repetitive HAEs may increase the incidence of cell death, and argues for the greater adoption of methods aimed at reducing mechanical loading on the brain from repetitive HAEs, both through reduction of the number of HAEs, and development of better protective equipment.

8.4 Rugby

Rugby is a sport that is very similar to football in terms of physicality and overall objective, which makes it a sport of interest for examining HAEs sustained by these athletes. In rugby games, it was seen that although forwards tended to sustain more HAEs than backs, there was not a difference in the magnitude of the HAEs. There were no differences in the PTA of a HAE if the team was in possession of the ball or not or if the event was caused by a ruck or a tackle. However, if on defense and in a ruck, this resulted in a higher PTA than if on offense in a ruck. This may be due to player vulnerability, awareness, and/or aggression while attempting to regain possession of the ball. Future works should examine the biomechanics of rugby and football players during collision events to ascertain similarities/differences that may help improve player safety.

8.5 Instrumented Helmet

Although it is extremely useful to measure the acceleration of the head to quantify the mechanical load on the brain, the acceleration of the head is actually the output of the system. The input of the collision is the hit or impact itself, and it is important to quantify this in order to fully understand the head-neck-helmet system. Strain gauges were used to quantify the deformation of the helmet during an impact and use that deformation to correlate to impact impulse and location. The strain gauges were able to provide the location of the impact and some had increasing activation with increasing impact impulse, demonstrating that this is a viable option for capturing impact characteristics.

REFERENCES

- [1] D. K. Menon, K. Schwab, D. W. Wright, A. I. Maas, *et al.*, “Position statement: Definition of traumatic brain injury,” *Archives of Physical Medicine and Rehabilitation*, vol. 91, no. 11, pp. 1637–1640, 2010.
- [2] E. L. Breedlove, M. Robinson, T. M. Talavage, K. E. Morigaki, U. Yoruk, K. O’Keefe, J. King, L. J. Leverenz, J. W. Gilger, and E. A. Nauman, “Biomechanical correlates of symptomatic and asymptomatic neurophysiological impairment in high school football,” *Journal of Biomechanics*, vol. 45, no. 7, pp. 1265–1272, 2012.
- [3] J. A. Langlois, W. Rutland-Brown, and M. M. Wald, “The epidemiology and impact of traumatic brain injury: A brief overview,” *The Journal of Head Trauma Rehabilitation*, vol. 21, no. 5, pp. 375–378, 2006.
- [4] A. M. Black, L. E. Sergio, and A. K. Macpherson, “The epidemiology of concussions: Number and nature of concussions and time to recovery among female and male canadian varsity athletes 2008 to 2011,” *Clinical Journal of Sport Medicine*, vol. 27, no. 1, pp. 52–56, 2017.
- [5] C. M. Baugh, P. T. Kiernan, E. Kroshus, D. H. Daneshvar, P. H. Montenegro, A. C. McKee, and R. A. Stern, “Frequency of head-impact-related outcomes by position in NCAA division I collegiate football players,” *Journal of Neurotrauma*, vol. 32, no. 5, pp. 314–326, 2015.
- [6] M. McCrea, T. Hammeke, G. Olsen, P. Leo, and K. Guskiewicz, “Unreported concussion in high school football players: Implications for prevention,” *Clinical Journal of Sport Medicine*, vol. 14, no. 1, pp. 13–17, 2004.
- [7] V. G. Coronado, L. C. McGuire, M. Faul, D. E. Sugerman, and W. S. Pearson, “Traumatic brain injury epidemiology and public health issues,” in *Brain Injury Medicine: Principles and Practice*, 2nd ed., Demos Medical Publishing New York, 2013, pp. 84–100, ISBN: 9781936287277.
- [8] R. A. Stern, D. O. Riley, D. H. Daneshvar, C. J. Nowinski, R. C. Cantu, and A. C. McKee, “Long-term consequences of repetitive brain trauma: Chronic traumatic encephalopathy,” *PM&R*, vol. 3, no. 10, S460–S467, 2011.
- [9] H. S. Martland, “Punch drunk,” *Journal of the American Medical Association*, vol. 91, no. 15, pp. 1103–1107, 1928.
- [10] J. Corsellis, C. Bruton, and D. Freeman-Browne, “The aftermath of boxing,” *Psychological Medicine*, vol. 3, no. 3, pp. 270–303, 1973.

- [11] B. I. Omalu, S. T. DeKosky, R. L. Minster, M. I. Kamboh, R. L. Hamilton, and C. H. Wecht, "Chronic traumatic encephalopathy in a national football league player," *Neurosurgery*, vol. 57, no. 1, pp. 128–134, 2005.
- [12] B. I. Omalu, S. T. DeKosky, R. L. Hamilton, R. L. Minster, M. I. Kamboh, A. M. Shakir, and C. H. Wecht, "Chronic traumatic encephalopathy in a national football league player: Part II," *Neurosurgery*, vol. 59, no. 5, pp. 1086–1093, 2006.
- [13] B. I. Omalu, R. L. Hamilton, M. I. Kamboh, S. T. DeKosky, and J. Bailes, "Chronic traumatic encephalopathy (CTE) in a national football league player: Case report and emerging medicolegal practice questions," *Journal of Forensic Nursing*, vol. 6, no. 1, pp. 40–46, 2010.
- [14] J. Mez, D. H. Daneshvar, P. T. Kiernan, B. Abdolmohammadi, V. E. Alvarez, B. R. Huber, M. L. Alosco, T. M. Solomon, C. J. Nowinski, L. McHale, *et al.*, "Clinicopathological evaluation of chronic traumatic encephalopathy in players of american football," *JAMA*, vol. 318, no. 4, pp. 360–370, 2017.
- [15] A. C. McKee, R. C. Cantu, C. J. Nowinski, E. T. Hedley-Whyte, B. E. Gavett, A. E. Budson, V. E. Santini, H.-S. Lee, C. A. Kubilus, and R. A. Stern, "Chronic traumatic encephalopathy in athletes: Progressive tauopathy after repetitive head injury," *Journal of Neuropathology & Experimental Neurology*, vol. 68, no. 7, pp. 709–735, 2009.
- [16] C. M. Baugh, J. M. Stamm, D. O. Riley, B. E. Gavett, M. E. Shenton, A. Lin, C. J. Nowinski, R. C. Cantu, A. C. McKee, and R. A. Stern, "Chronic traumatic encephalopathy: Neurodegeneration following repetitive concussive and subconcussive brain trauma," *Brain Imaging and Behavior*, vol. 6, no. 2, pp. 244–254, 2012.
- [17] C. A. Tagge, A. M. Fisher, O. V. Minaeva, A. Gaudreau-Balderrama, J. A. Moncaster, X.-L. Zhang, M. W. Wojnarowicz, N. Casey, H. Lu, O. N. Kokiko-Cochran, *et al.*, "Concussion, microvascular injury, and early tauopathy in young athletes after impact head injury and an impact concussion mouse model," *Brain*, vol. 141, no. 2, pp. 422–458, 2018.
- [18] B. E. Gavett, R. A. Stern, and A. C. McKee, "Chronic traumatic encephalopathy: A potential late effect of sport-related concussive and subconcussive head trauma," *Clinics in Sports Medicine*, vol. 30, no. 1, pp. 179–188, 2011.
- [19] T. M. Talavage, E. A. Nauman, E. L. Breedlove, U. Yoruk, A. E. Dye, K. E. Mori-gaki, H. Feuer, and L. J. Leverenz, "Functionally-detected cognitive impairment in high school football players without clinically-diagnosed concussion," *Journal of Neurotrauma*, vol. 31, no. 4, pp. 327–338, 2014.

- [20] K. Abbas, T. E. Shenk, V. N. Poole, E. L. Breedlove, L. J. Leverenz, E. A. Nauman, T. M. Talavage, and M. E. Robinson, "Alteration of default mode network in high school football athletes due to repetitive subconcussive mild traumatic brain injury: A resting-state functional magnetic resonance imaging study," *Brain Connectivity*, vol. 5, no. 2, pp. 91–101, 2015.
- [21] K. Abbas, T. E. Shenk, V. N. Poole, M. E. Robinson, L. J. Leverenz, E. A. Nauman, and T. M. Talavage, "Effects of repetitive sub-concussive brain injury on the functional connectivity of default mode network in high school football athletes," *Developmental Neuropsychology*, vol. 40, no. 1, pp. 51–56, 2015.
- [22] S. Bari, D. O. Svaldi, I. Jang, T. E. Shenk, V. N. Poole, T. Lee, U. Dydak, J. V. Rispoli, E. A. Nauman, and T. M. Talavage, "Dependence on subconcussive impacts of brain metabolism in collision sport athletes: An MR spectroscopic study," *Brain Imaging and Behavior*, vol. 13, no. 3, pp. 735–749, 2019.
- [23] D. O. Svaldi, C. Joshi, M. E. Robinson, T. E. Shenk, K. Abbas, E. A. Nauman, L. J. Leverenz, and T. M. Talavage, "Cerebrovascular reactivity alterations in asymptomatic high school football players," *Developmental Neuropsychology*, vol. 40, no. 2, pp. 80–84, 2015.
- [24] I. Y. Chun, X. Mao, E. Breedlove, L. Leverenz, E. Nauman, and T. Talavage, "DTI detection of longitudinal WM abnormalities due to accumulated head impacts," *Developmental Neuropsychology*, vol. 40, no. 2, pp. 92–97, 2015.
- [25] M. L. Dashnaw, A. L. Petraglia, and J. E. Bailes, "An overview of the basic science of concussion and subconcussion: Where we are and where we are going," *Neurosurgical Focus*, vol. 33, no. 6, E5, 2012.
- [26] J. E. Bailes, A. L. Petraglia, B. I. Omalu, E. Nauman, and T. Talavage, "Role of subconcussion in repetitive mild traumatic brain injury: A review," *Journal of Neurosurgery*, vol. 119, no. 5, pp. 1235–1245, 2013.
- [27] S. C. Saunders, "A review of Miner's Rule and subsequent generalizations for calculating expected fatigue life," Boeing Scientific Research Labs Seattle WA Mathematical and Information ..., Tech. Rep., 1970.
- [28] T. Lee, R. Lycke, J. Auger, J. Music, M. Dziekan, S. Newman, T. Talavage, L. Leverenz, and E. Nauman, "Head acceleration event metrics in youth contact sports more dependent on sport than level of play," *Proceedings of the Institution of Mechanical Engineers, Part H: Journal of Engineering in Medicine*, vol. 235, no. 2, pp. 208–221, 2021.

- [29] L. M. Gessel, S. K. Fields, C. L. Collins, R. W. Dick, and R. D. Comstock, "Concussions among united states high school and collegiate athletes," *Journal of Athletic Training*, vol. 42, no. 4, p. 495, 2007.
- [30] A. E. Lincoln, S. V. Caswell, J. L. Almquist, R. E. Dunn, J. B. Norris, and R. Y. Hinton, "Trends in concussion incidence in high school sports: A prospective 11-year study," *The American Journal of Sports Medicine*, vol. 39, no. 5, pp. 958–963, 2011.
- [31] M. Marar, N. M. McIlvain, S. K. Fields, and R. D. Comstock, "Epidemiology of concussions among united states high school athletes in 20 sports," *The American Journal of Sports Medicine*, vol. 40, no. 4, pp. 747–755, 2012.
- [32] Z. Y. Kerr, A. Chandran, A. K. Nedimyer, A. Arakkal, L. A. Pierpoint, and S. L. Zuckerman, "Concussion incidence and trends in 20 high school sports," *Pediatrics*, vol. 144, no. 5, e20192180, 2019.
- [33] "2017-2018 high school athletics participation survey," 2018.
- [34] A. Schwarz, *Congress examins N.F.L. concussions*, *New York Times*, 2010.
- [35] M. Locker, *Football head impacts can cause brain changes without concussion*, *Time Magazine*, 2014.
- [36] G. Reynolds, *A single concussion may have a lasting impact*, *The New York Times*, 2016.
- [37] B. Omalu, J. Bailes, R. L. Hamilton, M. I. Kamboh, J. Hammers, M. Case, and R. Fitzsimmons, "Emerging histomorphologic phenotypes of chronic traumatic encephalopathy in american athletes," *Neurosurgery*, vol. 69, no. 1, pp. 173–183, 2011.
- [38] B. Omalu, G. W. Small, J. Bailes, L. M. Ercoli, D. A. Merrill, K.-P. Wong, S.-C. Huang, N. Satyamurthy, J. L. Hammers, J. Lee, *et al.*, "Postmortem autopsy-confirmation of antemortem [f-18] FDDNP-PET scans in a football player with chronic traumatic encephalopathy," *Neurosurgery*, vol. 82, no. 2, pp. 237–246, 2018.
- [39] B. I. Omalu, J. Bailes, J. L. Hammers, and R. P. Fitzsimmons, "Chronic traumatic encephalopathy, suicides and parasuicides in professional american athletes: The role of the forensic pathologist," *The American Journal of Forensic Medicine and Pathology*, vol. 31, no. 2, pp. 130–132, 2010.
- [40] J. C. Maroon, R. Winkelman, J. Bost, A. Amos, C. Mathyssek, and V. Miele, "Chronic traumatic encephalopathy in contact sports: A systematic review of all reported pathological cases," *PloS One*, vol. 10, no. 2, e0117338, 2015.

- [41] K. F. Bieniek, O. A. Ross, K. A. Cormier, R. L. Walton, A. Soto-Ortolaza, A. E. Johnston, P. DeSaro, K. B. Boylan, N. R. Graff-Radford, Z. K. Wszolek, *et al.*, “Chronic traumatic encephalopathy pathology in a neurodegenerative disorders brain bank,” *Acta Neuropathologica*, vol. 130, no. 6, pp. 877–889, 2015.
- [42] T. M. Talavage, E. A. Nauman, and L. J. Leverenz, “The role of medical imaging in the recharacterization of mild traumatic brain injury using youth sports as a laboratory,” *Frontiers in Neurology*, vol. 6, p. 273, 2016.
- [43] B. Johnson, T. Neuberger, M. Gay, M. Hallett, and S. Slobounov, “Effects of subconcussive head trauma on the default mode network of the brain,” *Journal of Neurotrauma*, vol. 31, no. 23, pp. 1907–1913, 2014.
- [44] B. Johnson, K. Zhang, M. Gay, S. Horovitz, M. Hallett, W. Sebastianelli, and S. Slobounov, “Alteration of brain default network in subacute phase of injury in concussed individuals: Resting-state fmri study,” *Neuroimage*, vol. 59, no. 1, pp. 511–518, 2012.
- [45] M. C. Stevens, D. Lovejoy, J. Kim, H. Oakes, I. Kureshi, and S. T. Witt, “Multiple resting state network functional connectivity abnormalities in mild traumatic brain injury,” *Brain Imaging and Behavior*, vol. 6, no. 2, pp. 293–318, 2012.
- [46] Y. Zhou, M. P. Milham, Y. W. Lui, L. Miles, J. Reaume, D. K. Sodickson, R. I. Grossman, and Y. Ge, “Default-mode network disruption in mild traumatic brain injury,” *Radiology*, vol. 265, no. 3, pp. 882–892, 2012.
- [47] D. C. Zhu, T. Covassin, S. Nogle, S. Doyle, D. Russell, R. L. Pearson, J. Monroe, C. M. Liszewski, J. K. DeMarco, and D. I. Kaufman, “A potential biomarker in sports-related concussion: Brain functional connectivity alteration of the default-mode network measured with longitudinal resting-state fmri over thirty days,” *Journal of Neurotrauma*, vol. 32, no. 5, pp. 327–341, 2015.
- [48] M. E. Robinson, T. E. Shenk, E. L. Breedlove, L. J. Leverenz, E. A. Nauman, and T. M. Talavage, “The role of location of subconcussive head impacts in FMRI brain activation change,” *Developmental Neuropsychology*, vol. 40, no. 2, pp. 74–79, 2015.
- [49] T. E. Shenk, M. E. Robinson, D. O. Svaldi, K. Abbas, K. M. Breedlove, L. J. Leverenz, E. A. Nauman, and T. M. Talavage, “FMRI of visual working memory in high school football players,” *Developmental Neuropsychology*, vol. 40, no. 2, pp. 63–68, 2015.
- [50] E. J. Matser, A. G. Kessels, M. D. Lezak, B. D. Jordan, and J. Troost, “Neuropsychological impairment in amateur soccer players,” *JAMA*, vol. 282, no. 10, pp. 971–973, 1999.

- [51] A. D. Witol and F. M. Webbe, “Soccer heading frequency predicts neuropsychological deficits,” *Archives of Clinical Neuropsychology*, vol. 18, no. 4, pp. 397–417, 2003.
- [52] M. R. Zhang, S. D. Red, A. H. Lin, S. S. Patel, and A. B. Sereno, “Evidence of cognitive dysfunction after soccer playing with ball heading using a novel tablet-based approach,” *PloS One*, vol. 8, no. 2, e57364, 2013.
- [53] M. L. Lipton, N. Kim, M. E. Zimmerman, M. Kim, W. F. Stewart, C. A. Branch, and R. B. Lipton, “Soccer heading is associated with white matter microstructural and cognitive abnormalities,” *Radiology*, vol. 268, no. 3, pp. 850–857, 2013.
- [54] I. K. Koerte, A. P. Lin, M. Muehlmann, S. Merugumala, H. Liao, T. Starr, D. Kaufmann, M. Mayinger, D. Steffinger, B. Fisch, *et al.*, “Altered neurochemistry in former professional soccer players without a history of concussion,” *Journal of Neurotrauma*, vol. 32, no. 17, pp. 1287–1293, 2015.
- [55] I. K. Koerte, E. Nichols, Y. Tripodis, V. Schultz, S. Lehner, R. Igbino, A. Z. Chuang, M. Mayinger, E. M. Klier, M. Muehlmann, *et al.*, “Impaired cognitive performance in youth athletes exposed to repetitive head impacts,” *Journal of neurotrauma*, vol. 34, no. 16, pp. 2389–2395, 2017.
- [56] W. F. Stewart, N. Kim, C. S. Ifrah, R. B. Lipton, T. A. Bachrach, M. E. Zimmerman, M. Kim, and M. L. Lipton, “Symptoms from repeated intentional and unintentional head impact in soccer players,” *Neurology*, vol. 88, no. 9, pp. 901–908, 2017.
- [57] J. W. O’Kane, A. Spieker, M. R. Levy, M. Neradilek, N. L. Polissar, and M. A. Schiff, “Concussion among female middle-school soccer players,” *JAMA Pediatrics*, vol. 168, no. 3, pp. 258–264, 2014.
- [58] E. McCuen, D. Svaldi, K. Breedlove, N. Kraz, B. Cumiskey, E. L. Breedlove, J. Traver, K. F. Desmond, R. E. Hannemann, E. Zanath, *et al.*, “Collegiate women’s soccer players suffer greater cumulative head impacts than their high school counterparts,” *Journal of Biomechanics*, vol. 48, no. 13, pp. 3720–3723, 2015.
- [59] D. O. Svaldi, E. C. McCuen, C. Joshi, M. E. Robinson, Y. Nho, R. Hannemann, E. A. Nauman, L. J. Leverenz, and T. M. Talavage, “Cerebrovascular reactivity changes in asymptomatic female athletes attributable to high school soccer participation,” *Brain Imaging and Behavior*, vol. 11, no. 1, pp. 98–112, 2017.
- [60] K. M. Breedlove, E. L. Breedlove, M. Robinson, V. N. Poole, J. R. King, P. Rosenberger, M. Rasmussen, T. M. Talavage, L. J. Leverenz, and E. A. Nauman, “Detecting neurocognitive and neurophysiological changes as a result of subconcussive blows among high school football athletes,” *Athletic Training and Sports Health Care*, vol. 6, no. 3, pp. 119–127, 2014.

- [61] E. A. Nauman, K. M. Breedlove, E. L. Breedlove, T. M. Talavage, M. E. Robinson, and L. J. Leverenz, "Post-season neurophysiological deficits assessed by impact and fmri in athletes competing in american football," *Developmental Neuropsychology*, vol. 40, no. 2, pp. 85–91, 2015.
- [62] V. N. Poole, E. L. Breedlove, T. E. Shenk, K. Abbas, M. E. Robinson, L. J. Leverenz, E. A. Nauman, U. Dydak, and T. M. Talavage, "Sub-concussive hit characteristics predict deviant brain metabolism in football athletes," *Developmental Neuropsychology*, vol. 40, no. 1, pp. 12–17, 2015.
- [63] K. Merchant-Borna, P. Asselin, D. Narayan, B. Abar, C. M. Jones, and J. J. Bazarian, "Novel method of weighting cumulative helmet impacts improves correlation with brain white matter changes after one football season of sub-concussive head blows," *Annals of Biomedical Engineering*, vol. 44, no. 12, pp. 3679–3692, 2016.
- [64] B. Cummiskey, D. Schiffmiller, T. M. Talavage, L. Leverenz, J. J. Meyer, D. Adams, and E. A. Nauman, "Reliability and accuracy of helmet-mounted and head-mounted devices used to measure head accelerations," *Proceedings of the Institution of Mechanical Engineers, Part P: Journal of Sports Engineering and Technology*, vol. 231, no. 2, pp. 144–153, 2017.
- [65] J. R. Gay and K. H. Abbott, "Common whiplash injuries of the neck," *Journal of the American Medical Association*, vol. 152, no. 18, pp. 1698–1704, 1953.
- [66] F. Torres and S. K. Shapiro, "Electroencephalograms in whiplash injury: A comparison of electroencephalographic abnormalities with those present in closed head injuries," *Archives of Neurology*, vol. 5, no. 1, pp. 28–35, 1961.
- [67] A. K. Ommaya, F. Faas, and P. Yarnell, "Whiplash injury and brain damage: An experimental study," *JAMA*, vol. 204, no. 4, pp. 285–289, 1968.
- [68] A. K. Ommaya and P. Yarnell, "Subdural haematoma after whiplash injury," *The Lancet*, vol. 294, no. 7614, pp. 237–239, 1969.
- [69] K. Koshino, M. Tanaka, S. Kubota, M. Nakano, and K. Kawamoto, "Activated irregular spike and wave complex in traumatic cervical syndrome," *Brain and Nerve*, vol. 24, no. 1, pp. 49–55, 1972.
- [70] L. Barnsley, S. Lord, and N. Bogduk, "Whiplash injury," *Pain*, vol. 58, no. 3, pp. 283–307, 1994.
- [71] A. N. Guthkelch, "Infantile subdural haematoma and its relationship to whiplash injuries," *British Medical Journal*, vol. 2, no. 5759, pp. 430–431, 1971.

- [72] J. Caffey, “The whiplash shaken infant syndrome: Manual shaking by the extremities with whiplash-induced intracranial and intraocular bleedings, linked with residual permanent brain damage and mental retardation,” *Pediatrics*, vol. 54, no. 4, pp. 396–403, 1974.
- [73] I. Blumenthal, “Shaken baby syndrome,” *Postgraduate Medical Journal*, vol. 78, no. 926, pp. 732–735, 2002.
- [74] A. Dmitrienko, C. Chuang-Stein, and R. B. D’Agostino, *Pharmaceutical statistics using SAS: a practical guide*. SAS Institute, 2007.
- [75] B. Cummiskey, G. N. Sankaran, K. G. McIver, D. Shyu, J. Markel, T. M. Talavage, L. Leverenz, J. J. Meyer, D. Adams, and E. A. Nauman, “Quantitative evaluation of impact attenuation by football helmets using a modal impulse hammer,” *Proceedings of the Institution of Mechanical Engineers, Part P: Journal of Sports Engineering and Technology*, vol. 233, no. 2, pp. 301–311, 2019.
- [76] K. M. Guskiewicz, J. P. Mihalik, V. Shankar, S. W. Marshall, D. H. Crowell, S. M. Oliaro, M. F. Ciocca, and D. N. Hooker, “Measurement of head impacts in collegiate football players: Relationship between head impact biomechanics and acute clinical outcome after concussion,” *Neurosurgery*, vol. 61, no. 6, pp. 1244–1253, 2007.
- [77] J. M. Stamm, A. P. Bourlas, C. M. Baugh, N. G. Fritts, D. H. Daneshvar, B. M. Martin, M. D. McClean, Y. Tripodis, and R. A. Stern, “Age of first exposure to football and later-life cognitive impairment in former nfl players,” *Neurology*, vol. 84, no. 11, pp. 1114–1120, 2015.
- [78] M. L. Alosco, J. Mez, Y. Tripodis, P. T. Kiernan, B. Abdolmohammadi, L. Murphy, N. W. Kowall, T. D. Stein, B. R. Huber, L. E. Goldstein, *et al.*, “Age of first exposure to tackle football and chronic traumatic encephalopathy,” *Annals of Neurology*, vol. 83, no. 5, pp. 886–901, 2018.
- [79] G. E. Schneider, “Is it really better to have your brain lesion early? a revision of the “Kennard principle”,” *Neuropsychologia*, vol. 17, no. 6, pp. 557–583, 1979.
- [80] M. Field, M. W. Collins, M. R. Lovell, and J. Maroon, “Does age play a role in recovery from sports-related concussion? a comparison of high school and collegiate athletes,” *The Journal of Pediatrics*, vol. 142, no. 5, pp. 546–553, 2003.
- [81] R. Pulella, J. Raber, T. Pfankuch, D. M. Ferriero, C. P. Claus, S.-E. Koh, T. Yamauchi, R. Rola, J. R. Fike, and L. J. Noble-Haeusslein, “Traumatic injury to the immature brain results in progressive neuronal loss, hyperactivity and delayed cognitive impairments,” *Developmental Neuroscience*, vol. 28, no. 4-5, pp. 396–409, 2006.

- [82] A. V. Lavallee, R. P. Ching, and D. J. Nuckley, “Developmental biomechanics of neck musculature,” *Journal of Biomechanics*, vol. 46, no. 3, pp. 527–534, 2013.
- [83] R. C. Cantu and M. Hyman, *Concussions and our kids: America’s leading expert on how to protect young athletes and keep sports safe*. Houghton Mifflin Harcourt, 2012.
- [84] V. N. Poole, K. Abbas, T. E. Shenk, E. L. Breedlove, K. M. Breedlove, M. E. Robinson, L. J. Leverenz, E. A. Nauman, T. M. Talavage, and U. Dydak, “MR spectroscopic evidence of brain injury in the non-diagnosed collision sport athlete,” *Developmental Neuropsychology*, vol. 39, no. 6, pp. 459–473, 2014.
- [85] S. P. Broglio, J. J. Sosnoff, S. Shin, X. He, C. Alcaraz, and J. Zimmerman, “Head impacts during high school football: A biomechanical assessment,” *Journal of Athletic Training*, vol. 44, no. 4, pp. 342–349, 2009.
- [86] S. P. Broglio, T. Surma, and J. A. Ashton-Miller, “High school and collegiate football athlete concussions: A biomechanical review,” *Annals of Biomedical Engineering*, vol. 40, no. 1, pp. 37–46, 2012.
- [87] J. T. Eckner, M. Sabin, J. S. Kutcher, and S. P. Broglio, “No evidence for a cumulative impact effect on concussion injury threshold,” *Journal of Neurotrauma*, vol. 28, no. 10, pp. 2079–2090, 2011.
- [88] B. Schnebel, J. T. Gwin, S. Anderson, and R. Gatlin, “In vivo study of head impacts in football: A comparison of national collegiate athletic association division I versus high school impacts,” *Neurosurgery*, vol. 60, no. 3, pp. 490–496, 2007.
- [89] S. Tiernan, G. Byrne, and D. M. O’Sullivan, “Evaluation of skin-mounted sensor for head impact measurement,” *Proceedings of the Institution of Mechanical Engineers, Part H: Journal of Engineering in Medicine*, vol. 233, no. 7, pp. 735–744, 2019.
- [90] T. B. Hoshizaki, A. Post, M. Kendall, J. Cournoyer, P. Rousseau, M. D. Gilchrist, S. Brien, M. Cusimano, and S. Marshall, “The development of a threshold curve for the understanding of concussion in sport,” *Trauma*, vol. 19, no. 3, pp. 196–206, 2017.
- [91] C. Karton and T. B. Hoshizaki, “Concussive and subconcussive brain trauma: The complexity of impact biomechanics and injury risk in contact sport,” *Handbook of Clinical Neurology*, vol. 158, pp. 39–49, 2018.
- [92] R. A. Oeur, M. D. Gilchrist, and T. B. Hoshizaki, “Parametric study of impact parameters on peak head acceleration and strain for collision impacts in sport,” *International Journal of Crashworthiness*, vol. 26, no. 1, pp. 16–25, 2021.

- [93] Y. Feng, T. M. Abney, R. J. Okamoto, R. B. Pless, G. M. Genin, and P. V. Bayly, “Relative brain displacement and deformation during constrained mild frontal head impact,” *Journal of the Royal Society Interface*, vol. 7, no. 53, pp. 1677–1688, 2010.
- [94] H. Zou, J. P. Schmiedeler, and W. N. Hardy, “Separating brain motion into rigid body displacement and deformation under low-severity impacts,” *Journal of Biomechanics*, vol. 40, no. 6, pp. 1183–1191, 2007.
- [95] W. N. Hardy, C. D. Foster, M. J. Mason, K. H. Yang, A. I. King, and S. Tashman, “Investigation of head injury mechanisms using neutral density technology and high-speed biplanar x-ray,” SAE Technical Paper, Tech. Rep., 2001.
- [96] P. V. Bayly, T. Cohen, E. Leister, D. Ajo, E. Leuthardt, and G. Genin, “Deformation of the human brain induced by mild acceleration,” *Journal of Neurotrauma*, vol. 22, no. 8, pp. 845–856, 2005.
- [97] J. P. Mihalik, D. R. Bell, S. W. Marshall, and K. M. Guskiewicz, “Measurement of head impacts in collegiate football players: An investigation of positional and event-type differences,” *Neurosurgery*, vol. 61, no. 6, pp. 1229–1235, 2007.
- [98] J. J. Crisco, R. Fiore, J. G. Beckwith, J. J. Chu, P. G. Brolinson, S. Duma, T. W. McAllister, A.-C. Duhaime, and R. M. Greenwald, “Frequency and location of head impact exposures in individual collegiate football players,” *Journal of Athletic Training*, vol. 45, no. 6, pp. 549–559, 2010.
- [99] S. M. Duma, S. J. Manoogian, W. R. Bussone, P. G. Brolinson, M. W. Goforth, J. J. Donnenwerth, R. M. Greenwald, J. J. Chu, and J. J. Crisco, “Analysis of real-time head accelerations in collegiate football players,” *Clinical Journal of Sport Medicine*, vol. 15, no. 1, pp. 3–8, 2005.
- [100] T. A. Lee, R. J. Lycke, P. J. Lee, C. M. Cudal, K. J. Torolski, S. E. Bucherl, N. Leiva-Molano, P. S. Auerbach, T. M. Talavage, and E. A. Nauman, “Distribution of head acceleration events varies by position and play type in north american football,” *Clinical Journal of Sport Medicine: Official Journal of the Canadian Academy of Sport Medicine*, 2020.
- [101] S. T. DeKosky, M. D. Ikonomic, and M. Sam Gandy, “Traumatic brain injury—football, warfare, and long-term effects,” *The New England Journal of Medicine*, vol. 363, no. 14, pp. 1293–1296, 2010.
- [102] J. C. Maroon, R. Winkelman, J. Bost, A. Amos, C. Mathyssek, and V. Miele, “Correction: Chronic traumatic encephalopathy in contact sports: A systematic review of all reported pathological cases,” *PloS One*, vol. 10, no. 6, e0130507, 2015.

- [103] L.-N. Hazrati, M. C. Tartaglia, P. Diamandis, K. Davis, R. E. Green, R. Wennberg, J. C. Wong, L. Ezerins, and C. H. Tator, "Absence of chronic traumatic encephalopathy in retired football players with multiple concussions and neurological symptomatology," *Frontiers in Human Neuroscience*, vol. 7, no. 222, pp. 1–9, 2013.
- [104] A. C. McKee, T. D. Stein, C. J. Nowinski, R. A. Stern, D. H. Daneshvar, V. E. Alvarez, H.-S. Lee, G. Hall, S. M. Wojtowicz, C. M. Baugh, *et al.*, "The spectrum of disease in chronic traumatic encephalopathy," *Brain*, vol. 136, no. 1, pp. 43–64, 2013.
- [105] J. E. Bailes, R. C. Turner, B. P. Lucke-Wold, V. Patel, and J. M. Lee, "Chronic traumatic encephalopathy: Is it real? the relationship between neurotrauma and neurodegeneration," *Neurosurgery*, vol. 62, pp. 15–24, CN_suppl_1 2015.
- [106] R. C. Turner, B. P. Lucke-Wold, M. J. Robson, J. M. Lee, and J. E. Bailes, "Alzheimer's disease and chronic traumatic encephalopathy: Distinct but possibly overlapping disease entities," *Brain Injury*, vol. 30, no. 11, pp. 1279–1292, 2016.
- [107] M. Alosco, A. Kasimis, J. Stamm, A. Chua, C. Baugh, D. Daneshvar, C. Robbins, M. Mariani, J. Hayden, S. Conneely, *et al.*, "Age of first exposure to american football and long-term neuropsychiatric and cognitive outcomes," *Translational Psychiatry*, vol. 7, no. 9, e1236–e1236, 2017.
- [108] M. L. Alosco, Y. Tripodis, J. Jarnagin, C. M. Baugh, B. Martin, C. E. Chaisson, N. Estochen, L. Song, R. C. Cantu, A. Jeromin, *et al.*, "Repetitive head impact exposure and later-life plasma total tau in former national football league players," *Alzheimer's & Dementia: Diagnosis, Assessment & Disease Monitoring*, vol. 7, pp. 33–40, 2017.
- [109] P. S. Auerbach and I. Waggoner William H., "It's time to change the rules," *JAMA*, vol. 316, no. 12, pp. 1260–1261, Sep. 2016, ISSN: 0098-7484. DOI: [10.1001/jama.2016.8184](https://doi.org/10.1001/jama.2016.8184). eprint: <https://jamanetwork.com/journals/jama/articlepdf/2556128/jpo160023.pdf>. [Online]. Available: <https://doi.org/10.1001/jama.2016.8184>.
- [110] S. P. Broglio, J. T. Eckner, D. Martini, J. J. Sosnoff, J. S. Kutcher, and C. Randolph, "Cumulative head impact burden in high school football," *Journal of Neurotrauma*, vol. 28, no. 10, pp. 2069–2078, 2011.
- [111] D. J. Wiebe, B. A. D'Alonzo, R. Harris, M. Putukian, and C. Campbell-McGovern, "Association between the experimental kickoff rule and concussion rates in ivy league football," *JAMA*, vol. 320, no. 19, pp. 2035–2036, 2018.
- [112] D. Martini, J. Eckner, J. Kutcher, and S. Broglio, "Subconcussive head impact biomechanics: Comparing differing offensive schemes," *Medicine and Science in Sports and Exercise*, vol. 45, no. 4, pp. 755–761, 2013.

- [113] E. A. Nauman, T. M. Talavage, and P. S. Auerbach, “Mitigating the consequences of subconcussive head injuries,” *Annual Review of Biomedical Engineering*, vol. 22, pp. 387–407, 2020.
- [114] I. Jang, I. Y. Chun, J. R. Brosch, S. Bari, Y. Zou, B. R. Cummiskey, T. A. Lee, R. J. Lycke, V. N. Poole, T. E. Shenk, *et al.*, “Every hit matters: White matter diffusivity changes in high school football athletes are correlated with repetitive head acceleration event exposure,” *NeuroImage: Clinical*, no. 101930, pp. 1–16, 2019.
- [115] D. O. Svaldi, C. Joshi, E. C. McCuen, J. P. Music, R. Hannemann, L. J. Leverenz, E. A. Nauman, and T. M. Talavage, “Accumulation of high magnitude acceleration events predicts cerebrovascular reactivity changes in female high school soccer athletes,” *Brain Imaging and Behavior*, pp. 1–11, 2018.
- [116] E. A. Nauman and T. M. Talavage, “Subconcussive trauma,” *Handbook of Clinical Neurology*, vol. 158, pp. 245–255, 2018.
- [117] C. A. Emery and A. M. Black, “Are rule changes the low-hanging fruit for concussion prevention in youth sport?” *JAMA Pediatrics*, vol. 173, no. 4, pp. 309–310, 2019.
- [118] A. L. Schranz, K. Y. Manning, G. A. Dekaban, L. Fischer, T. Jevremovic, K. Blackney, C. Barreira, T. J. Doherty, D. D. Fraser, A. Brown, *et al.*, “Reduced brain glutamine in female varsity rugby athletes after concussion and in non-concussed athletes after a season of play,” *Human Brain Mapping*, vol. 39, no. 4, pp. 1489–1499, 2018.
- [119] T. W. McAllister, J. C. Ford, L. A. Flashman, A. Maerlender, R. M. Greenwald, J. G. Beckwith, R. P. Bolander, T. D. Tosteson, J. H. Turco, R. Raman, *et al.*, “Effect of head impacts on diffusivity measures in a cohort of collegiate contact sport athletes,” *Neurology*, vol. 82, no. 1, pp. 63–69, 2014.
- [120] S. Tremblay, L. C. Henry, C. Bedetti, C. Larson-Dupuis, J.-F. Gagnon, A. C. Evans, H. Theoret, M. Lassonde, and L. D. Beaumont, “Diffuse white matter tract abnormalities in clinically normal ageing retired athletes with a history of sports-related concussions,” *Brain*, vol. 137, no. 11, pp. 2997–3011, 2014.
- [121] J. J. Bazarian, T. Zhu, B. Blyth, A. Borrino, and J. Zhong, “Subject-specific changes in brain white matter on diffusion tensor imaging after sports-related concussion,” *Magnetic Resonance Imaging*, vol. 30, no. 2, pp. 171–180, 2012.
- [122] V. A. Cubon, M. Putukian, C. Boyer, and A. Dettwiler, “A diffusion tensor imaging study on the white matter skeleton in individuals with sports-related concussion,” *Journal of Neurotrauma*, vol. 28, no. 2, pp. 189–201, 2011.

- [123] L. C. Henry, J. Tremblay, S. Tremblay, A. Lee, C. Brun, N. Lepore, H. Theoret, D. Ellemberg, and M. Lassonde, “Acute and chronic changes in diffusivity measures after sports concussion,” *Journal of Neurotrauma*, vol. 28, no. 10, pp. 2049–2059, 2011.
- [124] M. A. Lancaster, D. V. Olson, M. A. McCrea, L. D. Nelson, A. A. LaRoche, and L. T. Muftuler, “Acute white matter changes following sport-related concussion: A serial diffusion tensor and diffusion kurtosis tensor imaging study,” *Human Brain Mapping*, vol. 37, no. 11, pp. 3821–3834, 2016.
- [125] T. W. McAllister, J. C. Ford, S. Ji, J. G. Beckwith, L. A. Flashman, K. Paulsen, and R. M. Greenwald, “Maximum principal strain and strain rate associated with concussion diagnosis correlates with changes in corpus callosum white matter indices,” *Annals of Biomedical Engineering*, vol. 40, no. 1, pp. 127–140, 2012.
- [126] S. M. Mustafi, J. Harezlak, K. M. Koch, A. S. Nencka, T. B. Meier, J. D. West, C. C. Giza, J. P. DiFiori, K. M. Guskiewicz, J. P. Mihalik, *et al.*, “Acute white-matter abnormalities in sports-related concussion: A diffusion tensor imaging study from the ncaa-dod care consortium,” *Journal of Neurotrauma*, vol. 35, no. 22, pp. 2653–2664, 2018.
- [127] N. Marchi, J. J. Bazarian, V. Puvenna, M. Janigro, C. Ghosh, J. Zhong, T. Zhu, E. Blackman, D. Stewart, J. Ellis, *et al.*, “Consequences of repeated blood-brain barrier disruption in football players,” *PloS One*, vol. 8, no. 3, 2013.
- [128] J. J. Bazarian, T. Zhu, J. Zhong, D. Janigro, E. Rozen, A. Roberts, H. Javien, K. Merchant-Borna, B. Abar, and E. G. Blackman, “Persistent, long-term cerebral white matter changes after sports-related repetitive head impacts,” *PloS One*, vol. 9, no. 4, 2014.
- [129] K. Arfanakis, V. M. Haughton, J. D. Carew, B. P. Rogers, R. J. Dempsey, and M. E. Meyerand, “Diffusion tensor MR imaging in diffuse axonal injury,” *American Journal of Neuroradiology*, vol. 23, no. 5, pp. 794–802, 2002.
- [130] N. Bahrami, D. Sharma, S. Rosenthal, E. M. Davenport, J. E. Urban, B. Wagner, Y. Jung, C. G. Vaughan, G. A. Gioia, J. D. Stitzel, *et al.*, “Subconcussive head impact exposure and white matter tract changes over a single season of youth football,” *Radiology*, vol. 281, no. 3, pp. 919–926, 2016.
- [131] C. W. Christman, M. S. Grady, S. A. Walker, K. L. Holloway, and J. T. Povlishock, “Ultrastructural studies of diffuse axonal injury in humans,” *Journal of Neurotrauma*, vol. 11, no. 2, pp. 173–186, 1994.
- [132] E. M. Davenport, C. T. Whitlow, J. E. Urban, M. A. Espeland, Y. Jung, D. A. Rosenbaum, G. A. Gioia, A. K. Powers, J. D. Stitzel, and J. A. Maldjian, “Abnormal

- white matter integrity related to head impact exposure in a season of high school varsity football,” *Journal of Neurotrauma*, vol. 31, no. 19, pp. 1617–1624, 2014.
- [133] G. Douaud, T. E. Behrens, C. Poupon, Y. Cointepas, S. Jbabdi, V. Gaura, N. Golestani, P. Krystkowiak, C. Verny, P. Damier, *et al.*, “In vivo evidence for the selective subcortical degeneration in Huntington’s disease,” *Neuroimage*, vol. 46, no. 4, pp. 958–966, 2009.
 - [134] G. Douaud, S. Jbabdi, T. E. Behrens, R. A. Menke, A. Gass, A. U. Monsch, A. Rao, B. Whitcer, G. Kindlmann, P. M. Matthews, *et al.*, “DTI measures in crossing-fibre areas: Increased diffusion anisotropy reveals early white matter alteration in MCI and mild Alzheimer’s disease,” *Neuroimage*, vol. 55, no. 3, pp. 880–890, 2011.
 - [135] K. D. B. Foss, W. Yuan, J. A. Diekfuss, J. Leach, W. Meehan, C. A. DiCesare, G. Solomon, D. K. Schneider, J. MacDonald, J. Dudley, *et al.*, “Relative head impact exposure and brain white matter alterations after a single season of competitive football: A pilot comparison of youth versus high school football,” *Clinical Journal of Sport Medicine*, vol. 29, no. 6, pp. 442–450, 2019.
 - [136] N. Gajawelli, Y. Lao, M. L. Apuzzo, R. Romano, C. Liu, S. Tsao, D. Hwang, B. Wilkins, N. Lepore, and M. Law, “Neuroimaging changes in the brain in contact versus noncontact sport athletes using diffusion tensor imaging,” *World Neurosurgery*, vol. 80, no. 6, pp. 824–828, 2013.
 - [137] M. S. Grady, M. R. McLaughlin, C. W. Christman, A. B. Valadka, C. L. Fligner, and J. T. Povlishock, “The use of antibodies targeted against the neurofilament subunits for the detection of diffuse axonal injury in humans,” *Journal of Neuropathology & Experimental Neurology*, vol. 52, no. 2, pp. 143–152, 1993.
 - [138] V. E. Johnson, W. Stewart, and D. H. Smith, “Axonal pathology in traumatic brain injury,” *Experimental Neurology*, vol. 246, pp. 35–43, 2013.
 - [139] K. Kantarci, M. E. Murray, C. G. Schwarz, R. I. Reid, S. A. Przybelski, T. Lesnick, S. M. Zuk, M. R. Raman, M. L. Senjem, J. L. Gunter, *et al.*, “White-matter integrity on DTI and the pathologic staging of Alzheimer’s disease,” *Neurobiology of Aging*, vol. 56, pp. 172–179, 2017.
 - [140] I. K. Koerte, D. Kaufmann, E. Hartl, S. Bouix, O. Pasternak, M. Kubicki, A. Rauscher, D. K. Li, S. B. Dadachanji, J. A. Taunton, *et al.*, “A prospective study of physician-observed concussion during a varsity university hockey season: White matter integrity in ice hockey players. part 3 of 4,” *Neurosurgical Focus*, vol. 33, no. 6, E3, 2012.
 - [141] M. F. Kraus, T. Susmaras, B. P. Caughlin, C. J. Walker, J. A. Sweeney, and D. M. Little, “White matter integrity and cognition in chronic traumatic brain injury: A diffusion tensor imaging study,” *Brain*, vol. 130, no. 10, pp. 2508–2519, 2007.

- [142] S. Kuzminski, M. Clark, M. Fraser, C. Haswell, R. Morey, C. Liu, K. Choudhury, K. Guskiewicz, and J. Petrella, "White matter changes related to subconcussive impact frequency during a single season of high school football," *American Journal of Neuroradiology*, vol. 39, no. 2, pp. 245–251, 2018.
- [143] Y. Lao, M. Law, J. Shi, N. Gajawelli, L. Haas, Y. Wang, and N. Leporé, "A T1 and DTI fused 3D corpus callosum analysis in pre- vs. post-season contact sports players," in *10th International Symposium on Medical Information Processing and Analysis*, International Society for Optics and Photonics, vol. 9287, 2015, 92870O.
- [144] C. Mac Donald, K. Dikranian, S.-K. Song, P. Bayly, D. Holtzman, and D. Brody, "Detection of traumatic axonal injury with diffusion tensor imaging in a mouse model of traumatic brain injury," *Experimental Neurology*, vol. 205, no. 1, pp. 116–131, 2007.
- [145] C. L. Mac Donald, K. Dikranian, P. Bayly, D. Holtzman, and D. Brody, "Diffusion tensor imaging reliably detects experimental traumatic axonal injury and indicates approximate time of injury," *Journal of Neuroscience*, vol. 27, no. 44, pp. 11 869–11 876, 2007.
- [146] S. Magnoni, C. L. Mac Donald, T. J. Esparza, V. Conte, J. Sorrell, M. Macrì, G. Bertani, R. Biffi, A. Costa, B. Sammons, *et al.*, "Quantitative assessments of traumatic axonal injury in human brain: Concordance of microdialysis and advanced mri," *Brain*, vol. 138, no. 8, pp. 2263–2277, 2015.
- [147] M. C. Mayinger, K. Merchant-Borna, J. Hufschmidt, M. Muehlmann, I. R. Weir, B.-S. Rauchmann, M. E. Shenton, I. K. Koerte, and J. J. Bazarian, "White matter alterations in college football players: A longitudinal diffusion tensor imaging study," *Brain Imaging and Behavior*, vol. 12, no. 1, pp. 44–53, 2018.
- [148] G. D. Myer, K. B. Foss, S. Thomas, R. Galloway, C. A. DiCesare, J. Dudley, B. Gadd, J. Leach, D. Smith, P. Gubanich, *et al.*, "Altered brain microstructure in association with repetitive subconcussive head impacts and the potential protective effect of jugular vein compression: A longitudinal study of female soccer athletes," *British Journal of Sports Medicine*, vol. 53, no. 24, pp. 1539–1551, 2019.
- [149] G. D. Myer, W. Yuan, K. D. Barber Foss, D. Smith, M. Altaye, A. Reches, J. Leach, A. W. Kiefer, J. C. Khoury, M. Weiss, *et al.*, "The effects of external jugular compression applied during head impact exposure on longitudinal changes in brain neuroanatomical and neurophysiological biomarkers: A preliminary investigation," *Frontiers in Neurology*, vol. 7, no. 74, pp. 1–14, 2016.
- [150] G. D. Myer, W. Yuan, K. D. B. Foss, S. Thomas, D. Smith, J. Leach, A. W. Kiefer, C. Dicesare, J. Adams, P. J. Gubanich, *et al.*, "Analysis of head impact exposure and brain microstructure response in a season-long application of a jugular vein compres-

- sion collar: A prospective, neuroimaging investigation in american football,” *British Journal of Sports Medicine*, vol. 50, no. 20, pp. 1276–1285, 2016.
- [151] J. Pan, I. D. Connolly, S. Dangelmajer, J. Kintzing, A. L. Ho, and G. Grant, “Sports-related brain injuries: Connecting pathology to diagnosis,” *Neurosurgical Focus*, vol. 40, no. 4, E14, 2016.
 - [152] J. Povlishock, D. Becker, C. Cheng, and G. Vaughan, “Axonal change in minor head injury,” *Journal of Neuropathology & Experimental Neurology*, vol. 42, no. 3, pp. 225–242, 1983.
 - [153] J. T. Povlishock and D. I. Katz, “Update of neuropathology and neurological recovery after traumatic brain injury,” *The Journal of Head Trauma Rehabilitation*, vol. 20, no. 1, pp. 76–94, 2005.
 - [154] H. D. Rosas, D. S. Tuch, N. D. Hevelone, A. K. Zaleta, M. Vangel, S. M. Hersch, and D. H. Salat, “Diffusion tensor imaging in presymptomatic and early Huntington’s disease: Selective white matter pathology and its relationship to clinical measures,” *Movement Disorders: Official Journal of the Movement Disorder Society*, vol. 21, no. 9, pp. 1317–1325, 2006.
 - [155] D. K. Schneider, R. Galloway, J. J. Bazarian, J. A. Diekfuss, J. Dudley, J. L. Leach, R. Mannix, T. M. Talavage, W. Yuan, and G. D. Myer, “Diffusion tensor imaging in athletes sustaining repetitive head impacts: A systematic review of prospective studies,” *Journal of Neurotrauma*, vol. 36, no. 20, pp. 2831–2849, 2019.
 - [156] Y. Shitaka, H. T. Tran, R. E. Bennett, L. Sanchez, M. A. Levy, K. Dikranian, and D. L. Brody, “Repetitive closed-skull traumatic brain injury in mice causes persistent multifocal axonal injury and microglial reactivity,” *Journal of Neuropathology & Experimental Neurology*, vol. 70, no. 7, pp. 551–567, 2011.
 - [157] S. R. Shultz, D. F. MacFabe, K. A. Foley, R. Taylor, and D. P. Cain, “Sub-concussive brain injury in the long-evans rat induces acute neuroinflammation in the absence of behavioral impairments,” *Behavioural Brain Research*, vol. 229, no. 1, pp. 145–152, 2012.
 - [158] S. M. Slobounov, A. Walter, H. C. Breiter, D. C. Zhu, X. Bai, T. Bream, P. Seidenberg, X. Mao, B. Johnson, and T. M. Talavage, “The effect of repetitive subconcussive collisions on brain integrity in collegiate football players over a single football season: A multi-modal neuroimaging study,” *Neuroimage: Clinical*, vol. 14, pp. 708–718, 2017.
 - [159] N. Sollmann, P. S. Echlin, V. Schultz, P. V. Viher, A. E. Lyall, Y. Tripodis, D. Kaufmann, E. Hartl, P. Kinzel, L. A. Forwell, *et al.*, “Sex differences in white matter alterations following repetitive subconcussive head impacts in collegiate ice hockey players,” *Neuroimage: Clinical*, vol. 17, pp. 642–649, 2018.

- [160] M. Sundman, P. M. Doraiswamy, and R. Morey, “Neuroimaging assessment of early and late neurobiological sequelae of traumatic brain injury: Implications for CTE,” *Frontiers in Neuroscience*, vol. 9, no. 334, pp. 1–15, 2015.
- [161] W. Yuan, K. D. Barber Foss, S. Thomas, C. A. DiCesare, J. A. Dudley, K. Kitchen, B. Gadd, J. L. Leach, D. Smith, M. Altaye, *et al.*, “White matter alterations over the course of two consecutive high-school football seasons and the effect of a jugular compression collar: A preliminary longitudinal diffusion tensor imaging study,” *Human Brain Mapping*, vol. 39, no. 1, pp. 491–508, 2018.
- [162] P. J. Basser and D. K. Jones, “Diffusion-tensor MRI: Theory, experimental design and data analysis—a technical review,” *NMR in Biomedicine: An International Journal Devoted to the Development and Application of Magnetic Resonance In Vivo*, vol. 15, no. 7-8, pp. 456–467, 2002.
- [163] C. Beaulieu, “The basis of anisotropic water diffusion in the nervous system—a technical review,” *NMR in Biomedicine: An International Journal Devoted to the Development and Application of Magnetic Resonance In Vivo*, vol. 15, no. 7-8, pp. 435–455, 2002.
- [164] A. Chutinet and N. S. Rost, “White matter disease as a biomarker for long-term cerebrovascular disease and dementia,” *Current Treatment Options in Cardiovascular Medicine*, vol. 16, no. 292, pp. 1–12, 2014.
- [165] A. A. Hirad, J. J. Bazarian, K. Merchant-Borna, F. E. Garcea, S. Heilbronner, D. Paul, E. B. Hintz, E. van Wijngaarden, G. Schifitto, D. W. Wright, *et al.*, “A common neural signature of brain injury in concussion and subconcussion,” *Science Advances*, vol. 5, no. 8, eaau3460, 2019.
- [166] H. S. Levin, E. Wilde, M. Troyanskaya, N. J. Petersen, R. Scheibel, M. Newsome, M. Radaideh, T. Wu, R. Yallampalli, Z. Chu, *et al.*, “Diffusion tensor imaging of mild to moderate blast-related traumatic brain injury and its sequelae,” *Journal of Neurotrauma*, vol. 27, no. 4, pp. 683–694, 2010.
- [167] J. M. Ling, A. Pena, R. A. Yeo, F. L. Merideth, S. Klimaj, C. Gasparovic, and A. R. Mayer, “Biomarkers of increased diffusion anisotropy in semi-acute mild traumatic brain injury: A longitudinal perspective,” *Brain*, vol. 135, no. 4, pp. 1281–1292, 2012.
- [168] D. R. Miller, J. P. Hayes, G. Lafleche, D. H. Salat, and M. Verfaellie, “White matter abnormalities are associated with chronic postconcussion symptoms in blast-related mild traumatic brain injury,” *Human Brain Mapping*, vol. 37, no. 1, pp. 220–229, 2016.
- [169] M. Smits, G. C. Houston, D. W. Dippel, P. A. Wielopolski, M. W. Vernooij, P. J. Koudstaal, M. M. Hunink, and A. van der Lugt, “Microstructural brain injury in

- post-concussion syndrome after minor head injury,” *Neuroradiology*, vol. 53, no. 8, pp. 553–563, 2011.
- [170] P.-H. Yeh, B. Wang, T. R. Oakes, L. M. French, H. Pan, J. Graner, W. Liu, and G. Riedy, “Postconcussional disorder and PTSD symptoms of military-related traumatic brain injury associated with compromised neurocircuitry,” *Human Brain Mapping*, vol. 35, no. 6, pp. 2652–2673, 2014.
 - [171] K. Zhang, B. Johnson, D. Pennell, W. Ray, W. Sebastianelli, and S. Slobounov, “Are functional deficits in concussed individuals consistent with white matter structural alterations: Combined FMRI & DTI study,” *Experimental Brain Research*, vol. 204, no. 1, pp. 57–70, 2010.
 - [172] T. Mueggler, H. Pohl, C. Baltes, D. Riethmacher, U. Suter, and M. Rudin, “MRI signature in a novel mouse model of genetically induced adult oligodendrocyte cell death,” *Neuroimage*, vol. 59, no. 2, pp. 1028–1036, 2012.
 - [173] U. I. Tuor, M. Morgunov, M. Sule, M. Qiao, D. Clark, D. Rushforth, T. Foniok, and A. Kirton, “Cellular correlates of longitudinal diffusion tensor imaging of axonal degeneration following hypoxic–ischemic cerebral infarction in neonatal rats,” *NeuroImage: Clinical*, vol. 6, pp. 32–42, 2014.
 - [174] M. Linder, *3d arrow plot*. [Online]. Available: <https://www.mathworks.com/matlabcentral/fileexchange/28324-3d-arrow-plot>, MATLAB Central File Exchange.
 - [175] K. Hua, J. Zhang, S. Wakana, H. Jiang, X. Li, D. S. Reich, P. A. Calabresi, J. J. Pekar, P. C. van Zijl, and S. Mori, “Tract probability maps in stereotaxic spaces: Analyses of white matter anatomy and tract-specific quantification,” *Neuroimage*, vol. 39, no. 1, pp. 336–347, 2008.
 - [176] D. Bonekamp, L. M. Nagae, M. Degaonkar, M. Matson, W. M. Abdalla, P. B. Barker, S. Mori, and A. Horská, “Diffusion tensor imaging in children and adolescents: Reproducibility, hemispheric, and age-related differences,” *Neuroimage*, vol. 34, no. 2, pp. 733–742, 2007.
 - [177] T. J. Eluvathingal, K. M. Hasan, L. Kramer, J. M. Fletcher, and L. Ewing-Cobbs, “Quantitative diffusion tensor tractography of association and projection fibers in normally developing children and adolescents,” *Cerebral Cortex*, vol. 17, no. 12, pp. 2760–2768, 2007.
 - [178] K. M. Hasan, A. Sankar, C. Halphen, L. A. Kramer, M. E. Brandt, J. Juranek, P. T. Cirino, J. M. Fletcher, A. C. Papanicolaou, and L. Ewing-Cobbs, “Development and organization of the human brain tissue compartments across the lifespan using diffusion tensor imaging,” *Neuroreport*, vol. 18, no. 16, pp. 1735–1739, 2007.

- [179] K. M. Hasan, A. Kamali, L. A. Kramer, A. C. Papnicolaou, J. M. Fletcher, and L. Ewing-Cobbs, "Diffusion tensor quantification of the human midsagittal corpus callosum subdivisions across the lifespan," *Brain Research*, vol. 1227, pp. 52–67, 2008.
- [180] C. Lebel, L. Walker, A. Leemans, L. Phillips, and C. Beaulieu, "Microstructural maturation of the human brain from childhood to adulthood," *Neuroimage*, vol. 40, no. 3, pp. 1044–1055, 2008.
- [181] D. J. Mabbott, M. Noseworthy, E. Bouffet, S. Laughlin, and C. Rockel, "White matter growth as a mechanism of cognitive development in children," *Neuroimage*, vol. 33, no. 3, pp. 936–946, 2006.
- [182] E. A. Olson, P. F. Collins, C. J. Hooper, R. Muetzel, K. O. Lim, and M. Luciana, "White matter integrity predicts delay discounting behavior in 9-to 23-year-olds: A diffusion tensor imaging study," *Journal of Cognitive Neuroscience*, vol. 21, no. 7, pp. 1406–1421, 2009.
- [183] D. Qiu, L.-H. Tan, K. Zhou, and P.-L. Khong, "Diffusion tensor imaging of normal white matter maturation from late childhood to young adulthood: Voxel-wise evaluation of mean diffusivity, fractional anisotropy, radial and axial diffusivities, and correlation with reading development," *Neuroimage*, vol. 41, no. 2, pp. 223–232, 2008.
- [184] V. J. Schmithorst, M. Wilke, B. J. Dardzinski, and S. K. Holland, "Correlation of white matter diffusivity and anisotropy with age during childhood and adolescence: A cross-sectional diffusion-tensor MR imaging study," *Radiology*, vol. 222, no. 1, pp. 212–218, 2002.
- [185] V. J. Schmithorst and W. Yuan, "White matter development during adolescence as shown by diffusion MRI," *Brain and Cognition*, vol. 72, no. 1, pp. 16–25, 2010.
- [186] L. Snook, L.-A. Paulson, D. Roy, L. Phillips, and C. Beaulieu, "Diffusion tensor imaging of neurodevelopment in children and young adults," *Neuroimage*, vol. 26, no. 4, pp. 1164–1173, 2005.
- [187] L. Snook, C. Plewes, and C. Beaulieu, "Voxel based versus region of interest analysis in diffusion tensor imaging of neurodevelopment," *Neuroimage*, vol. 34, no. 1, pp. 243–252, 2007.
- [188] W. Rugby, *Laws of the game rugby union*, 2020.
- [189] D. A. King, P. A. Hume, C. Gissane, and T. N. Clark, "Similar head impact acceleration measured using instrumented ear patches in a junior rugby union team during matches in comparison with other sports," *Journal of Neurosurgery: Pediatrics*, vol. 18, no. 1, pp. 65–72, 2016.

- [190] D. King, P. Hume, C. Gissane, and T. Clark, “Head impacts in a junior rugby league team measured with a wireless head impact sensor: An exploratory analysis,” *Journal of Neurosurgery: Pediatrics*, vol. 19, no. 1, pp. 13–23, 2017.
- [191] D. King, P. A. Hume, M. Brughelli, and C. Gissane, “Instrumented mouthguard acceleration analyses for head impacts in amateur rugby union players over a season of matches,” *The American Journal of Sports Medicine*, vol. 43, no. 3, pp. 614–624, 2015.
- [192] J. J. Crisco, B. J. Wilcox, J. G. Beckwith, J. J. Chu, A.-C. Duhaime, S. Rowson, S. M. Duma, A. C. Maerlender, T. W. McAllister, and R. M. Greenwald, “Head impact exposure in collegiate football players,” *Journal of Biomechanics*, vol. 44, no. 15, pp. 2673–2678, 2011.
- [193] N. Leiva-Molano, R. J. Rolley, T. Lee, K. G. McIver, G. Sankaran, J. J. Meyer, D. E. Adams, E. Breedlove, T. M. Talavage, and E. A. Nauman, “Evaluation of impulse attenuation by football helmets in the frequency domain,” *Journal of Biomechanical Engineering*, vol. 142, no. 6, 2020.
- [194] A. J. Merrell, W. F. Christensen, M. K. Seeley, A. E. Bowden, and D. T. Fullwood, “Nano-composite foam sensor system in football helmets,” *Annals of Biomedical Engineering*, vol. 45, no. 12, pp. 2742–2749, 2017.
- [195] T. A. Fodemski, *Protective helmet having a microprocessor controlled response to impact*, US Patent 8,127,373, Mar. 2012.
- [196] K. Hoffmann, *An introduction to stress analysis using strain gauges*.
- [197] *Strain gauges: HBM strain gauges*, Catalog.
- [198] O. Mete, M. Yalcin, and K. Genel, “Experimental and numerical studies on the folding response of annular-rolled Al tube,” *Thin-Walled Structures*, vol. 127, pp. 798–808, 2018.
- [199] *Tech note #122: Clear and understandable: Temperature compensation of strain gauge quarter bridge applications*, 2021. [Online]. Available: <https://www.hbm.com/en/10083/temperature-compensation-of-strain-gauge-quarter-bridges/>.
- [200] *Errors due to transverse sensitivity in strain gages*, Document Number 11059, 2011. [Online]. Available: <http://www.vishaypg.com/docs/11059/tn509tn5.pdf>.
- [201] A. P. Boresi, R. J. Schmidt, O. M. Sidebottom, *et al.*, *Advanced mechanics of materials*. Wiley New York, 1985, vol. 6.

- [202] D. Ferreira, Ed., *User's manual – release 10.4*, DIANA FEA BV, 2020. [Online]. Available: <https://dianafea.com/manuals/d104/Diana.html>.

A. APPENDIX A: METHODS

A.1 Outlier Analysis

Two separate outlier analysis methods were used. For each session, HAEs that occurred within a 10 second window were considered. If five or more HAEs occurred within those 10 seconds, all the readings in the time window were flagged. If the number of flagged HAEs in a session accounted for more than 50% of the impacts for that session, all the HAEs from that session were removed because this was indicative of a faulty sensor.

A second analysis was also applied to sessions where more than 100 HAEs were recorded since all sessions were observed and athletes never approached this many HAEs in a single session. If a session with 100 HAEs or greater had an impact rate of one impact per minute or greater, the session was removed. If the session had more than double the number of HAEs than the session with the greatest number of HAEs less than 100, the session was removed. The sensors were power cycled before redeploying for the next session.

A total of 151,304 HAEs for the 123 FB players (both high school and MS) and 48,562 HAEs for the 65 GS players occurred within the valid time windows for all the sessions. Although other studies have used video systems to limit analysis to HAEs in which direct head impacts occurred, in this study, threshold and outlier analysis lead to the acceptance of 31,774 (FB; 21.0%) and 8,368 (GS; 17.2%) HAEs as valid (used to generate Figure 2.2). Of these impacts, full-season athletes accounted for 30,675 (FB) and 8,238 (GS) HAEs.

A.2 Repair Data Calculation

Session type refers to the session and the players that participated (all practice, V game, FR practice, etc.). An impact rate was calculated for each player and each session type. For the i^{th} player and the j^{th} the impact rate was calculated by dividing the total number of recorded HAEs the i^{th} player sustained during j^{th} session type in a season by the total participation time the player registered for the j^{th} session type during a season, with n being the total number of j type sessions in a season.

$$Impact\ Rate_j^i = \frac{\sum_{k=1}^n HAEs_{jk}^i}{\sum_{k=1}^n Time_{jk}^i} \quad (A.1)$$

If the i^{th} player did not participate in a j^{th} session type, the impact rate for the i^{th} player's j^{th} session type was set to zero. The number of repair HAEs for the k^{th} session was calculated by multiplying the i^{th} player's impact rate for the corresponding j^{th} session type by the time missed in the k^{th} session.

$$Repair\ Data_{jk}^i = Impact\ Rate_j^i \times Missed\ Time_{jk}^i \quad (A.2)$$

Outlier days were also replaced using the same repair equation with the missed time equal to the total time for the session. The repair data resulted in 3,421 (football; 10.0%) and 176 (soccer; 2.09%) of the total accepted. This brings the total number of HAEs for all analyses (other than in Figure 2.2) to 34,096 (FB) and 8,414 (GS).

B. APPENDIX B: METRIC GENERATION

B.1 Histograms

Only recorded HAEs for full and partial seasons of data were used to generate the histograms and were separated by sport and level of play. The recorded HAEs were sorted based on the PTA and were binned at 20 g intervals with a lower bound of 20 g. The percentage of HAEs in each bin was determined by dividing the number of recorded HAEs in each bin by the total number of recorded HAEs for that group.

B.2 Number of HAEs

Only players with full seasons of data were used to calculate median number of HAEs per contact session and total HAEs per season. The HAEs were separated by player and session. The total number of HAEs for each session was calculated adding the recorded data and any repair data needed for missing session time. If the player did not register an HAE for a session, it was considered a non-contact session and these sessions were excluded when calculating the session median number of HAEs. Regardless of session type (game or practice), the median number of HAEs per contact session was determined for each player. For the total number of HAEs, a player's recorded number of HAEs and repair data were summed to produce an accurate HAE total.

$$Total\ HAEs^i = \sum_{j=1}^m \sum_{k=1}^n (HAEs_{jk}^i + Repair\ Data_{jk}^i) \quad (B.1)$$

B.3 Cumulative PTA and PAA

To calculate the cumulative PTA for a season, a player's recorded HAE PTAs were summed. The repair HAEs were sorted by session type. The total number of repair HAEs for each session type was then multiplied by the average event PTA for that specific session type.

$$Repair\ PTA^i = \sum_{j=1}^m \left(\sum_{k=1}^n Repair\ Data_{jk}^i \right) \times Average\ PTA_j^i \quad (B.2)$$

The repair HAE magnitude was added to the recorded HAE cumulative PTA. An equivalent process was conducted for PAA.

B.4 Contact Sessions

A contact session is a session that had at least one HAE in the session. The percent of contact sessions is the number of contact sessions divided by the total number of monitored sessions.

B.5 Linear Regressions

A player's cumulative PTA and PAA for the season were plotted against the total number of HAEs per season. The players were then grouped by level of play and a linear regression was performed for each group. The intercepts for these plots were fixed at the origin because it is not possible for a player to accumulate any PTA or PAA without registering a HAE in a season. Players who accumulated more than 40% of their HAEs for the season in a single session (noted by the filled-in marker) were removed from the session-season regression, but the data points were still plotted.

VITA

Taylor A. Lee

Education

Ph.D. May 2021, Mechanical Engineering

Jan 2020 - May 2021

M.S. December 2019, Mechanical Engineering

Aug 2016 - Dec 2019

Purdue University, West Lafayette, IN, U.S.A

- **Associated Research Groups:** Human Injury Research and Regenerative Technologies (HIRRT) Lab, Purdue Neurotrauma Group, Auckland University of Technology Sports Performance Research Institute New Zealand (AUT SPRINZ)
- **Advisory Committee:** Professors Eric Nauman (Chair), Thomas Talavage, Scott Lawrance, and Jeffrey Rhoads
- **Affiliations:** College of Engineering, School of Mechanical Engineering
- **Research Focus:** Determining methods to reduce the mechanical load, and subsequent neurological changes, on the brains of contact sport athletes during play.
- **Relevant Coursework:** MRI Theory, Continuum Mechanics, Dynamics, Mixture Theory, Statistics, Finite Element Methods, Human Motion Kinetics, Uncertainty Quantification
- **Fellowships:** Fulbright US Student (New Zealand 2020), National Science Foundation Graduate Research Fellowships Program (Grant No. DGE-1333468), Purdue Doctoral Fellowship
- **Related Projects:** Designed and developed elbow brace for Isaac Haas in the NCAA Sweet 16 game in 34 hours
- **GPA:** 4.0/4.0

B.Sc. May 2016, Bioengineering

Aug 2012 - May 2016

University of California at Berkeley, Berkeley, CA, U.S.A

- **Associated Research Group:** Medical Polymer Group (MPG)
- **Relevant Coursework:** Orthopedic Biomechanics, Properties of Biological Materials, Biomedical Physiology, Instrumentation, Fluid Mechanics, Biomechanics, Biochemistry, Electronic Techniques for Engineers, Properties of Materials
- **GPA:** 3.97/4.0 (Summa cum laude)

Work Experience

R&D Mechanical Engineer Summer Intern

Jun 2015 - Aug 2015

ExploraMed, Mountain View, CA, U.S.A

Medical device company that developed the Willow Wearable Breast Pump

- Designed and conducted tests for product analysis and product specifications
- Prototyped multiple designs in SolidWorks
- Built, characterized and debugged R&D and clinical trial units
- Cross department collaboration with quality, clinical, R&D and software
- Wrote documentation for FDA submission

Undergraduate Research Assistant

Jun 2013 - May 2016

Medical Polymer Group, Berkeley, CA, U.S.A

Mechanical Engineering lab at UC Berkeley that tests and evaluates polymers used in medical implants

- Scored and analyzed damaged glenoid that were removed from a patient
- Organized and maintained database for all shoulder implants
- Manufactured UHWMPE compression test samples

Technical Qualifications

- **Computer Experience:** Excel, MATLAB, ImageJ, SolidWorks, Photoshop, SAS, Stata, R

Activities

- **West Lafayette High School Softball Coach** (2017-Present)
- **Tau Beta Pi Member** (2014-Present)
- **Community Service** (2015-Present): Graduate Mentor for Official Mechanical Engineering Graduate students Association, Mentor for Introduce a Girl to Engineering 2017, Spoke on a student panel for Hopkins Outreach Day
- **University of California Intercollegiate NCAA Div. I, PAC-12 Softball** (2012-2013): NFCA-National Scholar Athlete (2012), Varsity Letter Winner (2012-2013)

PUBLICATIONS

Peer Reviewed Journals

- T. A. Lee, R. J. Lycke, P. J. Lee, C. M. Cudal, K. J. Torolski, S. E. Bucherl, N. Leiva-Molano, P. S. Auerbach, T. M. Talavage, and E. A. Nauman, “Distribution of head acceleration events varies by position and play type in north american football,” *Clinical Journal of Sport Medicine: Official Journal of the Canadian Academy of Sport Medicine*, 2020.
- T. Lee, R. Lycke, J. Auger, J. Music, M. Dziekan, S. Newman, T. Talavage, L. Leverenz, and E. Nauman, “Head acceleration event metrics in youth contact sports more dependent on sport than level of play,” *Proceedings of the Institution of Mechanical Engineers, Part H: Journal of Engineering in Medicine*, vol. 235, no. 2, pp. 208–221, 2021.
- H. Yang, Z. Liang, N. L. Vike, T. Lee, J. Rispoli, E. Nauman, T. Talavage, and Y. Tong, “Characterizing Near-Infrared Spectroscopy Signal Under Hypercapnia,” *Journal of Biophotonics*, vol. 13, no. 11, p. e202000173, 2020.
- N. Leiva-Molano, R. J. Rolley, T. Lee, K. G. McIver, G. Sankaran, J. J. Meyer, D. E. Adams, E. Breedlove, T. M. Talavage, and E. A. Nauman, “Evaluation of impulse attenuation by football helmets in the frequency domain,” *Journal of Biomechanical Engineering*, vol. 142, no. 6, 2020.
- S. Bari, D. O. Svaldi, I. Jang, T. E. Shenk, V. N. Poole, T. Lee, U. Dydak, J. V. Rispoli, E. A. Nauman, and T. M. Talavage, “Dependence on subconcussive impacts of brain metabolism in collision sport athletes: An MR spectroscopic study,” *Brain Imaging and Behavior*, vol. 13, no. 3, pp. 735–749, 2019.
- I. Jang, I. Y. Chun, J. R. Brosch, S. Bari, Y. Zou, B. R. Cummiskey, T. A. Lee, R. J. Lycke, V. N. Poole, T. E. Shenk, et al., “Every hit matters: White matter diffusivity changes in high school football athletes are correlated with repetitive head acceleration event exposure,” *NeuroImage: Clinical*, no. 101930, pp. 1–16, 2019.
- F. Ansari, T. Lee, L. Malito, A. Martin, S. Gunther, S. Harmsen, T. Norris, M. Ries, D. Van Citters, and L. Pruitt, Analysis of severely fractured glenoid components: clinical consequences of biomechanics, design, and materials selection on implant performance.

Abstracts, Conference Presentations, and Technical Reports

- Yang H, Yao J, Wang JH, Liang Z, Kish B, Tu J, Lee T, Vike N, Kashyap P, Bari S, Zou Y, Jang I, Vincent J, Mao X, Tamer G, Nauman E, Talavage T and Tong Y. Characterizing Near-Infrared Spectroscopy Signal Under Hypercapnia. BMES 2019 Annual meeting, October 16-19, 2019.
- Zou Y, Lee T, Lycke RJ, Jang I, Vike NL, Nauman EA, Talavage TM, Rispoli JV. High -G Head Collisions are Associated with Short-Term White Matter Microstructural Deficits in High School Football Athletes. Neurotrauma 2018. Toronto, August 11-16, 2018. Published by Journal of Neurotrauma, Aug 1, 2018 (Vol. 35, No. 16, pp. A143-A144).
- Talavage TM, Lee T, Lycke RJ, Nauman EA. Necessity for Personalized Sensor Systems for Accurate Measurement of Head Acceleration Events in Youth Contact Sports. Neurotrauma 2018. Toronto, Canada, August 11-16, 2018. Published by Journal of Neurotrauma, Aug 1, 2018 (Vol. 35, No. 16, pp. A143-A144).
- Lycke R, Lee T, Sankaran G, McIver K, Talavage T, Nauman E. Traumatic Brain Injury in Sport: The Importance of Individualized Analysis and Monitoring. Health and Disease: Science Technology, Culture and Policy Research Poster Session. West Lafayette, IN, March 1, 2018.
- Lee T, Auger J, Music J, et al. (2017). Head impacts for middle school football players comparable to high school players. Biomedical Engineering Society 2017 Annual Meeting. Phoenix, AZ.